

Universidade do Minho
Escola de Engenharia

Joana Maria Marques da Silva

**Nanostructured 3D Constructs based
on Chitosan and Chondroitin Sulphate
Multilayers for Cartilage Tissue
Engineering**



Universidade do Minho

Escola de Engenharia

Joana Maria Marques da Silva

**Nanostructured 3D Constructs based
on Chitosan and Chondroitin Sulphate
Multilayers for Cartilage Tissue
Engineering**

Dissertação de Mestrado
Ciclo de Estudos Integrados Conducentes ao Grau de
Mestre em Engenharia Biomédica
Área de Especialização em Biomateriais, Reabilitação e
Biomecânica

Trabalho realizado sob a orientação do
Professor Doutor João Filipe Colardelle da Luz Mano

Outubro de 2011

É AUTORIZADA A REPRODUÇÃO INTEGRAL DESTA DISSERTAÇÃO APENAS PARA EFEITOS DE INVESTIGAÇÃO, MEDIANTE DECLARAÇÃO ESCRITA DO INTERESSADO, QUE A TAL SE COMPROMETE;

Universidade do Minho, ____/____/_____

Assinatura: _____

ACKNOWLEDGMENTS

The thesis developed during this school year was the final step of this journey started in the 2006/2007 academic year. So, let me express my sincere thanks to all those who contributed directly or indirectly throughout this journey, especially in this thesis.

First, I would like to acknowledge my supervisor, Professor João Filipe Colardelle da Luz Mano, for all the support, advices, availability and opportunities given. My ERASMUS experience was the result of his encouragement.

I would also like to thank Rui Costa for the confidence, guidance and availability throughout the work done. To Praveen for the support and availability along the endless hours spent during scaffold production, thank you so much!

To all researchers and staff of 3B's I would like to thanks the good environment and help they provided throughout this work. A special recognition goes to Álvaro Leite and Sofia Caridade for their support in handling the robot and for always being ready to help. I would like to thanks Ivo Aroso and Mariana Oliveira for all their help and support provided in the FTIR and DMA analysis, respectively. Finally, I wish to thank Tírcia Santos for all the “tricks” transmitted during histology assay.

Half of my thesis was developed during my ERASMUS experience, so I would like to thank Professor Marcel Karperien that welcomed me on his work group, in Twente University, during 6 months, for the personal and professional growth that my staying there represented. I wish to thanks, Nicole Georgi who taught me so much about cell culture and a wide range of cellular tests. Thank you for all the support, availability and transmitted knowledge. To the cartilage group I would like to thanks, for all the valuable discussions and suggestions along the six months. Finally, to the TR Team, thank you for welcome me in their group!!

I cannot forget to acknowledge the friends that I made during my ERASMUS. It is impossible to refer all of you but I would like to say that they were very important during this journey!!! Thanks

for the company, good environment and happy hours. To all the residents of our home called Calslaan 24 as well as our neighbours from Calslaan 26 and the Portuguese “ghetto” thank you so much for the good moments lived together, I will never forget you!!!!

To my colleagues and friends of Biomedical Engineering thank you for everything you have given me throughout these years.

I would like to dedicate special words to Diana, Catarina, Vanessa, Nélon and João Vieira that share with me this trajectory through all these years. They have been very special friends. Thank you so much for all the support and friendship!

Sara I cannot finish this thesis without saying thank you so much for all the support, endless friendship and for all the advices, it is time to say after 5 years, yes I did it!!

To Bianca, for her friendship, company over this year that we spent together. I must say that you became my right arm!! I am pretty sure that without you this year, especially the lived moments during our ERASMUS, it would not be the same. Thank you for everything!!!

Thanks to my sisters Sofia and Raquel and to my brother Pedro, my brother-in-law Hélder and to my little nieces, Inês and Joaninha. They always gave me constant support, and they are so important in my life. Raquel, I must say thank you for all the support and patience during this year and for almost known my entire thesis.

At last but not least, to my parents for always be there for me, supporting my decisions. Thank you so much for everything!!! This thesis would not exist without you, and it is for you that I dedicate this thesis.

ABSTRACT

Articular cartilage damage is a persistent and increasing problem with the aging population, and treatments to achieve biological repair remain a challenge. The lack of efficient modalities of treatments has prompted research into tissue engineering (TE). TE approaches are a promising strategy for improving the rate of repair of articular cartilage lesions by combining cells, biomaterials and microenvironmental factors. The work developed at this thesis was aimed to study the potential of nanostructured scaffolds based on layer-by-layer (LbL) methodology to be used in articular cartilage TE. The polyelectrolytes used for producing these structures were two polysaccharides: chitosan (polycation) and chondroitin sulphate (polyanion). These polyelectrolytes were chosen due to its biocompatibility and positive influence on cartilage.

The sequential combination of these polyelectrolytes led to a decrease in frequency and increase in dissipation as seen using quartz microbalance (QCM), indicating the development of a multilayered film. For the proof of concept, biological assays were first performed in multilayered surfaces with bovine chondrocytes (bch). No cytotoxic effects of the film were found. Thus, the formation of a nanostructured film was transposed to a three-dimensional (3D) level combining LbL and leaching of spherical sacrificial templates. The homogenous distribution of polysaccharides in the scaffolds was confirmed by Fourier transformed infrared spectroscopy (FTIR). Morphological analysis of the scaffolds was based on scanning electron microscope (SEM), optical microscopy, and histology. The results showed a high porosity, which leads to swollen structure when immersed in phosphate buffered saline (PBS). The enzymatic degradation tests, using PBS and enzymatic solution with lysozyme and hyaluronidase, showed that the scaffold has a gradual degradation, and as expected the rate of degradation was higher in the enzymatic solution. Mechanical properties of the scaffold were evaluated using dynamic mechanical analysis (DMA). The results revealed that scaffold exhibit viscoelastic behaviour which corroborates the results obtained at QCM.

The applicability of the nanostructured scaffold for cartilage was evaluated in cellular assays with bch and human mesenchymal cells (hMSCs). Tests of cell viability, SEM and quantification of DNA revealed that scaffolds promote cell adhesion and proliferation. Differentiation studies demonstrated the production of glycosaminoglycans (GAGs) by both cells. These results confirmed the maintenance of phenotype of bch and the chondrogenic differentiation of hMSCs. Thus, we believe the scaffolds developed may have potential use in cartilage TE approaches.

RESUMO

Os danos da cartilagem articular são um problema persistente e crescente com o envelhecimento da população, pelo que os tratamentos para obter a reparação biológica continuam a ser um desafio. A falta de tratamentos eficientes impulsionou a investigação de estratégias de engenharia de Tecidos (TE), as quais são estratégias promissoras para melhorar a taxa de reparação de lesões da cartilagem articular, combinando células, biomateriais e factores microambientais. O trabalho desenvolvido nesta tese teve como objectivo estudar o potencial de “scaffolds” nanoestruturados baseados na metodologia de “*layer-by-layer*” (LbL) para estratégias de TE da cartilagem articular. Os materiais utilizados para a produção destas estruturas foram dois polissacarídeos: o quitosano (policatão) e o sulfato de condroitina (polianião). Estes foram seleccionados devido à sua biocompatibilidade e influência positiva na cartilagem.

A combinação sequencial destes polielectrólitos leva a uma diminuição da frequência e aumento da dissipação na microbalança de quartzo (QCM), indicando o desenvolvimento de um filme com multicamadas. Para comprovar a aplicabilidade destas estruturas, primeiramente foram realizados ensaios biológicos em superfícies com multicamadas, utilizando condrócitos bovinos (bch). O filme produzido não apresentou qualquer efeito citotóxico. Assim, a formação de um filme nanoestruturado foi transposta para o nível tridimensional (3D) combinando LbL com lixiviação de partículas de sacrifício esféricas. A presença dos polissacarídeos nos “scaffolds” foi confirmada pela espectroscopia de infravermelhos por transformadas de Fourier (FTIR). A análise morfológica dos “scaffolds” foi baseada em microscopia electrónica de varrimento (SEM), microscopia óptica, bem como cortes histológicos. Os resultados obtidos demonstraram uma elevada porosidade, o que leva à dilatação da estrutura quando imersa em tampão fosfato salino (PBS). Os testes de degradação enzimática realizados, usando PBS e uma solução enzimática composta por lisozima e hialuronidase, demonstraram que a degradação dos “scaffolds” ocorreu de forma gradual e tal como esperado foi mais acentuada na solução enzimática. As propriedades mecânicas dos “scaffolds” foram avaliadas usando análise dinâmica mecânica (DMA). Os resultados revelaram que os “scaffolds” exibem um comportamento viscoelástico o que corrobora os resultados obtidos na QCM.

A aplicabilidade destas estruturas para a cartilagem avaliou-se em ensaios celulares com bch e células humanas mesenquimais (hMSCs). Os testes de viabilidade celular, SEM e quantificação de DNA revelaram que os “scaffolds” promovem a adesão celular e proliferação. Estudos de diferenciação demonstraram a produção de glucosaminoglicanos (GAGs) de ambas as células. Estes resultados confirmam a manutenção de fenótipo dos bch e a diferenciação condrogénica de hMSCs. Desta forma, acreditamos que os “scaffolds” desenvolvidos terão uma potencial utilização em estratégias de TE para a cartilagem.

TABLE OF CONTENTS

Acknowledgments	iii
Abstract	v
Resumo	vi
Table of contents	vii
List of abbreviations	xi
List of figures	xvii
List of tables	xxi
List of equations	xxiii
Chapter I	1
Chapter I - General Introduction	3
I-1. Motivation and Outline.....	3
I-2. Cartilage tissue organization	4
I-3. Articular cartilage associated diseases	5
I-4. Articular cartilage repair therapies	6
I-5. Cell source.....	8
I-6. Microenvironmental factors	9
I-6.1. Scaffold requirements for cartilage tissue engineering	11
I-7. Scaffold processing techniques for cartilage applications.....	12
I-7.1. Layer-by-layer methodology.....	14
I-7.1.1. Parameters.....	16
I-8. Polymeric material used in articular cartilage tissue engineering.....	17
I-8.1. Synthetic polymers	18
I-8.2. Natural polymers.....	18
I-8.2.1. Chitosan	19

I-8.2.2.	Chondroitin sulphate	20
I-8.2.3.	Combination of chitosan and chondroitin sulphate	22
I-9.	Conclusion and future perspectives.....	23
I-10.	References	24

Chapter II..... 33

Chapter II - Materials and methods 35

II-1.	Materials	35
II-2.	Methods.....	36
II-2.1.	Layer-by-layer (LbL) assembly in 2D surfaces	36
II-2.2.	Scaffolds production by LbL.....	37
II-2.3.	Physicochemical characterization of scaffolds and surfaces	37
II-2.3.1.	Build-up Mechanism for film constructed	37
II-2.3.2.	Morphology.....	38
II-2.3.2.1.	Optical microscope	38
II-2.3.2.2.	Scanning electron microscopy (SEM).....	38
II-2.3.3.	Fourier transform infrared spectroscopy.....	38
II-2.3.4.	Swelling test.....	39
II-2.3.5.	Enzymatic Degradation.....	39
II-2.3.6.	Mechanical Properties.....	40
II-2.4.	Cellular assays	41
II-2.4.1.	Bovine articular chondrocytes and human mesenchymal stem cells culture	41
II-2.4.2.	Cell viability and morphology	42
II-2.4.2.1.	Live dead assay	42
II-2.4.2.2.	MTT assay	42
II-2.4.2.3.	SEM	43
II-2.4.3.	DNA quantification	43

II-2.4.4. Histology	43
II-3. Statistical Analysis.....	44
II-4. References.....	44
Chapter III	45
Chapter III - Nanostructured 3D constructs based on chitosan and chondroitin sulphate multilayers for cartilage tissue engineering	47
Abstract	47
III-1. Introduction.....	49
III-2. Materials and methods.....	50
III-2.1. Materials.....	50
III-2.2. Methods.....	50
III-2.2.1. Build-up Mechanism for film constructed	50
III-2.2.2. LbL assembly in 2D surfaces	51
III-2.2.3. Scaffolds production by LbL	51
III-2.2.4. Physicochemical characterization	52
III-2.2.4.1. Morphology	52
III-2.2.4.2. Fourier transform infrared (FTIR) spectroscopy.....	52
III-2.2.4.3. Swelling test.....	52
III-2.2.4.4. Enzymatic Degradation	52
III-2.2.4.5. Mechanical Test	53
III-2.3. Cellular assays	53
III-2.3.1. Bovine articular chondrocytes and human mesenchymal stem cells culture	53
III-2.3.2. Cell viability	54
III-2.3.2.1. Live /dead assay	55
III-2.3.2.2. MTT assay.....	55

III-2.3.2.3. Scanning electron microscopy observation	55
III-2.3.3. DNA quantification	55
III-2.3.4. Histology.....	56
III-3. Statistical Analysis	56
III-4. Results and discussion	57
III-4.1. Build-up Mechanism for film constructed.....	57
III-4.2. Multilayer surface	58
III-4.2.1. Cell behaviour in multilayers.....	58
III-4.3. Nanostructured Scaffolds: Physicochemical characterization.....	61
III-4.3.1. Scaffold preparation and morphology.....	61
III-4.3.2. Fourier transform infrared spectroscopy.....	62
III-4.3.3. Swelling ability	64
III-4.3.4. Enzymatic degradation	64
III-4.4. Cells behaviour in nanostructured scaffolds.....	66
III-4.4.1. Cell viability and adhesion \ morphology.....	66
III-4.4.2. Cell proliferation.....	68
III-4.5. Histology	69
III-5. Conclusion	71
III-6. References	72

Chapter IV..... 75

Chapter IV - General Conclusion and Future Perspectives 77

IV-1. General Conclusions.....	77
IV-2. Future perspectives	78

LIST OF ABBREVIATIONS

A

α -MEM	Alpha modified Eagle's medium
ATR	Attenuated total reflection
ASAC	Ascorbic acid 2-phosphate

B

bch	Bovine chondrocytes
BMP	Bone morphogenetic protein

C

CHT	Chitosan
CS	Chondroitin sulphate
cm	Centimetre
Cps	Centipoise
CPD	Critical point dryer

D

2D	Bi-dimensional
3D	Three-dimensional
Δ D	Dissipation changes
Da	Dalton
DCM	Dichloromethane
DD	Degree of deacetylation
dL	Double layer
DMA	Dynamic mechanical analysis
DMEM	Dulbecco's modified Eagle's medium
DNA	Deoxyribonucleic acid

E

E'	Storage modulus
ECM	Extracellular matrix
e.g.	For example
EGF	Epidermal growth factor

F

Δf	Frequency changes
$\Delta f_i/n$	Normalized frequency changes
FBS	Fetal bovine serum
FGF	Fibroblast growth factor
FITC	Fluorescein isothiocyanate
FTIR	Fourier transform infrared

G

g	Gram
GAGs	Glycosaminoglycans
GFs	Growth Factors

H

h	Hours
H&E	Haematoxylin and eosin
hMSCs	Human mesenchymal stem cells
Hz	Hertz

I

IGF	Insulin-like growth factor
ILs	Interleukins
ITS	Insulin-Transferrin-selenite

K

KBr	Potassium Bromide
kV	Kilovolt

L

LB	Langmuir Blodgett
LbL	Layer-by-layer

M

μg	Micrograms
μL	Microliters
μm	Micrometre
μM	Micromolar
M	Molar
Mw	Molecular weight
MHz	Megahertz
min	Minutes
mL	Mililiters
mM	Milimolar
mm	Milimeter
MMP	Matrix metalloproteinase
MSCs	Mesenchymal Stem cells
MTT	M3-(4,5-dimethylthiazol-2-yl)-2,5-diphenyltetrazolium bromide

N

n	Overtone
nm	Nanometre
NaCl	Sodium chloride
NaOH	Sodium hydroxide

P

p	Statistical level of significance
PBA	Poly(butyl acrylate)
PBS	Phosphate buffered saline solution
PBT	Poly(butylene terephthalate)
PCL	Poly(ϵ - caprolactone)
PCR	Polymeric chain reaction
PDGF	Platelet derived growth factor
PDLA	Poly(D- lactic acid)
PDLLA	Poly(D,L- lactic acid)
PE	Poly(ethylene)
PEI	Poly(ethylene imine)
PEG	Poly(ethylene glycol)
PEMs	Polyelectrolyte multilayers
PEMA	Poly(ethyl methacrylate)
PEO	Poly(ethylene oxide)
PET	Poly(ethylene terephthalate)
PGA	Poly(glycol acid)
PHA	Poly(hydroxyalkanoate)
PHB	Poly(hydroxybutyrate)
PHBV	Poly(3-hydroxybutyrate-co-3-hydroxyvaluate)
PLLA	Poly(L-lactic acid)
PLGA	Poly(lactic-co glycolic) acid
PMMA	Poly(methyl methacrylate)
PNIPAAM	Poly(N-isopropylacrylamide)
PPF	Poly(propylene fumarate)
PU	Poly(urethane)
PTFE	Poly(tetrafluoroethylene)
PVA	Poly(vinyl alcohol)

Q

QCM Quartz crystal microbalance

R

RNA Ribonucleic acid

S

s Second

SAMs Self-assembled monolayers

SD Standard deviation

SEM Scanning electron microscopy

T

th Thickness

Tan δ Loss factor

TE Tissue engineering

TGF- β Transforming growth factor beta

TNF- α Tumor necrosis factor alpha

Tris-EDTA Tris(hydroxymethyl)aminomethane ethylenediaminetetraacetic

U

UV Ultra-violet

W

W_d Weight of dried scaffold

W_f Weight after incubation in PBS or enzymatic solution

W_i Initial weight of scaffold

WL Weight loss

W_w Weight of swollen scaffold

w/v Weight/volume

Wnts Wingless family

v

v/v

Volume/volume

LIST OF FIGURES

Chapter I -	General Introduction	3
Figure I-1:	Zonal organization in normal articular cartilage: superficial zone (SZ), middle zone (MZ), Deep zone (DZ), and Calcified zone (CZ) below which is the subchondral bone SB). Each zone is distinct in cell morphology (A), GAGs distribution (B), Collagen organization (C) and changes in oxygen levels (D)[adapted from [6, 18]].....	5
Figure I-2:	Comparison between partial thickness defects and full thickness defects [28].	6
Figure I-3:	General scheme representing cartilage TE approaches: <i>in ex vivo</i> TE and <i>in vivo</i> TE (adapted from [36]).	8
Figure I-4:	Chondrocytes phenotype shift during dedifferentiation [adapted from table [38]].	9
Figure I-5:	Schematic representation of drawbacks associated with LB and SAMs [adapted from [104, 107]].....	15
Figure I-6:	Chemical structure of chitin and chitosan[adapted from [138]].....	19
Figure I-7:	Structures of disaccharides forming chondroitin sulphate. Different groups on R1, R2 and R3 give rise to different types of CS: R1=R2=R3=H non-sulphated chondroitin, R1=[SO₃ –]and R2=R3= H chondroitin-4-sulphate; R2=[SO₃ –]and R1=R3=H chondroitin-6-sulphate; R2=R3=[SO₃ –]and R1=H chondroitin-2,6-disulphate; R1=R2=[SO₃ –]and R3=H chondroitin-4,6-disulphate; R1=R3=[SO₃ –] and R2=H chondroitin-2,4-disulphate; R1=R2=R3=[SO₃ –] trisulphated chondroitin [175].	21
Chapter II -	Materials and methods.....	35
Figure II-1:	Diagram illustrating the sequential step to prepare surfaces coated with chitosan and chondroitin sulphate. 1) First glass coverslips were	

	immersed into a polycationic solution of chitosan solution. 2) The coverglasses are subsequent immersed in washing solution with NaCl. 3) Immersion in polyanionic solution of chondroitin sulphate solution. 4) Immersion in NaCl solution. These sequential steps have been repeated until reach 10 double layers (dL).....	36
Figure II-2:	Schematic diagram of the produced scaffolds. A) Paraffin wax spheres coated with PEI, B) Addition of polyelectrolytes, C) Leaching with DCM and freeze dried process.....	37
Chapter III -	Nanostructured 3D constructs based on chitosan and chondroitin sulphate multilayers for cartilage tissue engineering.....	47
Figure III-1:	Build-up monitoring of the CHT/CS polyelectrolyte multi-layered using QCM for film constructed: A) Normalized frequency ($\Delta f_7/7$) and dissipation changes (ΔD_7) obtain at 35 MHz, 1) deposition of CHT, 2) washing step and 3) deposition of CS; B) Estimated thickness (th) evolution and SEM micrographs of the multilayer surface with 10 dL (inset image).	57
Figure III-2:	Live/dead assay and SEM micrographs of bch seeded on glass coverslips coated with chitosan and chondroitin sulphate at day 1 (A, B), 3 (C, D), 7 (E, F), 14 (G, H) and 21 (I, J) of culture in proliferation medium.	59
Figure III-3:	Percentage of surface area coverage with cells at 1, 3, 7, 14 and 21 days of culture. Significant differences for $p < 0.01 (**)$ were found.	60
Figure III-4:	Scaffold characterization: A) Production steps of scaffolds: LbL and leaching of free-packet paraffin spheres, B) Optical Microscopy image of the scaffolds after the leaching of the core material, C) SEM micrographs of cross-sections (two different magnifications) and Histological cross-sections of the scaffolds after staining with alcian blue (E) and eosin (D).....	62
Figure III-5:	Physicochemical characterization of scaffolds: A) FTIR measurements of CHT/CS scaffolds and pure polysaccharides (CHT and CS), B) Swelling	

	test up to 3 days (The inset graphic expands the water uptake for the first 5 hours), C) Weight loss of the scaffolds in PBS (▲) and in an enzymatic solution at 37°C (■).....	63
Figure III-6:	Variations of (A) Storage modulus (E') and (b) loss factor (tanδ) of the CHT/CS scaffolds obtained by LbL methodology. Experiments are reported for dry samples (■) and hydrated samples in PBS at 37°C (●).....	66
Figure III-7:	Live/dead assay, MTT assay and cross-section SEM micrographs of Bch seeded on scaffold at day 1(A, B, C), 3(D, E, F), 14 (G, H, I) and 21(J, K, L) of culture in proliferation medium.	67
Figure III-8:	Live/dead assay, MTT assay and cross-section SEM micrographs of hMSCs seeded on scaffold at day 1(A, B, C), 3(D, E, F), 14 (G, H, I) and 21(J, K, L) of culture in proliferation medium.	68
Figure III-9:	DNA assay on the scaffolds seeded with bch and hMSCs in differentiation medium. Significant differences between each cell type at different time points were found for $p < 0.05$ (*) and $p < 0.01$ (**).	69
Figure III-10:	Histological cross-sections of scaffolds seeded with bch stained by H&E and Alcian blue at different days of culture in differentiation medium.....	70
Figure III-11:	Histological cross-sections of scaffolds seeded with hMSCs stained by H&E and Alcian blue at different days of culture in differentiation medium.	71

LIST OF TABLES

Chapter I -	General Introduction	3
Table I-1:	Regulatory effects of GFs and cytokines in articular cartilage	10
Table I-2:	Scaffolds requirement for TE.....	11
Table I-3:	Overview of techniques to prepare scaffolds for TE.....	13
Table I-4:	Overview of techniques to prepare scaffolds for TE (continuation)	14
Table I-5:	Examples of parameters varied in LbL technique and their influence on final structure of film	16
Table I-6:	Materials already used for articular cartilage TE	17

LIST OF EQUATIONS

Chapter II -	Materials and methods.....	35
Equation II-1:	Determination of water uptake.....	39
Equation II-2:	Determination of WL (%)	40
Chapter III -	Nanostructured 3D constructs based on chitosan and chondroitin sulphate multilayers for cartilage tissue engineering	47
Equation III-1:	Determination of water uptake.....	52
Equation III-2:	Determination of WL (%)	53



“Learning never exhausts the mind”

Leonardo da Vinci

CHAPTER I

GENERAL INTRODUCTION

Chapter I

General Introduction

I-1. MOTIVATION AND OUTLINE

Every year millions of people suffer from cartilage damage which is normally associated with sports and progressive ageing [1-3]. Owing to specific properties of cartilage, such as low capacity of self-repair, available treatments are not completely successful, so new challenges are required [4, 5]. The ideal cartilage treatment would provide the integration of hyaline cartilage with the surrounding tissue, would also reproduce the unique zonal architecture of cartilage, would be cost-effective, and would be accomplished with one surgery. Several cartilage regeneration techniques are available and may satisfy many of the characteristics of an ideal cartilage repair method. However, the future of cartilage repair seems to be intimately associated with tissue engineering (TE) approaches, such as various types of scaffolds, has been demonstrated to own promising therapeutic advantages in restoring both the structure and function of the damaged articular cartilage [6, 7]. Thus, besides some promising results, new approaches are still need to be clinically accepted.

The goal of this work is to process three-dimensional (3D) porous structures based on layer-by-layer (LbL) methodology for cartilage TE. The polyelectrolytes selected were chitosan, natural abundant, and chondroitin sulphate present in articular cartilage. Chitosan was chosen due to its cationic nature that allows the interactions with anionic species, such as glucosaminoglycans (GAGs). The choice of chondroitin sulphate was related with its highly negative charge density which together with gives rises to the compressive behaviour of cartilage.

Structures based on chitosan and chondroitin sulphate share the advantage of these two polysaccharides and thereby the hypothesis of this work is the positive influence of this combination in structured based on LbL for cartilage TE applications.

I-2. CARTILAGE TISSUE ORGANIZATION

Cartilage is a connective tissue that comprises most of the embryonic skeleton [8, 9]. Three different types of cartilage have been distinguished based on their histological and biomechanical properties: fibrous, elastic and hyaline cartilage[8]. The most prevalent type is hyaline cartilage that covers articulating surface and protects against the damage due to repetitive load and friction associated with joint movement [10, 11]. Articular cartilage and nasal septal cartilage are examples of hyaline cartilage [8].

Articular cartilage is an avascular, aneural, alymphatic, anisotropic and acellular (low amount of chondrocytes) tissue [2, 12]. This tissue is mainly composed of fluid, comprising up to 80 % of the total weight, while solid matrix contribute only with 20 % [13-15]. The fluid content is composed by water, gases, metabolites and a large amount of cations to balance the negatively charge GAGs in the extracellular matrix (ECM). The solid matrix is mostly composed by collagen type II fibrils, smaller amount of type IX, X, XI, V and VI collagen molecules, noncollagenous proteins (glycoproteins) and proteoglycans molecules [13, 15, 16]. Proteoglycans are large molecules composed of a protein core with polysaccharide side chains attached. The primary proteoglycan in articular cartilage is aggrecan which consist of a core protein that is heavily glycosylated with negatively charge GAGs, like chondroitin sulphate and keratin sulphate. Aggrecan molecules have the ability to interact with hyaluronic acid to form large proteoglycans aggregates via link proteins [5, 15, 17]. As a result, the proteoglycans network can be thought as a mesh that is interlaced within the more organized collagen structure. The collagen structure gives tissue tensile strength and hinders expansion of the aggrecan molecules [17]. Other proteoglycans essential for articular cartilage are: biglycans, decorin and fibromodulin [1]. Glycoproteins have a small amount of oligosaccharide associated with protein core. This polypeptide is responsible to stabilize the ECM matrix and aid in chondrocytes matrix interaction [8, 15].

In articular cartilage four zones can be distinguished by differences in water and proteoglycans concentrations, gene expression, levels of oxygen, cell size, cell shape, metabolic activity, collagen fibril diameter and orientation (Figure I-1)[6, 18]. The first zone is the superficial that has two distinct layers: an acellular sheet of predominantly collagen fibres and a second layer composed of flattened chondrocytes. This zone plays important role for compressive strength of the tissue and possibly in isolation of cartilage from immune systems. The second zone is the middle or transitional that is composed of spherical chondrocytes randomly oriented on collagen. The third

zone is the deep or radial zone that has the largest diameter collagen fibrils, the higher concentration of proteoglycans and the least concentration of water. The last zone (calcified) is a zone of mineralized tissue, hypertrophic and with circular chondrocytes. This zone lies closest to the subchondral bone and act as a transition from soft hyaline cartilage to bone [15, 19].

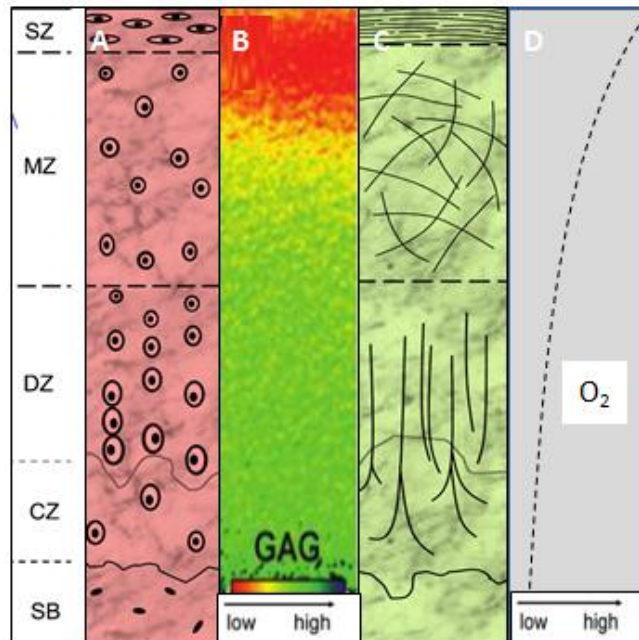


Figure I-1: Zonal organization in normal articular cartilage: superficial zone (SZ), middle zone (MZ), Deep zone (DZ), and Calcified zone (CZ) below which is the subchondral bone (SB). Each zone is distinct in cell morphology (A), GAGs distribution (B), Collagen organization (C) and changes in oxygen levels (D) [adapted from [6, 18]].

I-3. ARTICULAR CARTILAGE ASSOCIATED DISEASES

Traumatic injury and age-related degenerative diseases associated with cartilage are one of the most common health problems worldwide [20, 21]. Age-related diseases occur due to changes in the composition of ECM and organization of chondrocytes. With increasing of age there are changes in the zonal distribution of chondrocytes and as result the deeper layers have an increased number of cells when compared with the superficial layers. Other change is a decrease in the hydration of the matrix with a corresponding increase in compressive stiffness. The size of proteoglycans aggregates also decreases with the age [1].

The poor regeneration of adult articular cartilage is intrinsically associated with the limited number of chondrocytes, reduced repairs elements, absence of blood supply and innervations [22, 23]. In contrast to the adult cartilage, young cartilage has capacity to accelerate synthesis of ECM.

Spontaneous repair in adult cartilage usually results in primarily fibrous tissue at the superficial layers and fibrocartilage (mechanically and chemically inferior to hyaline cartilage). These repair tissues are unable to withstand the higher compressive loads during sports practice or even normal gaits and the predilection for the development of degeneration diseases (e.g. osteoarthritis) [14, 24, 25].

There are three main types of articular cartilage injury: matrix disruption, osteochondral or full thickness defects and chondral or partial thickness defects [26, 27]. Matrix disruption occurs from blunt trauma or age related matrix and it is responsible for ECM damaged. Full-thickness defects extend through the cartilage layer and penetrate the subchondral bone. As a result, the defects are filled within a fibrin clot. On the other hand, partial thickness defects do not penetrate the subchondral bone and immediately following the injury nearby cells begin to proliferate. This type of defect is not easily repaired as the full thickness defects because spontaneous repair is only achieved when the defects penetrates the subchondral bones, probably triggering a response from the mesenchymal stem cells (MSCs) presents in the marrow (Figure I-2) [14, 27, 28].

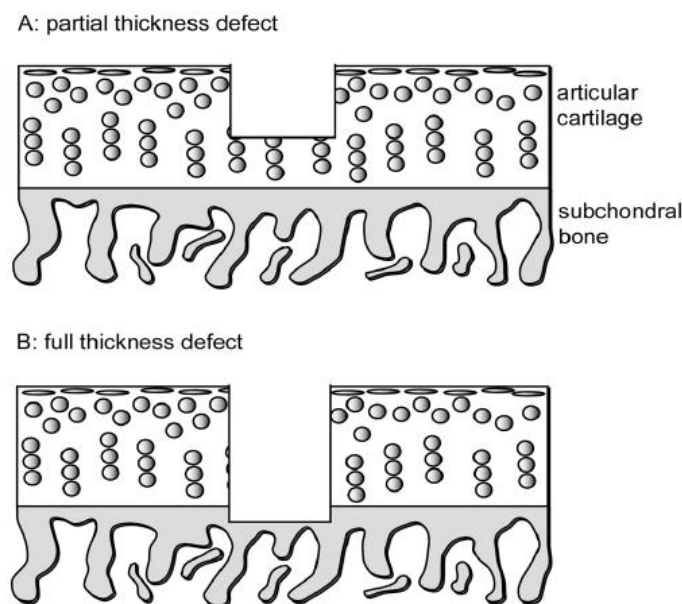


Figure I-2: Comparison between partial thickness defects and full thickness defects [28].

I-4. ARTICULAR CARTILAGE REPAIR THERAPIES

Millions of people require treatment to repair damaged cartilage due to limitation of its natural self-repair [29]. The therapies for articular cartilage defects can be divided into two major

categories: conservative treatments and surgical procedures. The conservative treatments include physical therapies (e.g.: ice, supply of orthothesis) and/or drug administration. Nevertheless, these treatments only can modify and improve symptoms nevertheless none of these can heal cartilage defects. Conversely, the surgical procedures can reconstruct the surface of articular cartilage and there are several different types available. Surgical procedures include arthroscopy techniques (e.g.: bone marrow stimulating procedure, osteotomy, chondral shaving, debridement, lavage, abrasion arthroplasty, osteochondral drilling, microfracture, total joint arthroplasty, distraction of joints) and procedures that follow autogenic and allogenic tissue transplantation principles (osteochondral transplantation- mosaicplasty, perichondral / periosteal grafting) [2, 30, 31].

A wide range of clinical options emerged to repair focal lesions and damage to the articular cartilage. These approaches reduce the pain increase the immobility but present a limited extent and a short-term period. Thus, TE strategies are a significant clinical option in the treatment of damaged or diseased cartilage [13, 15, 32]. The principles of TE rely on the use of cells, biomaterials and microenvironmental factors, alone or in combination [33-35].

The advantages of TE approaches is the use of scaffolds that can provide the initial structure support and retain cells in the defective area which is follow degraded when the cells secrete their own ECM. General TE approaches for cartilage repair require some steps that are represented in Figure I-3. Briefly, cells are firstly isolated via biopsy from patient and then in order to obtain a large amount of cells bi-dimensional (2D) expansion is required. Due to the de-differentiation process and cartilage complex three-dimensional (3D) geometry isolated cells are reintroduced into a 3D environment, namely scaffold. Bioactive, biomechanical and chemical factors, as well as bioreactors, can be used to stimulate cartilage regeneration. Two basic methodologies are normally applied in cartilage TE approaches: *ex vivo* TE and *in vivo* TE. In *ex vivo* TE strategy the tissue is completely generated in vitro while *in vivo* TE strategies the construct is implanted with or without prior *in vitro* cultivation and allowed to mature *in vivo* [4, 36].

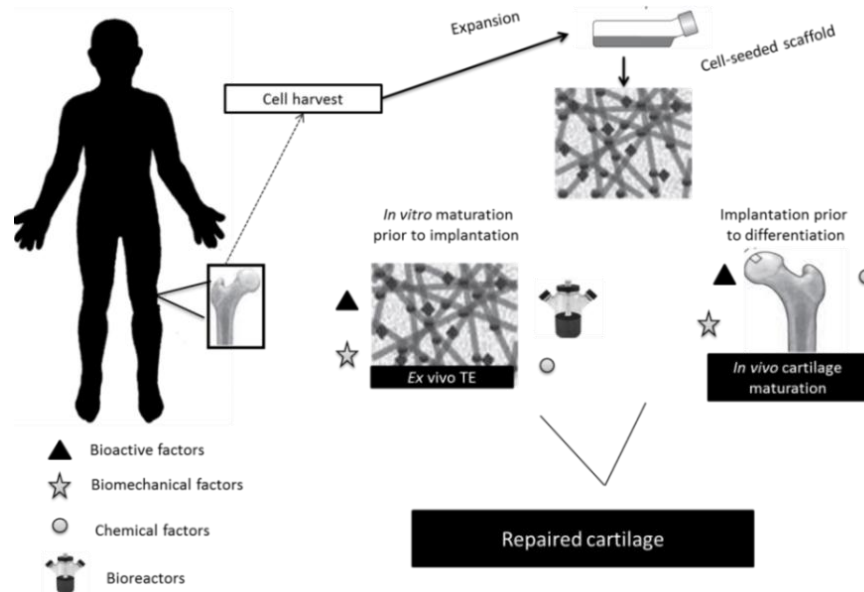


Figure I-3: General scheme representing cartilage TE approaches: *in ex vivo* TE and *in vivo* TE (adapted from [36]).

I-5. CELL SOURCE

The optimal source for cartilage TE approaches is still being identified. As a result, wide ranges of cells have been already tested such as chondrocytes, stem cells and genetically modified cells [4, 7, 37, 38]. Chondrocytes are the most obvious choice, because they are found in native cartilage and are responsible for secretion of the ECM. The sources normally used for cartilage repair are: auricular cartilage, articular cartilage, nasoseptal cartilage and costal cartilage. These cells, like the others, reside, proliferate and differentiate inside the body within a complex 3D environment. However, in contrast with other cell types, the isolated chondrocytes in 2D culture lose their differentiated phenotype [4, 5, 39]. The de-differentiation process is accompanied by morphological/cytoskeletal changes, different ECM synthesis and cell surface receptors profile (Figure I-4). The de-differentiation process can be limited when chondrocytes are cultured in a 3D environment [5, 38].

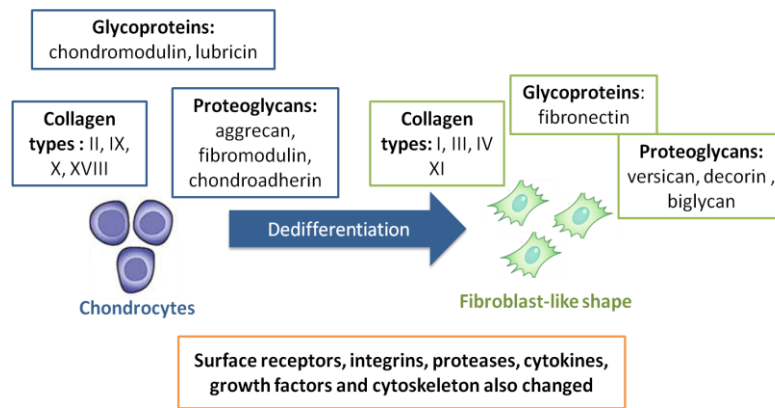


Figure I-4: Chondrocytes phenotype shift during dedifferentiation [adapted from table [38]].

MSCs are a promising strategy for articular cartilage due to their easy availability and multilineage differentiation capacity. These cells can differentiate into different cell types when stimulated by microenvironmental factors that are the driving motor for its differentiation [4, 5, 39-46]. The chondrogenic differentiation involves a 3D structure, growth and environmental factors. However, MSCs also have some limitations associated with *in vitro* expansion due to the potential loss of differentiation potential. Moreover, other potential obstacles exist, including cellular senescence and death, hypertrophy, and graft integration [44]. The most challenging problem in cartilage TE using MSCs is the terminal differentiation to hypertrophy, characterized by high levels expression of alkaline phosphatase and collagen type X [44].

I-6. MICROENVIRONMENTAL FACTORS

The microenvironmental factors are namely composed of mechanical and signalling molecules [47]. The signalling molecules should try to reproduce the natural sequence of signals guiding spontaneous tissue repair and cells. These molecules involved the use of bioactive molecules, generally represented by growth factors (GFs) and cytokines [48].

GFs are polypeptides secreted by a wide range of cells and play a role in either stimulating or inhibiting transmission of signals. The signals transmitted regulate cellular activities, such as migration, differentiation, proliferation and gene expression. These polypeptides elicit cellular action by binding to specific cellular receptors present on the surface of target cells that initiate a cascade of biological events to stimulate the regenerative process [48-52]. Cytokines are molecules secreted by immune cells to act on damaged or infected tissue. For cartilage regenerative process it has been shown that there are several essential GFs and cytokines that provide regulatory effects

on chondrocytes or stem cells involved in chondrocytes maturation and cartilage formation [50-57]. The GFs and cytokines for cartilage applications include: TGF- β superfamily, IGF, FGF, BMP, platelet derived growth factor (PDGF), epidermal growth factor (EGF), interleukins (ILs) and tumor necrosis factor (TNF- α) (Table I-1).

Table I-1: Regulatory effects of GFs and cytokines in articular cartilage

GFs and cytokines	Function
TGF-β superfamily	Increase proteoglycans synthesis (TGF- β 1); Prevent ECM degradation (TGF- β 1); Induce inhibition of matrix metalloproteinase(MMP) (TGF- β 1); Stimulate chondrogenic differentiation of progenitor cells (TGF- β 1), chondrocyte proliferation (TGF- β 1) and maturation (TGF- β 3); Induce chemotaxis of inflammatory cells [36, 50, 58].
IGF - 1	Promote chondrocyte proliferation; Prevent apoptosis; Induce chondrogenic differentiation of progenitor cells; Stimulate chondrocyte proliferation; Prevent ECM degradation (inhibition of MMP) [36, 48, 59].
FGF	Promote chondrocyte proliferation; Stimulate deoxyribonucleic acid (DNA) and ribonucleic acids (RNA) synthesis; Promote ossification; Induce chemotaxis of inflammatory cells; Stimulate MMP and matrix degradation; Augment neovascularization [4, 36, 40, 51].
BMP	Stimulate prechondrogenic condensation and differentiation into chondrocytes (BMP-2, 4, 5, 6, 7); Induce the matrix synthesis (BMP-2, 4, 6, and 7) and sometimes degradation (BMP-2); Promote ossification (BMP-2) [4, 36, 40, 51].
PDGF	Up-regulated the number of IL-1 per chondrocytes growth and differentiation of MSCs; Stimulate MMP and ECM degradation; Promote ossification [4, 36, 40, 51].
EGF	Induce chondrocytes proliferation; Induce matrix degradation [51].
ILs	Induce MMP inhibition (IL-4, 6) and stimulation (IL-1 β , 17, 18); Induce matrix degradation (IL-1 β , 18) [4, 36, 40, 51].
TNF-α	Stimulate MMP and matrix degradation [4, 36, 40, 51].

The mechanical factors applied to cartilage cultured *in vitro* may affect the synthesis and organization of components of articular cartilage. These factors stimuli cellular functions and may be transmitted to cells by forces affecting the cellular microenvironment. The mechanical factors normally applied are: oxygen tension and mechanical loading (deformation, hydrostatic pressure, fluid flow, shear stress and dynamic compression) [4, 5, 56].

I-6.1. Scaffold requirements for cartilage tissue engineering

Scaffolds provide the 3D environment that guides the differentiation and the development of the cartilaginous tissue. Such constructs should be designed with the adequate mechanical and physical-chemical characteristics, in order to mimic the native ECM structure and function [60-62]. As a result a number of requirements are necessary to be full filled and illustrated on Table I-2.

Table I-2: Scaffolds requirement for TE.

Scaffold Requirements	Biological and material basis
Porosity	Promote the integration of cells into the scaffolds which allow them to generate their own ECM; Enhance implant fixation; Affect mechanical properties [60, 61, 63].
Pore size	Affect cell infiltration, migration and distribution; Improve ECM deposition and distribution [61, 64, 65].
Interconnectivity	Promotes cell migration throughout all the volume of the construct; Influence the diffusion of physiological nutrients and gases to cells and the removal of metabolic waste from cells [60, 61, 64].
Surface characteristics (topography, chemistry, surface energy or wettability)	Affect protein adsorption and cell adhesion; Increase the interaction with the surrounding environment; Control cell migration, phenotype maintenance and intracellular signalling; Improve the recruitment of cells and the healing at the tissue-scaffold interface [66-69].
Biocompatibility	Prevents inflammatory or immunologic reactions that comprise the host tissue; Support cell adhesion and proliferation [60, 70].
Appropriate mechanical properties	Prevent leakage or extrusion after implantation; Support mechanical loading; Provide the correct stress environment for the neo-tissue [71].
Structural anisotropy	Promotes native anisotropic tissue structure [60, 72].
Cell adhesiveness	Improve cell seeding for delivery and retention of cells; Promote maintenance of chondrogenic phenotype [60].
Bioactivity	Act as delivery vehicles for biologics included: cells, genes, peptides and GFs [73].
Controlled degradation rate	Promote new tissue ingrowth and remodelling of the ECM; Match healing of new tissue assuring the initial strength of the scaffold [67, 74].
Geometry and architecture	Support 3D tissue growth; Control the morphological of the growing tissue; Support cell proliferation and differentiation [75].

Ideally, scaffold should fulfill, a serie of requirements (Table I-2) to promote matrix synthesis and optimal chondrocytes homing. The ability of scaffold to bond and integrate with native tissue is critical for obtain an homogeneous and functional repair [76].

Among the scaffolds requirements the porous network is a driving parameter in their design because is intimately connected to their mechanical properties (e.g: an increase in porosity results in a more flexible structure). The scaffolds should ideally mimic the mechanical properties of the native tissue. However this can result in a scaffold with low porosity and a decrease in nutrients diffusion, which can lead to possible necrosis. As a result, a balance between mechanical properties and porosity must be found. [67, 70, 76].

A wide range of scaffolds were already used, such as hydrogels, sponges, membranes, foams, fibrous meshes (microfiber and nanofiber-biomimetic the ECM, agglomerate particles, microspheres or composite of these materials [70, 77-83]. For all these scaffolds macro and micro-structural properties affect the cell survival, signaling growth, propagation and reorganization [35, 65]. So far none currently available scaffolds fulfill all of the requirements and consequently a highly variable effects were already related in the growth, differentiation and maintenance of cells [36].

I-7. SCAFFOLD PROCESSING TECHNIQUES FOR CARTILAGE APPLICATIONS

Scaffolds are central element to TE strategies and a wide range of fabrication technologies have been developed to prepare them. Manufacturing processes should assure a high level of control over macro and micro-structural properties [84-86].

The different technologies used in scaffolds production dictates the type of structure and also affects some characteristics such as: mechanical properties, degradation behaviour, biocompatibility and surface properties [84-86]. The techniques normally used for scaffold production in TE approaches are presented in Table I-3 and Table I-4.

Table I-3: Overview of techniques to prepare scaffolds for TE

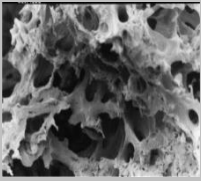
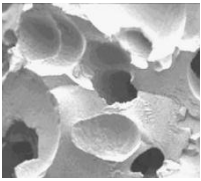
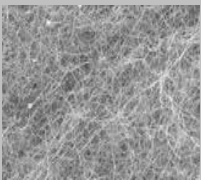

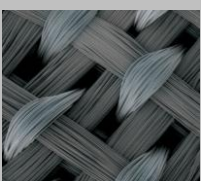
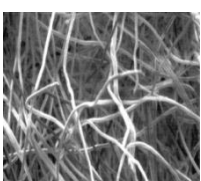
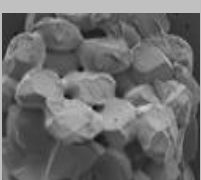
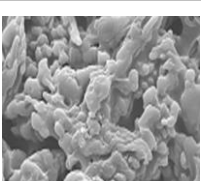
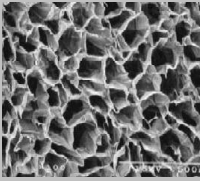
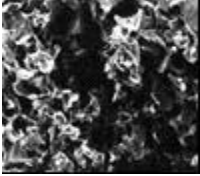
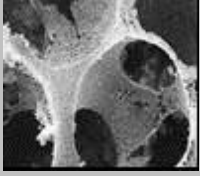
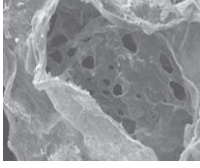
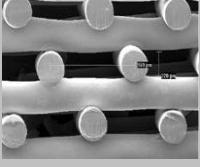
Technique		Characteristics
Melt based process: Compression moulding, injection moulding and extrusion		Production of complex 3D shapes; High reproducibility; High-throughput; Difficult to control porosity and pore size; Difficult to obtain high porosities and interconnectivities [87, 88].
Solvent casting and particle leaching		Very simple method; High porous structure; High surface area-to-volume ratios; Interconnectivity can be prevented; Easily and independent control of porosity and pore size; Solvent is often toxic and is not always possible to assure total removal [84, 89].
Electrospinning		Generate fibers that mimic the nanometer scale of fiber that compose ECM; Combine nano and micro fibers; Enhancement of surface area; Difficult for cell proliferate towards the interior of scaffolds [90, 91].
Fiber bonding		Large surface area for control cell attachment; Good interconnectivity among pores; Difficult to control porosity; Increase the mechanical properties of scaffolds when compared with the non-woven technologies [84, 85, 92, 93].
Woven fabric: Braiding and Knitting.		Insufficient mechanical properties [19, 94, 95].
Non-woven fabric		High porosity; Insufficient mechanical properties [19].
Precipitation and particle aggregation		High adhesion between particles; High interconnectivity; Obtain scaffolds with mean pores varying between 100 to 400 μm ; Possible release of GF; Porosity can be easily controlled by microsphere diameter; Low porosity [96].
Supercritical fluid technology: Gas foaming, gas foaming + particle leaching and phase inversion		Obtain dry porous structures without residual solvent; High porosity; Partially interconnected pores; Highly pure materials ideal for medical application; Only few types of polymers can be used; Low solubility of proteins in SCO_2 ; Avoid high temperature and organic solvent, allowing to incorporate the incorporation of bioactive agents [97-99].

Table I-4: Overview of techniques to prepare scaffolds for TE (continuation)

Technique	Characteristics
Freeze drying	 <p>Simplicity of operation; Large porosity (91-95 %); Small median pore size (13-35 μm); Usually low interconnectivities; Difficulty ensure structural stability and adequate mechanical properties after subsequent hydration [100, 101].</p>
Membrane lamination	 <p>Irregular pore size; Tedious process [102].</p>
Hydrocarbon templating	 <p>Allows incorporation of proteins; Control over interconnectivity [103].</p>
Layer by layer (LbL) methodology	 <p>Generally associated with surface modification; Allows a production of a porous structure with highly interconnectivity [104, 105].</p>
Rapid Prototyping and its subdivision	 <p>More precision than the conventional techniques; Ability to produce complex shaped objects; incorporation of GF is possibly; Well-defined internal and external architecture; Porosity is low; Mechanical properties need to be improved [8, 106].</p>

I-7.1. Layer-by-layer methodology

The design of a thin solid film at the molecular level has been first reported in 20th century and two techniques dominated this field: Langmuir-Blodgett (LB) and self-assembled monolayers (SAMs). However, both present some drawbacks, which limited their application in biological field as represented in Figure I-5 [104].

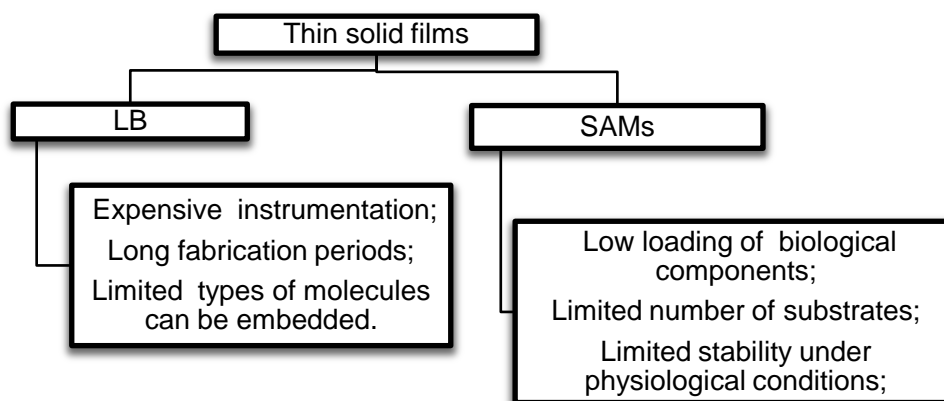


Figure I-5: Schematic representation of drawbacks associated with LB and SAMs [adapted from [104, 107]].

A new technology called layer-by-layer, LbL, was developed by *Decher* and co-workers in 1992. LbL emerged as a simple technique to build films on a solid substrate with precise control of thickness and surface charge. As a result in comparison with LB technique, LbL is more simple and faster and result in more stable films while in comparison with SAM allows higher loadings of biological interesting species [104, 107-109].

LbL consists in alternately deposition of polyanions and polycations or bipolar amphiphiles that self-assembled and self-organize on the material surface leading to the formation of polyelectrolyte multilayer films (PEMs). The deposition of PEMs by LbL has emerged as promising technique because only requires a charged substrate and allows the functionalization of it. The substrate can range from planar to non-planar templates, such as colloids or microcapsules [110-114].

The driving forces of this process include electrostatic as well as non-electrostatic interactions, namely: hydrophobic interactions, *van der Waals* forces and charge transfer [115-117]. This technique is not only applicable for polyelectrolyte/ polyelectrolyte systems, but it can be expanded to almost any type of charged species, including inorganic molecules clusters, nanoparticles, nanotubes, nanowires, nanoplates, organic dyes, dendrimers, porphyrins, biological polysaccharides, polypeptides, RNA and DNA, proteins and viruses [104].

LbL have been applied in various areas including TE such as in biomimetic coatings, drug delivery, protein adsorption, bioactive coatings, biosensors and the coating of living cells [104, 117-124].

I-7.1.1. Parameters

LbL methodology allow the production of tuned PEMs by varying several parameters, as represented in Table I-5 [114].

Table I-5: Examples of parameters varied in LbL technique and their influence on final structure of film

Parameters	Influence on final structure
Decrease of ionic strength	Decrease of mass deposition, swelling, smoothing and stiffness [116, 125].
Decrease of molecular weight	Influence the viscoelastic properties; Increase of the thickness; Increase the diffusion [112, 116, 125].
Increase of number of layers	Increase the thickness of the film and mechanical properties [124, 126].
Composition	Influence physic-chemical, mechanical properties and biological properties [104, 114].
Increase of charge density	Decrease of thickness; Increase the ion pairing [112].
pH	Affect the porosity, roughness and thickness [114, 127].
Sterical and thermodynamical parameters	Limited the diffusion ability [117].
Strength of polyelectrolytes	Decrease the hydration and thickness of layers[128].
Hydrophilicity of polyelectrolytes	Affect the swelling ability and thickness.
Increase of ion pairing	Increase stiffness; Decrease mobility, degradation rate and swelling ability [128].
Increase of film hydration	Increase the delivery of active compounds [117].
Cross-link	Increase the mechanical properties [129].
Terminal layer	Affect biological properties such as cellular behaviour and the surface energy [104, 114, 117].
Increase of Temperature	The exponential growth becomes dominant [117].
Topography: Roughness; Presence of microstructures.	Affect cellular adhesion [130].

LbL normally is used as a technique for surface modification, production of microcapsules and reservoirs for loading bioactive molecules. However, in 2011 *Praveen et al.* developed a technology for produced nanostructured 3D constructs combining LbL technology and 3D template leaching [105]. This thesis will mainly focus on such methodology in order to produce highly porous aimed to be used in cartilage TE.

I-8. POLYMERIC MATERIAL USED IN ARTICULAR CARTILAGE TISSUE ENGINEERING

The selection of material for scaffolds still remains a fundamental key for the design and development of tissue engineering constructs. A wide variety of materials, both synthetic and natural, have been used in cartilage application taking account the need of avoiding any adverse foreign host response (Table I-6) [67, 131, 132]. As a result, the scaffold can be natural, synthetic or hybrid (natural and synthetic).

Table I-6: Materials already used for articular cartilage TE

Categories of biomaterials		Polymers used
Natural polymers	Synthetic polymers	Carbon fibers [3]; Poly (ethylene glycol) (PEG) [5]; Poly (vinyl alcohol) (PVA) [133]; Poly (L-lactic acid) (PLLA) [5, 42]; Poly (D-lactic acid) (PDLA) [5, 42]; Poly (D,L-lactic acid) (PDLLA) [5, 42]; Poly (butyl acrylate) (PBA) [54]; Poly (methyl methacrylate) (PMMA) [134]; Poly (ethyl methacrylate) (PEMA) [42]; Poly (ethylene) (PE) [135]; Poly (tetrafluoroethylene) (PTFE) [42]; Poly (ϵ -caprolactone) (PCL) [75]; Poly (urethane) (PU) [42]; Poly (N-isopropylacrylamide) (PNiPAAM) [4]; Poly (glycol acid) (PGA) [54]; Poly (ethylene glycol/oxide) (PEO); Poly (lactic-co-glycolic acid) (PLGA) [42]; Poly (ethylene) (PET) [54]; Poly (propylene fumarate) (PPF) [136]; Poly (butylene terephthalate) (PBT) [135].
	Protein-based materials	Fibrin [5, 42, 133]; Laminin [5, 42, 133]; Gelatin [5, 42, 133]; Collagen [5, 42, 133]; Silk fibroin [4].
	Polysaccharide-based materials	Hyaluronic acid [42, 137]; Chitosan [138]; Agarose [42, 133]. Alginate [42, 133]; Cellulose [42, 133]; chondroitin sulphate [139]; Dermatan sulphate [140], Gellam gum [141].
	Bacterial polyesters	PHA (Poly (hydroxyalkanoate)):Poly (3-hydroxybutyrate-co-3-hydroxyvaluate) (PHBV) [142]; Poly (hydroxybutyrate) (PHB) [143].

I-8.1. Synthetic polymers

Synthetic polymers have been widely used for TE because they are more controllable and predictable than naturally derived polymers, whereas chemical and physical properties of the polymer can be tailored to match specific mechanical and degradation characteristics [4, 48]. Moreover, risks like toxicity, immunogenicity and infection are much lower for pure synthetic polymers. However, they have a lack of biological cues because these materials do not benefit from direct cell-scaffold interactions that could promote the desired cell response. In addition, some degradation products may be toxic or elicit an inflammatory response due to their accumulation and decrease of local pH derived of acidic products [48, 144].

I-8.2. Natural polymers

The growing interests in natural-based polymers relies on their economic and environmental aspects, as well as biocompatibility, biodegradability, low toxicity, low manufacture costs, low disposal costs and renewability [48, 145]. In addition, these polymers offer the advantage of being similar to biological macromolecules providing biological signalling, cell adhesion, cell responsive degradation and re-modelling [146-149]. Living organisms are able to synthesize natural polymers during the growth cycles. The synthesis is typically formed within cells by complex metabolic processes, generally included enzyme-catalysed, chain growth polymerization reactions of activated monomers. Natural polymers can be divided into three major classes: polysaccharides, proteins and bacterial polyesters, such as PHAs (PHB and PHBV) [34, 145, 148].

Polysaccharides derive from virtually any renewable resources, namely wood, plants, animals and microorganisms. Biochemically, these materials consist of monosaccharides linked by O-glycosidic linkages [34, 145, 148]. They may be linear or branched, and may have single or mixed linkage between monosaccharides units. Differences between the monosaccharides, linkage types, chain shapes and molecular weight, dictate their physical properties, such as solubility, gelation capability and surface properties. The interest of polysaccharides as a material used for TE are related with non-toxicity, renewability, water solubility, stability to pH variations and their capacity to be chemically modified in order to achieve high swelling in water. However, they have low mechanical, thermal and chemical stability. They also cannot be processed alone using melt-base techniques and are usually shaped by solvent-based methodologies. Natural-based polymers may

be combined with synthetic polymers to be processed using extrusion, injection moulding and compression moulding [34, 145, 146, 148, 150].

I-8.2.1. Chitosan

Among naturally derived polymers, chitin is one of the most abundant natural polymer that can be found in shells from crustaceans, cuticles insects and cell walls of fungi. The most important derivative of it is chitosan [151, 152]. Chitosan has been found as an excellent candidate in a broad spectrum of TE applications due to its characteristics, namely, biocompatibility, biodegradability, non-toxicity, remarkable affinity to proteins, along antitumoral, antibacterial, anticholesteremic, fungistatic and haemostatic properties [153-155]. This polysaccharide is obtained by a partial deacetylation of chitin under alkaline treatment (concentrated sodium hydroxide - NaOH) or by enzymatic hydrolysis in the presence of chitin deacetylase (Figure I-6) [138, 153, 155].

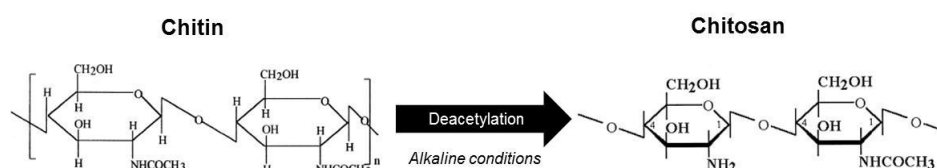


Figure I-6: Chemical structure of chitin and chitosan[adapted from [138].

Chitosan in solid state is a semicrystalline polymer with a high elastic modulus in the dry state owing to the high glass transition temperature [156, 157]. Structurally is a linear copolymer composed of glucosamine (deacetylated unit) and N -acetyl glucosamine (acetylated unit) units linked by β (1 \rightarrow 4) glycosidic bonds and it is normally insoluble in aqueous solutions above pH=7. However, in dilute acids (pH below 6), the free amine groups are protonated and the molecule becomes soluble [158-160]. Generally, chitosan has three types of reactive functional groups, an amino group (C [2] position), a primary (C [3] position) and secondary (C [6] position) hydroxyl groups. These groups allow modifications, such as covalent ionic or graft copolymerization, which is very useful for TE applications [153, 155, 161].

The degree of deacetylation (DD) measures the ratio between glucosamine and N-acetyl glucosamine in polymeric chains. Depending on the source and preparation procedure, chitosan molecular weight may range from 300 to over 1000 kDa with a DD from 30 % to 95 % [155, 162].

The DD influences physicochemical properties, such as solubility, crystallinity, biodegradability, swelling behaviour and biological properties [155, 162, 163]. The degradation of chitosan in human body has been reported to be carried out by enzymatic hydrolysis with lysozyme. Lysozyme is a primary enzyme responsible for *in vivo* degradation of chitosan which appear to target acetylated residues [138, 164]. Studies have demonstrated that chitosan and its degraded products are involved in the synthesis of the articular components, including chondroitin sulphate, dermatan sulphate, hyaluronic acid, keratan sulphate, and type II collagen [165]. The degradation kinetic of this material appears to be inversely related to DD, as it occurs for crystallinity [47, 163, 164].

For articular cartilage TE the ideal cell-carrier substance should mimic the natural environment in the articular cartilage ECM [166]. Most of the potential of chitosan for this application is its structural similarity with cartilage-specific ECM components such as GAGs [47, 138]. Moreover, chitosan cationic nature and high charge density in solution allows electrostatic interactions with anionic species, such as GAGs and proteoglycans [47, 138, 156]. Consequently, numerous studies *in vitro* and *in vivo* have been demonstrated a positive influence of chitosan on chondrocyte behaviour. *In vitro* studies developed by *Malafaya et al.* showed that human adipose derived MSCs seeded onto chitosan particles agglomerated scaffolds had a capacity to differentiate the chondrogenic lineage [78]. *In vivo* performance of chitosan-glycerophosphate gels were evaluated by *Chenite et al.* by mixing them with primary culture bovine chondrocytes (bch) and implanting subcutaneously in athymic mice. The implant area revealed several areas of remodelling chondrocytes secreting a matrix characteristic of normal cartilage [167]. *Lu et al.* has also demonstrated that chitosan solution injected into the knee articular cavity of rats led to significant increase in chondrocytes density [168]. *Mattioli-Belmonte et al.* showed that BMP-7 associated with N-dicarboxylmethyl chitosan induces or facilitates the repair of articular cartilage lesions in rabbits [169].

I-8.2.2. Chondroitin sulphate

Chondroitin sulphate is a linear, complex, sulphated unbranched polysaccharide belonging to the class of macromolecules known as GAGs [170-173]. It is composed of repeating disaccharide units of D-glucuronic acid and N-acetylgalactosamine linked by β -(1 \rightarrow 3) bonds. Like other natural polysaccharides, chondroitin sulphate derives from animal sources by extraction and purification

processes [170]. The animal sources generally used are chicken, porcine, bovine and cartilaginous fish such as sharks and skate [170, 174]. As a result chondroitin sulphate is a heterogeneous polysaccharide in terms of charge densities due to sulphate groups in varying amounts and linked in different positions, molecular masses, polydispersity, chemical properties, biological and pharmacological activities [175, 176].

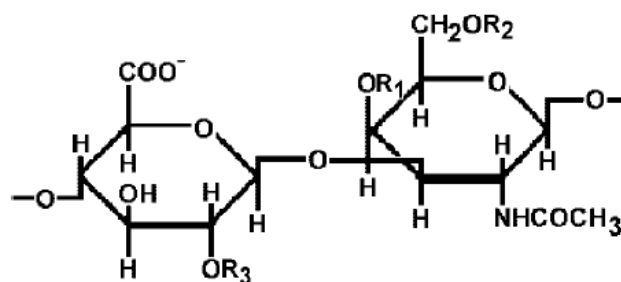


Figure I-7: Structures of disaccharides forming chondroitin sulphate. Different groups on R1, R2 and R3 give rise to different types of CS: R1=R2=R3=H non-sulphated chondroitin, R1=[SO₃⁻] and R2=R3=H chondroitin-4-sulphate; R2=[SO₃⁻] and R1=R3=H chondroitin-6-sulphate; R2=R3=[SO₃⁻] and R1=H chondroitin-2,6-disulphate; R1=R2=[SO₃⁻] and R3=H chondroitin-4,6-disulphate; R1=R3=[SO₃⁻] and R2=H chondroitin-2,4-disulphate; R1=R2=R3=[SO₃⁻] trisulphated chondroitin [175].

For cartilaginous tissues, this molecule (chondroitin-4-sulphate and chondroitin-6-sulphate) is an important structural component [177-180]. The tightly packed and highly charged sulphate groups of chondroitin sulphate generate electrostatic repulsion that provides much of the resistance of cartilage to compression and also cooperates in the shock absorbing capacity of aggrecans [47, 181]. Consequently, this polysaccharide with anionic nature enables efficient interaction with cationic molecules to form interesting structures [182, 183]. However, the major drawback of chondroitin sulphate is the high solubility in water, which limits its use alone in the solid state for biomedical applications, being frequently cross-linked or combined with other polymers, such as chitosan, hyaluronic acid, PVA, PLGA, PLLA, PCL, collagen, cellulose and gelatin [47, 177, 184-188]

Chondroitin sulphate is currently used as an ingredient in dietary supplements with the ultimate goal of relieving some of the pain and disability of patients with musculoskeletal pathologies, namely osteoarthritis [186, 189]. The benefits of chondroitin sulphate for the treatment of osteoarthritis are related with the stimulation of ECM production by chondrocytes, suppression of inflammatory mediators and inhibition of cartilage degeneration [190]. Thus, due to its nature, chondroitin sulphate has been used in the development of supports for cartilage TE

applications due to its chondroprotective ability and increased ECM synthesis [47, 191]. A number of recent studies have reported that chondroitin sulphate stimulates proliferation and matrix component production of seeded chondrocytes in collagen-GAG matrices *in vitro* [139, 192, 193]. *Yan et al.* reported *in vitro* and *in vivo* studies of a tri-copolymer matrix (collagen-chondroitin sulphate-chitosan). *In vitro* studies showed that chondrocytes adhered to the scaffold, where they proliferated and secreted ECM, filling the space within the scaffold. *In vivo* studies performed with subcutaneous implantation in nude mice demonstrated a homogeneous cartilaginous tissue similar to those of natural cartilage, when chondrocytes were seeded in collagen-chondroitin sulphate-chitosan matrix after implant of 12 weeks [194]. Collagen-GAG matrices were also used as a reservoir to GFs, namely IGF-I, and this combination demonstrate the increase of proteoglycan production *in vitro*. [195]. *Fan et al.* used PLGA–gelatin-chondroitin sulphate-hyaluronate hybrid scaffold and showed their capacity to induce differentiation of MSCs cells [196]. This material was also used in LbL methodology as polyanion and according to *Gong et al.* LbL assembly of chondroitin sulphate and collagen on aminolyzed PLLA porous scaffolds enhances their chondrogenesis [197].

I-8.2.3. Combination of chitosan and chondroitin sulphate

Several studies reported the combination between chitosan and chondroitin sulphate in various areas of TE, such as controlled release of drugs, conventional scaffolds, and surface modification with techniques like LbL methodology [47, 198-200]. Chitosan and chondroitin sulphate have analogous structures and this suggest that chitosan also can have specific interactions with GFs, receptors and adhesion proteins. However chitosan has poor mechanical strength limiting its application as biomaterial. Consequently combinations between this material and others became recurrent [191, 199, 201]. The combination with chondroitin sulphate occurs due to ionic interactions between the positively charged of chitosan and negatively charged of chondroitin sulphate. In 1976 this combination was called a film-like complex, due to their electrostatic interactions [202]. According to *Denuziere et al.* chitosan when associated with various polyelectrolytes has a protective effect against GAGs hydrolysis by their specific enzymes [191, 202].

For cartilage TE, the combination of chitosan with other materials, namely GAGs, reveals determinant due to the lack of other bioactive ECM components. The use of GAGs enhances the

chondrocytes differentiation and tissue formation. Chondroitin sulphate has been reported as beneficial to chondrocytes because it has chondroprotective ability and stimulate ECM synthesis [191, 201]. As a result the combination between this material and chitosan, according to *Yuan et al.*, enhance the hydrophilicity, biological compatibility and mechanical strength [201]. *Sechriest et al.* produced a chondroitin sulphate-chitosan support for chondrogenesis where bovine articular chondrocytes were seeded. The results show that chondrocytes establish focal adhesions maintaining a phenotype of differentiated chondrocytes with collagen type II and proteoglycan production [203]. *Chen et al.* also related that the use of composite chondroitin-6-sulphate-dermatan sulphate-chitosan scaffolds for cartilage TE is beneficial for ECM production [140].

I-9. CONCLUSION AND FUTURE PERSPECTIVES

Cartilage diseases generally derived from joint and systemic disorders affect millions of people worldwide with economic impact in the healthcare system. The scarcity of treatment modalities has motivated attempts for the cartilage TE approaches that can meet the functional demands of this tissue *in vivo* [31, 204]. Cartilage TE has key elements like cells, scaffolds and microenvironmental factors that can be used together or alone [9, 14, 35]. Each one of these elements is continuously being developed to achieve an adequate compromise between known biomaterials chemistry and structure as well as cell source, mechanical loadings, bioreactors and stimulation factors [4, 5, 7].

Despite the number of patented and applying products for FDA approval, extensive research will be needed to determine whether the results can be extended to the human situations. Thus, the goal of investigators working on this field is to develop a system with ability to promote the production of cartilage tissue and mimics native tissue properties, accelerating the restoration of this tissue function and its clinically applicability [7]. This is an ambitious goal, but significant progress and important advances have been made in recent years.

I-10. REFERENCES

1. Fox, A., A. Bedi, and A. Rodeo, *The Basic Science of Articular Cartilage: Structure, Composition and Function*. Sports Health, 2011. **1**: p. 461-468.
2. Fritz, J., et al., *Articular cartilage defects in the knee--Basics, therapies and results*. Injury, 2008. **39**(1, Supplement 1): p. 50-57.
3. Hunziker, E.B., *Articular cartilage repair: basic science and clinical progress. A review of the current status and prospects*. Osteoarthritis and Cartilage, 2001. **10**: p. 432-463.
4. Chung, C. and J.A. Burdick, *Engineering cartilage tissue*. Advanced Drug Delivery Reviews, 2008. **60**(2): p. 243-262.
5. Vinatier, C., et al., *Cartilage engineering: a crucial combination of cells, biomaterials and biofactors*. Trends in biotechnology, 2009. **27**(5): p. 307-314.
6. Klein, T., et al., *Tissue Engineering of Articular Cartilage with Biomimetic Zones*. Tissue Engineering part B., 2009. **15**: p. 143-157.
7. Cascio, B. and B. Sharma, *The Future of Cartilage Repair*. Oper Tech Sports Med., 2008. **16**: p. 221-224.
8. Woodfield, T.B.F., et al., *Design of porous scaffolds for cartilage tissue engineering using a three-dimensional fiber-deposition technique*. Biomaterials, 2004. **25**(18): p. 4149-4161.
9. Mandelbaum, B., et al., *Articular cartilage lesions of the knee*. The American Journal of Sports Medicine, 2011. **10**: p. 853-861.
10. Benz, K., et al., *Molecular analysis of expansion, differentiation, and growth factor treatment of human chondrocytes identifies differentiation markers and growth-related genes*. Biochemical and Biophysical Research Communications, 2002. **293**(1): p. 284-292.
11. Chang, C., A. Lauffenburger, and T. Morales, *Motile chondrocytes from newborn calf: migration properties and synthesis of collagen II*. OsteoArthritis and Cartilage, 2003. **11**: p. 603-612.
12. Tallheden, T., C. Karlsson, and A. Brunner, *Gene expression during redifferentiation of human articular chondrocytes*. OsteoArthritis and Cartilage, 2004. **12**: p. 525-535.
13. Buckwalter, J. and H. Mankin, *Institutional Course Lectures. The American Academy of orthopedic surgeons- Articular cartilage Part I: Tissue Design and chondrocytes-Matrix interactions*. 1997. **4**: p. 600-611.
14. LeBaron, R.G. and K.A. Athanasiou, *Ex vivo synthesis of articular cartilage*. Biomaterials, 2000. **21**(24): p. 2575-2587.
15. Temenoff, J. and A. Mikos, *Review: Tissue engineering for regeneration of articular cartilage*. Biomaterials, 2000. **21**: p. 431-440.
16. Lyu, S., W. Wuc, and C.e.a. Hou, *Study of cryopreservation of articular chondrocytes using the Taguchi method*. 2010. **60**: p. 165–176.
17. Athanasiou, K.A., E.M. Darling, and J.C. Hu, *Articular Cartilage Tissue Engineering* 2009: Morgan & Claypool.
18. Hayes, A., et al., *Macromolecular organization and in vitro growth characteristics of scaffold-free neocartilage grafts*. Journal of histochemistry&cytochemistry, 2011. **55**: p. 853-866.
19. Blitterswijk, C.A. and P. Thomsen, *Tissue engineering* 2008: Academic.
20. Heng, B., T. Cao, and E. Lee, *Directing stem cell differentiation into the chondrogenic lineage in vitro*. Stem cells, 2004. **22**: p. 1152-1167.
21. Zhao, X., S. Yu, and S. Wu, *Transfection of primary chondrocytes using chitosan-pEGFP nanoparticles* Journal of Controlled Release. , 2006. **112**: p. 223-228.
22. Baia, X., et al., *Cartilage-derived morphogenetic protein-1 promotes the differentiation of mesenchymal stem cells into chondrocytes*. Biochemical and Biophysical Research Communications, 2004., **325**: p. 453–464.
23. Wang, H. and R. Kandel, *Chondrocytes attach to hyaline or calcified cartilage and bone*. OsteoArthritis and Cartilage, 2004. **12**: p. 56-64.
24. Marijnissen, W., G. Van Osch, and J. Aigner, *Tissue-engineered cartilage using serially passaged articular chondrocytes. Chondrocytes in alginate, combined in vivo with a synthetic (E210) or biologic biodegradable carrier (DBM)*. Biomaterials, 2000. **21**: p. 571-580.
25. Elder, B., E. Kyriacos, and A. Athanasiou, *Extraction techniques for the decellularization of tissue engineered articular cartilage constructs*. Biomaterials, 2009. **30**: p. 3749-3756.

26. Kheir, E. and D. Shaw, *Management of articular cartilage defects*. Orthopaedics and Trauma, 2009. **23**: p. 266-273.
27. Temenoff, J.S. and A.G. Mikos, *Review: tissue engineering for regeneration of articular cartilage*. Biomaterials, 2000. **21**(5): p. 431-440.
28. Redman, S., S. Oldfield, and C. Archer, *Current strategies for articular cartilage repair*. European cells and materials, 2005. **9**: p. 23-32.
29. Katta, J., Z. Jin, and E. Ingham, *Biotribology of articular cartilage—A review of the recent advances*. Medical Engineering & Physics., 2008. **30**: p. 1349–1363.
30. Strehl, R., et al., *Long-term maintenance of human articular cartilage in culture for biomaterial testing*. Biomaterials, 2005. **26**(22): p. 4540-4549.
31. Cancedda, R., B. Dozina, and P. Giannonia, *Tissue engineering and cell therapy of cartilage and bone*. Matrix Biology, 2003. **22**: p. 81-91.
32. Bobic, V. and J. Noble, *Articular cartilage, to repair or not to repair*. J Bone Joint Surg Br, 2000. **82**: p. 165-166.
33. Khademhosseini, A., et al., *Microscale technologies for tissue engineering and biology*. PNAS, 2006. **103**: p. 2480–2487.
34. Kim, B.-S., et al., *Design of artificial extracellular matrices for tissue engineering*. Progress in Polymer Science, 2010. **In Press, Corrected Proof**.
35. Stevens, M.M. and J.H. George, *Exploring and Engineering the cell surface Interface*. Science, 2005. **3**: p. 1135-1138.
36. Chen, F.H., K.T. Rousche, and R.S. Tuan, *Technology Insight: adult stem cells in cartilage regeneration and tissue engineering*. Nat Clin Pract Rheum, 2006. **2**(7): p. 373-382.
37. Lia, W., R. Tulia, and C. Okafor, *A three-dimensional nanofibrous scaffold for cartilage tissue engineering using human mesenchymal stem cells*. Biomaterials, 2005. **26**: p. 599–609.
38. Schulze-Tanzil, G., *Activation and dedifferentiation of chondrocytes: Implications in cartilage injury and repair*. Annals of Anatomy, 2009. **191**: p. 325-338
39. Dausse, Y., L. Grossin, and G.e.a. Miralles, *Cartilage repair using new polysaccharidic biomaterials: macroscopic, histological and biochemical approaches in a rat model of cartilage defect*. Osteoarthritis and Cartilage, 2003. **11**: p. 16.28.
40. Heng, B., C. Tong, and C. Lee, *Directing stem cell differentiation into the chondrogenic lineage in vitro*. Stem Cells, 2004. **22**: p. 1152-1167.
41. Saraf, A. and A. Mikos, *Gene delivery strategies for cartilage tissue engineering*. Advanced Drug Delivery Reviews., 2006. **58**: p. 592-603.
42. Merceron, C., et al., *Adipose-derived mesenchymal stem cells and biomaterials for cartilage tissue engineering*. Joint Bone Spine, 2008. **75**(6): p. 672-674.
43. Hollander, A., S. Dickinson, and W. Kafinenah, *Stem Cells and cartilage development: Complexities of a simple tissue*. Stem Cells, 2010. **28**: p. 1992-1996.
44. Chen, F. and R. Tuan, *Adult Stem Cells for Cartilage Tissue Engineering and Regeneration*. Current Rheumatology Reviews., 2008. **4**: p. 161-170.
45. Varghese, J., et al., *Chondroitin sulfate based niches for chondrogenic differentiation of mesenchymal stem cells*. Matrix Biology, 2008. **27**: p. 12-21.
46. Chen, W., et al., *Compare the effects of chondrogenesis by culture of human mesenchymal stem cells with various type of the chondroitin sulfate C*. Journal of bioscience and bioengineering, 2011. **11**: p. 226-231.
47. Malafaya, P.B., G.A. Silva, and R.L. Reis, *Natural-origin polymers as carriers and scaffolds for biomolecules and cell delivery in tissue engineering applications*. Advanced Drug Delivery Reviews, 2007. **59**(4-5): p. 207-233.
48. Quaglia, F., *Bioinspired tissue engineering: The great promise of protein delivery technologies*. International Journal of Pharmaceutics, 2008. **364**(2): p. 281-297.
49. Holland, T.A. and A.G. Mikos, *Advances in drug delivery for articular cartilage*. Journal of Controlled Release, 2003. **86**(1): p. 1-14.
50. Zhang, S. and U. Hasan, *Nanoparticulate Systems for Growth Factor Delivery*. Pharmaceutical Research., 2009. **26**: p. 1561-1580.
51. Lee, S. and H. Shin, *Matrices and scaffolds for delivery of bioactive molecules in bone and cartilage tissue engineering*. Advanced Drug Delivery Reviews, 2007. **59**: p. 3393-33959.
52. Sokolsky-Papkov, M., K. Agashi, and A.e.a. Olaye, *Polymer carriers for drug delivery in tissue engineering*. . Advanced Drug Delivery Reviews, 2007. **59**: p. 181-206.

53. Biondi, M., et al., *Controlled drug delivery in tissue engineering*. Advanced Drug Delivery Reviews, 2008. **60**(2): p. 229-242.
54. Chen, R.R. and D.J. Mooney, *Polymeric Growth Factor Delivery Strategies for Tissue Engineering*. Pharmaceutical Research, 2003. **20**(8): p. 1103-1112.
55. Saraf, A. and A.G. Mikos, *Gene delivery strategies for cartilage tissue engineering*. Advanced Drug Delivery Reviews, 2006. **58**(4): p. 592-603.
56. Tabata, Y., *The importance of drug delivery systems in tissue engineering*. Pharmaceutical Science & Technology Today, 2000. **3**(3): p. 80-89.
57. Willerth, S.M., A. Rader, and S.E. Sakiyama-Elbert, *The effect of controlled growth factor delivery on embryonic stem cell differentiation inside fibrin scaffolds*. Stem Cell Research, 2008. **1**(3): p. 205-218.
58. Ragetly, G.R., et al., *Effect of chitosan scaffold microstructure on mesenchymal stem cell chondrogenesis*. Acta Biomaterialia, 2010. **6**(4): p. 1430-1436.
59. Derfoul, A., A. Miyoshi, and B.e.a. Freeman, *Glucosamine promotes chondrogenic phenotype in both chondrocytes and mesenchymal stem cells and inhibits MMP-13 expression and matrix degradation*. Osteoarthritis and Cartilage, 2007. **27**: p. 646-655.
60. Woodfield, T., *Cartilage Tissue Engineering: Instructive Cell- based tissue repair trough scaffold desig*, in *Tissue Regeneration2004*, University of Twente: Enschede.
61. Puppi, D., F. Chiellini, and A.e.a. Piras, *Polymeric materials for bone and cartilage repair*. Polymeric Science., 2010. **35**: p. 403-440.
62. Tognana, E., R. Padera, and F.e.a. Chen, *Development and remodeling of engineered cartilage-explant composites in vitro and in vivo*. . Osteoarthritis and Cartilage, 3005. **13**: p. 896-905.
63. Elder, B., E. Kyriacos, and A.e.a. Athanasiou, *Extraction techniques for the decellularization of tissue engineered articular cartilage constructs*. Biomaterials, 2009. **30**: p. 3749-3756.
64. Chen, G., T. Ushida, and T.e.a. Tateishi, *A biodegradable hybrid sponge nested with collagen microsponge*. Clin Orthop, 2001. **51**: p. 273-279.
65. Leong, K., C. Cheah, and C.e.a. Chua, *Solid freeform fabrication of three dimensional scaffolds for engineering replacement tissues and organs*. Biomaterials, 2003. **24**: p. 2363-2378.
66. Chu, P., J. Chen, and L.e.a. Wang, *Plasma-surface modification of biomaterials*. Mater Sci Eng., 2002. **36**: p. 143-206.
67. Hutmacher, D.B., *Scaffolds in tissue engineering bone and cartilage*. Biomaterials, 2000. **21**: p. 2529-2543.
68. McClary, K., T. Ugarova, and D.e.a. Grainger, *Modulating fibroblast adhesion, spreading and proliferation using sel-assembled monolayer films of alkylthiolates on gold*. . J Biomed Mater Res, 2000. **50**: p. 428-439.
69. Shin, H. and A.e.a. Mikos, *Biomimetic materials for tissue engineering*. Biomaterials, 2003. **24**: p. 4353-4364.
70. Iwasa, J., L. Engebresten, and Y.e.a. Shima, *Clinical application of scaffolds for cartilage tissue engineering*. Knee Surg Sports, 2009. **17**: p. 561-577.
71. Meyer, U., et al., *Fundamentals of Tissue Engineering and Regenerative Medicine2009*: Springer.
72. Covert, R., R. Ott, and D.e.a. Ku, *Friction characteristics of a potential articular cartilage biomaterial*. . Wear, 2003. **255**: p. 1064-1068.
73. Guldberg, R., C. Duvall, and A.e.a. Peister, *3D imaging of tissue integration with porous biomaterials*. Biomaterials, 2008. **29**: p. 3757-3761.
74. Ng, K., L. Kugler, and S.e.a. Doty, *Scaffold degradation elevates the collagen content and dynamic compressive modulus in engineered articular cartilage*. Osteoarthritis and Cartilage, 2009. **17**: p. 220-227.
75. Neves, S., et al., *Chitosan/Poly(3-caprolactone) blend scaffolds for cartilage repair*. 2010: p. 1-12.
76. Moroni, L. and J. Elisself, *Biomaterials engineered for integration*. Materials Today, 2008. **11**: p. 44-51.
77. Kang, S., O. Jeon, and B.e.a. Kim, *Poly(lactic-co-glycolic acid) microspheres as an injectable scaffold for cartilage tissue engineering*. . Tissue Engineering part A., 2005. **11**: p. 438-447.
78. Malafaya, P., J. Pedro, and A.e.a. Peterbauer, *Chitosan particles agglomerated scaffolds for cartilage and osteochondral tissue engineering approaches with adipose tissue*

- derived stem cells*. Journal of Materials Science: Materials in Medicine 2005. **16**: p. 1077-1085.
79. Moutos, F., B. Estes, and F. Guilak, *Multifunctional Hybrid Three-dimensionally Woven Scaffolds for Cartilage Tissue Engineering*. Macromolecular Bioscience, 2010. **10**: p. 1355-1364.
80. Tuli, R., W. Li, and R. Tuan, *Current state of cartilage tissue engineering*. Arthritis Res Ther. , 2003. **5**(235-242).
81. Viala, X. and F. Andreopoulos, *Novel Biomaterials for Cartilage Tissue Engineering*. Current Rheumatology Reviews,. 2009. **5**: p. 51-57.
82. Yamaoka, H., H. Asato, and T.e.a. Ogasawara, *Cartilage tissue engineering using human auricular chondrocytes embedded in different hydrogel materials*. Wiley InterScience, 2006: p. p. 1-11.
83. Zhao, H., L. Ma, and C.e.a. Gao, *A composite scaffold of PLGA microspheres/fibrin gel for cartilage tissue engineering: fabrication, physical properties, and cell responsiveness*. . Journal of Biomedical Materials Research. Part B, Applied Biomaterials., 2009. **88**: p. 240-249.
84. Ratner, B.D., *Biomaterials science: an introduction to materials in medicine*2004: Elsevier Academic Press.
85. Narayan, R., *Biomedical Materials*2009: Springer.
86. Lanza, R.P., R.S. Langer, and J. Vacanti, *Principles of tissue engineering*2007: Elsevier Academic Press.
87. Gomes, M.E., et al., *Alternative tissue engineering scaffolds based on starch: processing methodologies, morphology, degradation and mechanical properties*. Materials Science and Engineering: C, 2002. **20**(1-2): p. 19-26.
88. Neves, N.M., A. Kouyumdzhev, and R.L. Reis, *The morphology, mechanical properties and ageing behavior of porous injection molded starch-based blends for tissue engineering scaffolding*. Materials Science and Engineering: C, 2005. **25**(2): p. 195-200.
89. Chu, P.K. and X. Liu, *Biomaterials fabrication and processing handbook*2008: CRC Press/Taylor & Francis.
90. Sill, T.J. and A. von Recum, *Electrospinning: Applications in drug delivery and tissue engineering*. Biomaterials, 2008. **29**: p. 1989-2006.
91. Martins, A., R.L. Reis, and N.M. Neves, *Electrospinning: processing technique for tissue engineering scaffolding*. International Materials Reviews, 2008. **53**: p. 257-272.
92. Gomes, M., P.š.c. Malafaya, and R. Reis, *Fiber Bonding and Particle Aggregation as Promising Methodologies for the Fabrication of Biodegradable Scaffolds for Hard-Tissue Engineering*, in *Biodegradable Systems in Tissue Engineering and Regenerative Medicine*2004, CRC Press.
93. Mikos, A.G., et al., *Preparation of poly(glycolic acid) bonded fiber structures for cell attachment and transplantation*. Journal of Biomedical Materials Research, 1993. **27**(2): p. 183-189.
94. Moutos, F.T., L.E. Freed, and F. Guilak, *A biomimetic three-dimensional woven composite scaffold for functional tissue engineering of cartilage*. Nat Mater, 2007. **6**(2): p. 162-167.
95. Valonen, P.K., et al., *In vitro generation of mechanically functional cartilage grafts based on adult human stem cells and 3D-woven poly([var epsilon]-caprolactone) scaffolds*. Biomaterials, 2010. **31**(8): p. 2193-2200.
96. Malafaya, P., et al., *Chitosan particles agglomerated scaffolds for cartilage and osteochondral tissue engineering approaches with adipose tissue derived stem cells*. Journal of Materials Science: Materials in Medicine, 2006. **17**(7): p. 675-675.
97. Tentem, M., et al., *Green synthesis of a temperature sensitive hydrogel*. Green Chemistry, 2007. **9**: p. 75-79
98. Duarte, A.R., J.F. Mano, and R.L. Reis, *Supercritical fluids in biomedical and tissue engineering applications: a review*. International Materials Reviews, 2009. **54**: p. 215-222.
99. Duarte, A.R., J.F. Mano, and R.L. Reis, *Prespectives on: Supercritical Fluid Technology for 3D Tissue Engineering Scaffold Applications*. Journal of Bioactive and Compatible Polymers, 2009. **24**: p. 385-400.
100. Hsieh, C., et al., *Analysis of freeze-gelation and cross-linking oricesses for preparing porous chitosan scaffolds*. Carbohydrate Polymers, 2007. **67**: p. 124-132.

101. Chung, H.J. and T.G. Park, *Surface engineered and drug releasing pre-fabricated scaffolds for tissue engineering*. *Advanced Drug Delivery Reviews*, 2007. **59**(4-5): p. 249-262.
102. Mikos, A.G., et al., *Laminated three-dimensional biodegradable foams for use in tissue engineering*. *Biomaterials*, 1993. **14**(5): p. 323-330.
103. Shastri, V.P., I. Ivan Martin, and R. Langer, *Macroporous polymer foams by hydrocarbon templating*. *Proc Natl Acad Sci U S A.*, 2000. **97**: p. 1970–1975.
104. Tang, Z., et al., *Biomedical Applications of Layer-by-Layer Assembly: From Biomimetics to Tissue Engineering*. *Advanced Materials*, 2006. **18**: p. 3203-3224.
105. Sher, P., C.A. Custódio, and J.F. Mano, *Layer-By-Layer Technique for Producing Porous Nanostructured 3D Constructs Using Moldable Freeform Assembly of Spherical Templates*. *Small*, 2010: p. n/a-n/a.
106. Webster, T.J., *Nanotechnology for the regeneration of hard and soft tissues* 2007: World Scientific.
107. Sun, H. and N. Hu, *Size effect of polystyrene (PS) latex beads on electrochemical and electrocatalytic activity of layer-by-layer films of heme protein-coated PS beads with polyelectrolytes*. *Journal of Electroanalytical Chemistry*, 2006. **588**(2): p. 207-217.
108. Ma, L., et al., *Incorporation of basic fibroblast growth factor by a layer-by-layer assembly technique to produce bioactive substrates*. *Journal of Biomedical Materials Research Part B: Applied Biomaterials*, 2007. **83B**(1): p. 285-292.
109. Szarpak, A., et al., *Multilayer Assembly of Hyaluronic Acid/Poly(allylamine): Control of the Buildup for the Production of Hollow Capsules*. *Langmuir*, 2008. **24**(17): p. 9767-9774.
110. Richert, L., et al., *Improvement of Stability and Cell Adhesion Properties of Polyelectrolyte Multilayer Films by Chemical Cross-Linking*. *Biomacromolecules*, 2003. **5**(2): p. 284-294.
111. Liu, Y., et al., *Layer-by-layer assembly of biomacromolecules on poly(ethylene terephthalate) films and fiber fabrics to promote endothelial cell growth*. *Journal of Biomedical Materials Research Part A*, 2007. **81A**(3): p. 692-704.
112. Almodóvar, J., et al., *Layer-by-Layer Assembly of Polysaccharide-Based Polyelectrolyte Multilayers: A Spectroscopic Study of Hydrophilicity, Composition, and Ion Pairing*. *Biomacromolecules*, 2011. **12**(7): p. 2755-2765.
113. Picart, C., *Polyelectrolyte multilayer films: from physico-chemical properties to the control of cellular processes*. *Curr Med Chem*, 2008. **15**: p. 685-697.
114. Detzel, C.J., A.L. Larkin, and P. Rajagopalan, *Polyelectrolyte Multilayers in Tissue Engineering*. *Tissue Engineering part B.*, 2011. **17**: p. 1-13.
115. Serpe, M.J., C.D. Jones, and A.L. Lyon, *Layer by layer deposition of thermoresponsive microgel thin films*. *Langmuir*, 2003. **19**: p. 8759-8764.
116. Schneider, A., et al., *Multifunctional Polyelectrolyte Multilayer Films: Combining Mechanical Resistance, Biodegradability, and Bioactivity*. *Biomacromolecules*, 2006. **8**(1): p. 139-145.
117. Boudou, T., et al., *Multiple Functionalities of Polyelectrolyte Multilayer Films: New Biomedical Applications*. *Advanced Materials*, 2010. **22**(4): p. 441-467.
118. Zhu, H., J. Ji, and J. Shen, *Biomacromolecules Electrostatic Self-Assembly on 3-Dimensional Tissue Engineering Scaffold*. *Biomacromolecules*, 2004. **5**(5): p. 1933-1939.
119. Balkundi, S.S., et al., *Encapsulation of Bacterial Spores in Nanoorganized Polyelectrolyte Shells* Langmuir, 2009. **25**(24): p. 14011-14016.
120. Richert, L., et al., *Imaging cell interactions with native and crosslinked polyelectrolyte multilayers*. *Cell Biochemistry and Biophysics*, 2006. **44**(2): p. 273-285.
121. Go, D.P., et al., *Multilayered Microspheres for the Controlled Release of Growth Factors in Tissue Engineering*. *Biomacromolecules*, 2011. **12**(5): p. 1494-1503.
122. Zhao, Q. and B. Li, *pH-controlled drug loading and release from biodegradable microcapsules*. *Nanomedicine: Nanotechnology, Biology and Medicine*, 2008. **4**(4): p. 302-310.
123. Zhi, Z.-l., et al., *Polysaccharide Multilayer Nanoencapsulation of Insulin-Producing β -Cells Grown as Pseudoislets for Potential Cellular Delivery of Insulin*. *Biomacromolecules*, 2010. **11**(3): p. 610-616.
124. Costa, R.R., et al., *Stimuli-Responsive Thin Coatings Using Elastin-Like Polymers for Biomedical Applications*. *Advanced Functional Materials*, 2009. **19**(20): p. 3210-3218.
125. Richert, L., et al., *Layer by Layer Buildup of Polysaccharide Films: Physical Chemistry and Cellular Adhesion Aspects*. *Langmuir*, 2003. **20**(2): p. 448-458.

126. Zhang, J., et al., *Natural polyelectrolyte films based on layer-by layer deposition of collagen and hyaluronic acid*. *Biomaterials*, 2005. **26**(16): p. 3353-3361.
127. Martins, G., J.F. Mano, and N. Alves, *Nanostructured self-assembled films containing chitosan fabricated at neutral pH*. *Carbohydrate Polymers*, 2010. **80**: p. 570-573.
128. Crouzier, T. and C. Picart, *Ion Pairing and Hydration in Polyelectrolyte Multilayer Films Containing Polysaccharides*. *Biomacromolecules*, 2009. **10**(2): p. 433-442.
129. Alves, N.M., C. Picart, and J.F. Mano, *Self Assembling and Crosslinking of Polyelectrolyte Multilayer Films of Chitosan and Alginate Studied by QCM and IR Spectroscopy*. *Macromolecular Bioscience*, 2009. **9**(8): p. 776-785.
130. Mhanna, R.F., J. Vörös, and M. Zenobi-Wong, *Layer-by-Layer Films Made from Extracellular Matrix Macromolecules on Silicone Substrates*. *Biomacromolecules*, 2011. **12**(3): p. 609-616.
131. Stoop, R., *Smart biomaterials for tissue engineering of cartilage*. *Injury*, 2008. **39**(1, Supplement 1): p. 77-87.
132. Alves, N. and J.F. Mano, *Chitosan derivatives obtained by chemical modifications for biomedical and environmental applications*. *International Journal of Biological Macromolecules*, 2008. **43**: p. 402-414.
133. Cancedda, R., B. Dozina, and P.e.a. Giannonia, *Tissue engineering and cell therapy of cartilage and bone*. *Matrix Biology*., 2003. **22**: p. 81-91.
134. Pham, Q., U. Sharma, and A. Mikos, *Electrospinning of Polymeric Nanofibers for Tissue Engineering Applications: A Review*. *Tissue Engineering part C*., 2000. **12**: p. 1197-1211.
135. Frenkel, S.R. and P.E. Di Cesare, *Scaffolds for Articular Cartilage Repair*. *Annals of Biomedical Engineering*, 2004. **32**(1): p. 26-34.
136. Fisher, J., et al., *Thermoreversible hydrogel scaffolds for articular cartilage engineering*. *J Biomed Mater Res A* ., 2004. **71**: p. 268-274.
137. Correia, C., et al., *Chitosan Scaffolds Containing Hyaluronic Acid for Cartilage Tissue Engineering*. *Tissue Engineering: Part C*, 2010. **17**.
138. Francis Suh, J.K. and H.W.T. Matthew, *Application of chitosan-based polysaccharide biomaterials in cartilage tissue engineering: a review*. *Biomaterials*, 2000. **21**(24): p. 2589-2598.
139. Ko, C.-S., et al., *Type II collagen-chondroitin sulfate-hyaluronan scaffold cross-linked by genipin for cartilage tissue engineering*. *Journal of bioscience and bioengineering*, 2009. **107**(2): p. 177-182.
140. Chen, Y., et al., *Composite chondroitin-6-sulfate/dermatan sulfate/chitosan scaffolds for cartilage tissue engineering*. *Biomaterials*, 2007. **28**: p. 2294-2305.
141. Oliveira, J.T., et al., *Gellan gum: A new biomaterial for cartilage tissue engineering applications*. *Journal of Biomedical Materials Research Part A*, 2010. **93A**(3): p. 852-863.
142. Sun, J., et al., *Macroporous poly(3-hydroxybutyrate-co-3-hydroxyvalerate) matrices for cartilage tissue engineering*. *European Polymer Journal*, 2005. **41**(10): p. 2443-2449.
143. Deng, Y., et al., *Study on the three-dimensional proliferation of rabbit articular cartilage-derived chondrocytes on polyhydroxyalkanoate scaffolds*. *Biomaterials*, 2002. **23**(20): p. 4049-4056.
144. Kim, B., I. Park, and H.e.a. Takashib, *Design of artificial extracellular matrices for tissue engineering*. *Progress in Polymer Science* ., 2010.
145. Puppi, D., et al., *Polymeric materials for bone and cartilage repair*. *Progress in Polymer Science*, 2010. **35**(4): p. 403-440.
146. Chandra, R. and R. Rustgi, *Biodegradable Polymers*. Pergamon, 1998. **23**: p. 1273-1335.
147. Dang, J.M. and K.W. Leong, *Natural polymers for gene delivery and tissue engineering*. *Advanced Drug Delivery Reviews*, 2006. **58**(4): p. 487-499.
148. Mano, J.F., et al., *Natural origin biodegradable systems in tissue engineering and regenerative medicine: present status and some moving trends*. *Journal of Royal Society Interface*, 2007. **4**: p. 999-1030.
149. Zhang, X., et al., *Biodegradation of chemically modified wheat gluten-based natural polymer materials*. *Polymer Degradation and Stability*, 2010. **In Press, Corrected Proof**.
150. Seal, B.L., T.C. Otero, and A. Panitch, *Polymeric biomaterials for tissue and organ regeneration*. *Materials Science and Engineering: R: Reports*, 2001. **34**(4-5): p. 147-230.
151. Khor, E. and L.Y. Lim, *Implantable applications of chitin and chitosan*. *Biomaterials*, 2003. **24**(13): p. 2339-2349.
152. Shi, C., et al., *Therapeutic Potential of Chitosan and Its Derivatives in Regenerative Medicine*
1 This work was supported by "973" programs on severe trauma (NO.

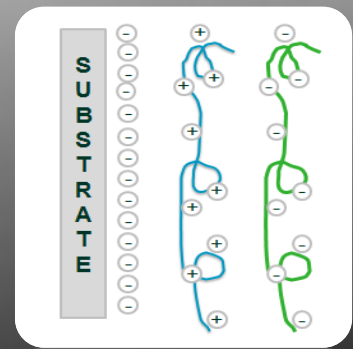
- 1999054205 and NO. 2005CB522605) from the Ministry of Science and Technology of China. The Journal of surgical research, 2006. **133**(2): p. 185-192.
153. Alves, N.M. and J.F. Mano, *Chitosan derivatives obtained by chemical modifications for biomedical and environmental applications*. International Journal of Biological Macromolecules, 2008. **43**(5): p. 401-414.
154. VandeVord, P.e.a., *Evaluation of biocompatibility of a chitosan scaffold in mice*. . Journal of Biomedical Materials Research, 2002. **59**: p. 585-590.
155. Kim, Y., S. Seo, and H.e.a. Moon, *Chitosan and its derivative for tissue engineering applications*. Biotechnology Advances, 2008. **26**: p. 1-21.
156. Martino, A. and M. Risbud, *Chitosan: A versatile biopolymer for orthopaedic tissue engineering*. Biomaterials, 2005. **26**: p. 5983-5990.
157. Nystrom, B.e.a., *Characterization of association phenomena in aqueous systems of chitosan of different hydrophobicity*. Advances in colloid and interface science, 1999: p. 79-81.
158. Freier, T., et al., *Controlling cell adhesion and degradation of chitosan films by N-acetylation*, . Biomaterials, 2005. **26**: p. 5872-5878.
159. Madhally, S. and M.H.e.a. . *Porous Chitosan scaffolds for tissue engineering*. Biomaterials, 1999. **20**: p. 1133-1142.
160. Rinaudo, M., *Chitin and chitosan: Properties and applications*. Progress in Polymer Science, 2006. **31**(7): p. 603-632.
161. Ravi Kumar, M.N.V., *A review of chitin and chitosan applications*. Reactive and Functional Polymers, 2000. **46**(1): p. 1-27.
162. Jayakumar, R., et al., *Novel chitin and chitosan nanofibers in biomedical applications*. Biotechnology Advances. **28**(1): p. 142-150.
163. Martins, A.M., et al., *Natural origin scaffolds with in situ pore forming capability for bone tissue engineering applications*. Acta Biomaterialia, 2008. **4**(6): p. 1637-1645.
164. Martins, A.M., et al., *Chitosan scaffolds incorporating lysozyme into CaP coatings produced by a biomimetic route: A novel concept for tissue engineering combining a self-regulated degradation system with in situ pore formation*. Acta Biomaterialia, 2009. **5**(9): p. 3328-3336.
165. Kim, S., J. Park, and Y.e.a. Cho, *Porous chitosan scaffold containing microspheres loaded with transforming growth factor-B1: Implications for cartilage tissue*. Journal of Controlled Release, 2003. **91**: p. 365-374.
166. Leea, J., K. Kimb, and L.e.a. Kwonb, *Effects of the controlled-released TGF-B1 from chitosan microspheres on chondrocytes cultured in a collagen/chitosan/glycosaminoglycan scaffold*. Biomaterials, 2004. **25**: p. 4163-4173.
167. Chenite, A., et al., *Novel injectable neutral solutions of chitosan form biodegradable gels in situ*. Biomaterials, 2000. **21**: p. 2155-2161.
168. Lu, J. and H. Mathew, *Effects of chitosan on rat knee cartilages*. Biomaterials, 1999. **20**: p. 1937-1944.
169. al., M.-B.e., *N,N dicarboxymethyl chitosan as delivery agent for bone morphogenetic protein in the repair of articular cartilage*. Med Biol Eng Comput, 1999. **37**: p. 130-134.
170. Maccari, F., F. Ferrarini, and N. Volpi, *Structural characterization of chondroitin sulfate from sturgeon bone*. Carbohydrate Research, 2010. **345**(11): p. 1575-1580.
171. Volpi, N. and F. Maccari, *Characterization of a low-sulfated chondroitin sulfate isolate isolated from the hemolymph of the freshwater snail Planorbium corneus*. Marine Biology, 2007. **152**(4): p. 1003-1007.
172. Bathe, M., G. Rutledge, and A.e.a. Grodzinsky, *Osmotic Pressure of Aqueous Chondroitin Sulfate Solution: A Molecular Modeling Investigation*. Biophysical Journal, 2005. **89**: p. 2357–2371.
173. Sugahara, K., T. Mikami, and T.e.a. Uyama, *Recent advances in the structural biology of chondroitin sulfate and dermatan sulfate*. Current Opinion in Structural Biology 2003, 13:612–620, 2003. **13**: p. 612–620.
174. Achura, R., et al., *Chondroitin sulfate proteoglycans of bovine cornea: structural characterization and assessment for the adherence of Plasmodium falciparum-infected erythrocytes*. Biochimica et Biophysica Acta (BBA) - General Subjects, 2004. **1701**: p. 109– 119.
175. Volpi, N., *Analytical aspects of pharmaceutical grade chondroitin sulfates*. Journal of Pharmaceutical Sciences, 2007. **96**(12): p. 3168-3180.

176. Lauder, R., *Chondroitin sulphate: A complex molecule with potential impacts on a wide range of biological systems*. Complementary Therapies in Medicine, 2009. **17**: p. 56–62.
177. Volpi, N., *Influence of charge density, sulfate group position and molecular mass on adsorption of chondroitin sulfate onto coral*. Biomaterials, 2002. **23**: p. 3015-3022.
178. Zhou, J., et al., *Immune modulation by chondroitin sulfate and its degraded disaccharide product in the development of an experimental model of multiple sclerosis*. Journal of Neuroimmunology, 2010. **223**: p. 55–64.
179. Möller, I., et al., *Effectiveness of chondroitin sulphate in patients with concomitant knee osteoarthritis and psoriasis: a randomized, double-blind, placebo-controlled study*. Osteoarthritis and Cartilage, 2010. **18**: p. S32-S40.
180. Ko, C., et al., *Type II collagen-chondroitin sulfate-hyaluronan scaffold cross-linked by genipin for cartilage tissue engineering*. Journal of Bioscience and Bioengineering, 2009. **2**: p. 177–182.
181. Roughley, P., M. Alini, and J. Antoniou, *The role of proteoglycans in aging, degeneration and repair of the intervertebral disc*. 2002: p. 869-874.
182. Sechriest, V., et al., *GAG-augmented polysaccharide hydrogel: A novel biocompatible and biodegradable material to support chondrogenesis*. Journal of Biomedical Materials Research, 2000. **49**: p. 531-541.
183. Huang, L., et al., *Preparation of chitosan/chondroitin sulfate complex microcapsules and application in controlled release of 5-fluorouracil*. Carbohydrate Polymers 2010. **80**: p. 168–173.
184. Lee, C., H. Breinan, and S.e.a. Nehrer, *Articular Cartilage Chondrocytes in Type I and Type II Collagen-GAG Matrices Exhibit Contractile Behavior in Vitro*. Tissue Engineering part A., 2000: p. 555-565.
185. Li, Q., C. Williams, and D.e.a. Sun, *Photocrosslinkable polysaccharides based on chondroitin sulfate*. Journal of Biomedical Materials Research Part A, 2004. **68**: p. 28-33.
186. Muradoa, M., et al., *Preparation of highly purified chondroitin sulphate from skate (*Raja clavata*) cartilage by-products. Process optimization including a new procedure of alkaline hydroalcoholic hydrolysis*. Biochemical Engineering Journal, 2010. **49**: p. 126–132.
187. Servaty, R., et al., *Hydration of polymeric components of cartilage — an infrared spectroscopic study on hyaluronic acid and chondroitin sulfate*. International Journal of Biological Macromolecules, 2001. **28**: p. 121–127.
188. Seog, J., et al., *Direct Measurement of Glycosaminoglycan Intermolecular Interactions via High-Resolution Force Spectroscopy*. Macromolecules, 2002. **35**(14): p. 5601-5615.
189. Trif, M., L. Moldovan, and M.e.a. Moisei, *Liposomes-entrapped chondroitin sulphate: Ultrastructural characterization and in vitro biocompatibility*. Micron 2008. **39**: p. 1042–1045.
190. Kubo, M., K. Ando, and T.e.a. Mimura, *Chondroitin sulfate for the treatment of hip and knee osteoarthritis: Current status and future trends*. Life Sciences 2009. **85**: p. 477–483.
191. Suh, J. and H.B. Matthew, Vol. 21, pp. 2589-2598., *Application of chitosan-based polysaccharide biomaterials in cartilage tissue engineering: a review*. Biomaterials, 2000. **21**: p. 2589-2598.
192. Pieper, J.S., et al., *Preparation and characterization of porous crosslinked collagenous matrices containing bioavailable chondroitin sulphate*. Biomaterials, 1999. **20**(9): p. 847-858.
193. van Susante, J.L.C., et al., *Linkage of chondroitin-sulfate to type I collagen scaffolds stimulates the bioactivity of seeded chondrocytes in vitro*. Biomaterials, 2001. **22**(17): p. 2359-2369.
194. Yan, J., N. Qi, and Q. Zhang, *Rabbit articular chondrocytes seeded on collagen-chitosan-Gag scaffold for cartilage tissue engineering in vivo*. Artificial Cells, Blood Substitutes, and biotechnology, 2007. **35**: p. 333-344.
195. Mullen, L., M. Chem, and S.e.a. Best, *Binding and release characteristics of Insuline-like growth factor-1 from a collagen-glycosaminoglycan scaffold*. Tissue Engineering part C., 2010. **16**: p. 1439-1448.
196. Fan, H., Y. Hu, and C.e.a. Zhang, *Cartilage regeneration using mesenchymal stem cells and a PLGA-gelatin/chondroitin/hyaluronate hybrid scaffold*. Biomaterials, 2006. **27**: p. 4573-4580.
197. Gong, Y., Y. Zhu, and Y.e.a. Liu, *Layer-by-layer assembly of chondroitin sulfate and collagen on aminolyzed poly-L-lactic acid) porous scaffolds to enhance their chondrogenesis*. Acta Biomaterialia, 2007. **3**: p. 677-685.

198. Dausse, Y., et al., *Cartilage repair using new polysaccharidic biomaterials: macroscopic, histological and biochemical approaches in a rat model of cartilage defect*. *Osteoarthritis and Cartilage*, 2003. **11**(1): p. 16-28.
199. Villanueva, I., et al., *Dynamic loading stimulates chondrocyte biosynthesis when encapsulated in charged hydrogels prepared from poly(ethylene glycol) and chondroitin sulfate*. *Matrix Biology*, 2010. **29**(1): p. 51-62.
200. Liu, Y., H. Tao, and C. Gao, *Surface modification of poly(ethylene terephthalate) via hydrolysis and layer-by-layer assembly of chitosan and chondroitin sulfate to construct cytocompatible layer for human endothelial cells*. *Colloids and Surfaces B: Biointerfaces*, 2005. **46**: p. 117-126.
201. Yuan, N.-Y., et al., *Fabrication and characterization of chondroitin sulfate-modified chitosan membranes for biomedical applications*. *Desalination*, 2008. **234**(1-3): p. 166-174.
202. Denuziere, A., D. Ferrier, and A. Domard, *Chitosan-chondroitin sulfate and chitosan-hyaluronate polyelectrolyte complexes physico-chemical aspects*. *Carbohydrate Polymers*, 1996. **29**: p. 317-323.
203. Sechriest, V.F., et al., *GAG-augmented polysaccharide hydrogel: A novel biocompatible and biodegradable material to support chondrogenesis*. *Journal of Biomedical Materials Research*, 2000. **49**(4): p. 534-541.
204. Cascio, B. and B.T. Sharma, *The Future of Cartilage Repair*. *Oper Tech Sports Med.* , 2008. **16**: p. 221-224.

“A scientist in his laboratory is not a mere technician: he is also a child confronting natural phenomena that impress him as though they were fairy tales...”

Marie Curie



CHAPTER II

MATERIALS AND METHODS

Chapter II

Materials and methods

The main aim of this Chapter is to describe in more detail the experimental work that was employed throughout the thesis. In this Chapter each technique and experimental details used will be highlighted.

II-1. MATERIALS

Chitosan (CHT) of medium molecular weight (M_w 190.000-310.000 Da, 75-85 % degree of deacetylation (DD), viscosity 200-800 cps) and chondroitin-4-sulphate (CS) (M_w 50.000 to 100.000 Da) were purchased from Sigma Aldrich. Before being used chitosan was purified by recrystallization. The first step was dissolved it in 1 % (w/v) acetic acid solution and then filtered into a Buckner flask under vacuum through porous membranes (Whatman® ashes filter paper, 20-25 μ m). The pH of solution was adjusted to 8 by adding a solution of sodium hydroxide that caused flocculation due to deprotonation and insolubility of the polymer at neutral pH. The polymer solution was then neutralized until the pH was equal to that of distilled water. Samples were frozen at -80°C and lyophilized.

The paraffin wax spheres were purchased from Jojoba Desert Whale (Tucson, USA) and then modified with polyethylene imine (PEI) (Sigma- Aldrich).

The glass coverslips with 13 mm (L4097-3) were purchased from Agar Scientific.

Lysozyme from chicken egg white (lyophilized powder ~ 10000 U/mg stored at 4°C) and hyaluronidase from bovine tests (Type VIII, 300 U/mg stored at -20°C) were purchased from Sigma- Aldrich.

II-2. METHODS

II-2.1. Layer-by-layer assembly in 2D surfaces

The CHT/CS polyelectrolytes multilayers (PEMs) were constructed onto glass coverslips. The glass coverslips were placed in 70 % (v/v) ethanol during 2 hours and then immersed in 0.15 M sodium chloride (NaCl) for 10 minutes. Then the glass coverslips were dried using nitrogen flow. For the layer-by-layer (LbL) coating CHT solution at 0.15 % (w/v) was dissolved in a 1 % acetic acid with 0.15 M (NaCl). The pH of solution was adjusted at 5.5. CS at the same concentration was dissolved in 0.15 M NaCl and the pH of solution was also adjusted to 5.5.

The multilayered film build-up started by immersing first the substrate in CHT over 10 min followed by immersion in 0.15 M NaCl solution during 5 min. Then the coverslips were dipped in CS solution for 10 min, followed by immersion in 0.15 M NaCl during 5 min (Figure II-1). After these four steps one double layer (dL) had been assembled. The process was repeated until 10 dL.

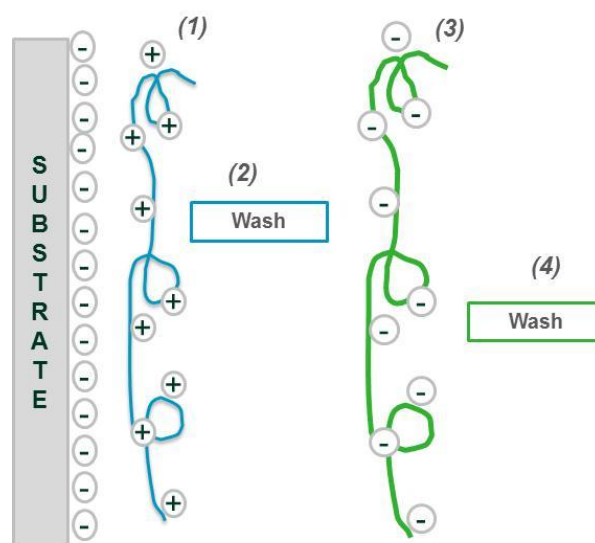


Figure II-1: Diagram illustrating the sequential step to prepare surfaces coated with chitosan and chondroitin sulphate. 1) First glass coverslips were immersed into a polycationic solution of chitosan solution. 2) The coverglasses are subsequent immersed in washing solution with NaCl. 3) Immersion in polyanionic solution of chondroitin sulphate solution. 4) Immersion in NaCl solution. These sequential steps have been repeated until reach 10 double layers (dL).

II-2.2. Scaffolds production by layer-by-layer

The PEMs was constructed onto free-packet paraffin spheres previously modified with PEI. Paraffin spheres modified with PEI (200 μm) were chosen as porogen and 150 mg of them placed into modified cylindrical containers with a porous base. Drop wise addition of polyelectrolytes and washing solutions over the top of assembly was done to form 10 dL of CHT and CS. The coated structure was placed in dichloromethane (DCM) to leach out the paraffin. After the leaching the samples were freeze dried.

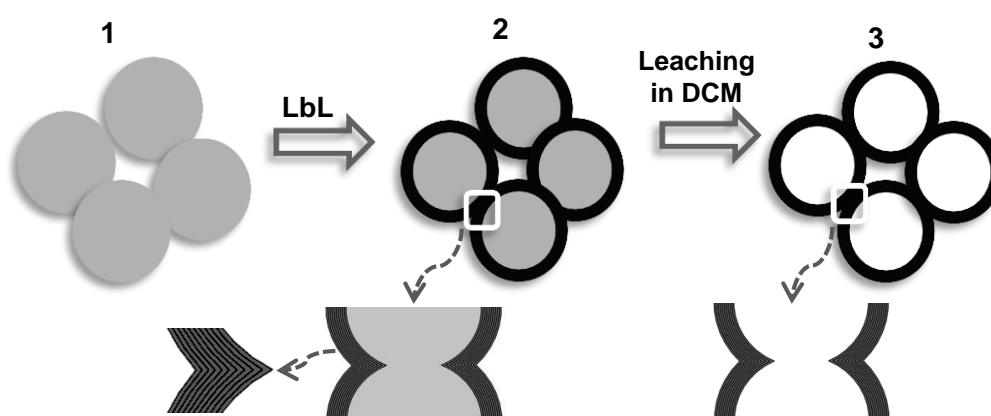


Figure II-2: Schematic diagram of the produced scaffolds. A) Paraffin wax spheres coated with PEI, B) Addition of polyelectrolytes, C) Leaching with DCM and freeze dried process.

II-2.3. Physicochemical characterization of scaffolds and surfaces

II-2.3.1. Build-up Mechanism for film constructed

The build-up process of the CHT and CS multilayers was followed *in situ* by quartz crystal microbalance (QCM-Dissipation, Q-Sense, Sweden). This technique consists in measuring the resonance frequency and dissipation changes (Δf and ΔD , respectively) of quartz crystal induced by polyelectrolyte adsorption on the AT cut quartz crystal. This crystal can be excited at its fundamental frequency (5 MHz) and at several overtones [1-3].

The crystals were cleaned in an ultrasound bath at 30°C using successively acetone, ethanol and isopropanol. Adsorption took place at pH 5.5 and at a constant flow rate of 50 $\mu\text{L min}^{-1}$. The polycationic solution (chitosan) was injected standing for 10 min to allow the adsorption equilibrium at the crystal surface to be reached. Subsequently, the rinsing step was carried out by

the injection of 0.15 M NaCl adjusted at pH 5.5 during 10 min. The same procedure was followed for the deposition of chondroitin sulphate. The steps were repeated to the desire number of layers. The frequency and dissipation were monitored in real time. The thickness of the film was estimated using the Voigt model through the *Q-Tools* Software, from Q-Sense.

II-2.3.2. Morphology

II-2.3.2.1. Optical microscope

The morphology of the scaffolds, after the leaching, was assessed immersing them in DCM, using transmitted light of Axioplan Imager Z1 microscope (Zeiss).

II-2.3.2.2. Scanning electron microscopy (SEM)

Scanning electron microscopy (SEM) has been routinely applied for the morphological analysis of structures developed for tissue engineering (TE) purposes. In SEM the specimen is scanned point by point with an electron beam, and secondary electrons that are emitted by the sample surface on irradiation with the electron beam are detected. In this way, a 3-D impression of the structures in the sample, or of their surface, respectively, is obtained [4].

After the freeze-dried process scaffolds morphology was performed in Philips XL 30 ESEM-FEG operated at 15 KV accelerating voltage and 250 x and 1000 x magnifications. Surface morphology was also assessed using the same equipment at 7.5 kV accelerating voltage and 250 x magnifications. All the samples were coated with a gold sputter (Cressington) for 40 s at a current of 40 mA.

II-2.3.3. Fourier transform infrared spectroscopy

The Fourier transform infrared spectroscopy (FTIR) is a conventional way to infer about the miscibility of polymers via a detailed structural analysis provided by active vibrational transitions. This is performed analysing the shifts of the characteristic bands of components. FTIR analysis can operate separately in transmission, reflection or attenuated reflection (ATR) mode, however in this case the surface has to be flat [5, 6]. FTIR measurements were recorded using an IRPrestige-21

spectrophotometer as the average of 34 individual scan over the range 4400 cm^{-1} to 400 cm^{-1} . The samples were combined with potassium bromide (KBr) to produce discs.

II-2.3.4. Swelling test

The water uptake ability of the scaffolds with known weight was determined by soaking them in phosphate buffered saline solution (PBS, Gibco) at pH=7.4 up to 3 days at 37°C. The swollen scaffolds were removed at predetermined time points ($t=15$ min, 30 min, 1 h, 2 h, 3 h, 4 h, 5 h, 1 day, 2 days and 3 days). The excess of water of each scaffold was removed using a filter paper (Whatman Pergamyn Paper) and then they were weighted with an analytical balance (Scaltec, Germany). The water uptake was calculated using Equation II-1, where W_w and W_d are the weights of swollen and dried scaffold, respectively.

$$\text{Water uptake (\%)} = \frac{W_w - W_d}{W_d} \times 100$$

Equation II-1: Determination of water uptake.

II-2.3.5. Enzymatic Degradation

The enzymatic degradation test is normally performed to evaluate the degradation rate of the scaffolds produced in simulated physiological environments. Scaffolds were placed at 37°C in PBS solution (pH=7.4) or at enzymatic solution containing 2 mg/ml of lysozyme and 0.33 mg/ml of hyaluronidase (pH=7.4) [7]. PBS and enzymatic solution were changed every third day. At predetermined time intervals $t=3, 7$ and 14 days the scaffolds were washed with distilled water to remove the salts. Then the scaffolds were immersed in ethanol 100 % and dried for 1 day at room temperature. The percentage of weight loss (WL) was calculated according to the following equation (Equation II-2), where W_i and W_f are the weights of dry scaffold and after incubation in PBS or enzymatic solution, respectively.

$$\%WL = \frac{W_i - W_f}{W_i} \times 100$$

Equation II-2: Determination of WL (%)

II-2.3.6. Mechanical Properties

Dynamical mechanical analysis (DMA) is common tool used in the laboratory for monitoring relaxation events, measurements of elastic modulus and damping factor and the analysis of interfacial phenomena, such as in composites and immiscible blends. In this technique, an oscillating force is applied to a sample and the material's response it will be a deformation. The deformation is measured as a function of time or/and temperature. From these measurements it is possible to calculate the storage modulus (E') and the loss factor ($\tan \delta$) versus time or temperature for one or more frequencies [8].

For this study, compression tests were carried out by dynamic mechanical analysis (DMA) using a Tritec 2000B equipment (Triton Technology, UK) in order to characterize the mechanical properties of cylindrical scaffolds in both dry and wet states. The sizes of samples were measured using a digital micrometer with precision of 0.001 mm. For the wet state, prior to any measurements the scaffolds were immersed in PBS until equilibrium was reached. The measurement was carried out at 37°C under full immersion of the sample in liquid bath (PBS) placed in a Teflon® reservoir. Experiments were carried out in compression mode following cycles of increasing frequency ranging from 0.1 to 15 Hz, with constant strain amplitude of 30 μm . The frequency range chosen covers the characteristic timescales of the periodic loads felt by the scaffold *in vivo* (e.g. typically frequency of skeletal movement and passage of blood, among others). The high frequency limit used in this study should provide information about the viscoelastic properties for the equivalent of short times (e.g. equivalent to a shock or sudden impact felt by the construct). Moreover, the frequency range used is within the typical frequency interval employed in DMA studies [9].

II-2.4. Cellular assays

II-2.4.1. Bovine articular chondrocytes and human mesenchymal stem cells culture

Two different cell types were used in this study, the bovine chondrocytes (bch) and human mesenchymal stem cells (hMSCs). Bch cells were isolated from freshly collected cartilage of a calf knee by 0.2 % collagenase. hMSCs were selected by adherence from the bone marrow of human donors undergoing total hip replacement. Ethical approval has been obtained from the Almelo and Enschede hospital.

The isolated bch were washed, centrifuged and re-suspended in chondrocytes proliferation medium containing dulbecco's modified eagle medium (DMEM, Invitrogen, USA), fetal bovine serum (FBS, 10 %, Sigma-Aldrich), non-essential aminoacids (0.1 mM, Sigma-Aldrich), penicillin/streptomycin (100 U/100 µg/mL, Invitrogen), proline (0.4 mM, Sigma-Aldrich) and Ascorbic acid 2-phosphate (ASAC, 0.2 mM, Invitrogen) in a humidified atmosphere with 5 % CO₂ and at 37°C. hMSCs were also washed, centrifuged and re-suspended in MSCs proliferation medium containing alpha modified eagle's medium (α-MEM, Invitrogen, USA), fetal bovine serum (FBS, 10 % Sigma-Aldrich), penicillin/streptomycin (100 U/100 µg/mL, Invitrogen), Glutamine (2 mM, Sigma-Aldrich), basic fibroblast growth factor (bFGF, 1 ng/mL, Sigma Aldrich) and ASAC (0.2 mM, Invitrogen) in a humidified atmosphere with 5 % CO₂ and at 37°C. bch and hMSCs were seeded in tissue culture flasks and the medium was change every third day until cells achieved 80 % of confluence. bch were used at passage 2 and hMSCs at passage 3.

Prior to cell seeding scaffolds were sterilized with 70 % (v/v) ethanol overnight and then rinsed three times in PBS, whereas surfaces were treated with ultraviolet (UV) light for 10 min to avoid the damage of the coating. Scaffolds and flat surfaces were then immersed for 4 hours in the medium appropriate for each cell type. For the scaffolds the seeding was performed by applying the cell suspension, with a concentration of 0.5×10^6 cells in 25 µL of medium (per scaffold). For surfaces the cell concentration was adjusted to 1.32×10^4 cells in 25 µL of medium (per surface).

After cell attachment for 2 hours (37°C in a 5 % CO₂), chondrocytes proliferation medium, MSCs proliferation medium or differentiation medium (DMEM, 2 mM glutamine (Gibco), 0.2 mM ASAC (Invitrogen), 100 µg/mL penicillin/Streptomycin (Invitrogen), 0.4 mM proline (Sigma-

Aldrich), 100 µg/mL sodium pyruvate (Sigma-Aldrich) and 50 mg/mL insulin-Transferrin-selenite (ITS+premix, BD biosciences), 10 ng/mL TGFβ-3 (R&D systems) and 0.1 µM dexamethasone (Sigma-Aldrich)) was added.

II-2.4.2. Cell viability and morphology

The cell viability and morphology were assessed with live/dead, MTT assay and SEM. The scaffolds were cut in half in order to perform live dead and MTT at 1, 3, 14 and 21 days. Scaffolds were further observed by SEM. For the surfaces live dead assay was performed at 1, 3, 7, 14 and 21 days, followed by SEM visualization. Medium was changed every third day to maintain an adequate supply of cell nutrients.

II-2.4.2.1. Live/dead assay

To perform this assay the medium was aspirated from the scaffolds and surfaces. The scaffolds and surfaces were then incubated with ethidium homodimer-1 (4 µM) and calcein-AM (2 µM) in PBS for 30 min at 37°C in a 5 % CO₂ atmosphere incubator. After 30 min the samples were immediately examined in an inverted fluorescent microscope (Nikon Eclipse E600) using Fluorescein isothiocyanate (FITC) and Texas Red Filter, as well as the *NIS element-F.30* software. The live/dead assay pictures obtained with surfaces were used to average the percentage of surface area covered with cells. The program used was *Image J*.

Calcein-AM is only capable of entering the cell membrane of living cells where it will be cleaved by esterases and produces green fluorescence. On the other side, ethidium homodimer-1 is only able to enter dead cells and bind to fragmented nucleic acid, emitting a red fluorescence [10].

II-2.4.2.2. MTT assay

The scaffolds were incubated in 900 µL of proliferation medium and 100 µL of MTT solution (5 mg/mL) per well for 2 hours at 37°C in 5 % CO₂. The MTT assay measures the metabolic activity of viable cells, once that the dissolved MTT can be converted to an insoluble purple formazan by dehydrogenase enzymes that catalyse the cleavage of the tetrazolium ring in MTT [11-14] Images were captured using a stereomicroscope with colour camera (Nikon SMZ-10A) and the *Qcapture* software.

II-2.4.2.3. SEM

Scaffolds and surfaces with cells were fixed in formalin 10 % and dehydrated using serial concentrations of ethanol [70 %, 80 %, 90 %, 96 % and 100 % (v/v), 30 min in each], before performing critical point drying (Balzers CPD 030). Finally, scaffolds and surfaces were mounted and gold sputtered. The analysis was performed in Philips XL 30 ESEM-FEG operated at 7.5-15 kV accelerating voltage and 1000 x-2500 x magnification

II-2.4.3. DNA quantification

Scaffolds seeded with bch and hMSCS in differentiation medium at 1, 14 and 35 days were washed with PBS and frozen at - 80°C before proteinase K (Sigma Aldrich) digestion. Then the scaffolds were digested with 1 mg/mL of proteinase K in tris (hydroxymethyl) aminomethane ethylenediaminetetraacetic (Tris\EDTA) buffer (pH=7.6) containing 18.5 µg/mL idoacetamide and 1 µg/mL pepstatin A (Sigma Aldrich) at 56°C for 20 hours. Quantification of total DNA in each sample was determined with CyQuant DNA kit according to manufacturer description (Molecular probes, Eugene, Orgeon, USA), using a spectrofluorometer (Victor3, Perkin-Elmer, USA) at an emission wavelength of 520 nm and an excitation wavelength of 480 nm.

II-2.4.4. Histology

Haematoxylin & eosin (H&E) and alcian blue stainings methods were used to analyse cell distribution and cartilage tissue formation, respectively. Scaffolds were fixed overnight in 10 % formalin, and then dehydrated using sequential ethanol series [70 %, 80 %, 90 %, 96 %, and 100 % (v/v), 30 min in each]. Once dehydrated, they were incubated in butanol overnight at 4°C. Ultimately, the scaffolds were incubated paraffin overnight at 56°C and then embedded in paraffin. Sections with 4.5 µm of thickness were cut using a microtome (MicroM HM355S). After deparaffinization with xylene and rehydration using a graded ethanol series [from 100 % to 70 % (v/v)], the samples were stained using the automatic stainer (MicroM HMS740). For H&E staining samples were stained with haematoxylin for 1 min and rinse up to 6 min before being stained with eosin for 30 s. For alcian blue staining the samples were placed in alcian blue solution (0.5%, pH=1) for 30 min and rinsed with tap water or distilled water for 4 min. In the last step nuclear fast red was added for 5 min before dehydration. Slides were assembled with resinous medium and

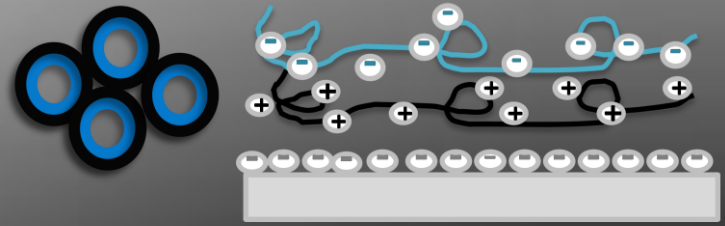
mounted slides were examined under a light of Axioplan Imager Z1 microscope (Zeiss). Representative images were captured using a digital camera (AxioCAM MRCE) and *Axiovision* software. Each assay was performed at 1, 14, 21 and 35 days of culture.

II-3. STATISTICAL ANALYSIS

The experiences developed were carried out in triplicate otherwise specified. The results were presented as mean \pm standard deviation (SD). Statistical analysis was performed using one way ANOVA analysis followed by Turkey test (Graph Pad Prism 5.0 for Windows). Statistical significance was set to p-value (p) <0.05 (*) and p<0.01 (**).

II-4. REFERENCES

1. Costa, R.R., et al., *Stimuli-Responsive Thin Coatings Using Elastin-Like Polymers for Biomedical Applications*. *Advanced Functional Materials*, 2009. **19**(20): p. 3210-3218.
2. Irwin, E., et al., *Analysis of interpenetrating polymer networks via quartz crystal microbalance with dissipation monitoring*. *Langumir*, 2005. **21**: p. 5529-5536.
3. Martins, G., J.F. Mano, and N. Alves, *Nanostructured self-assembled films containing chitosan fabricated at neutral pH*. *Carbohydrate Polymers*, 2010. **80**: p. 570-573.
4. Goldstein, J., *Scannine electron microscopy and X-ray microanalysis*2003.
5. Yampolskaya, G., B. Tarasevich, and A. Elenskii, *Secondary structure of globular proteins in adsorption layers at the solution-air interface by the Data of Fourier Transform IR spectroscopy*. *Colloid Journal*, 20005. **67**: p. 385-391.
6. Sasic, S. and Y. Ozaki, *Raman, Infrared, and Near-Infrared Chemical Imaging*2011: John Wiley & Sons.
7. Correia, C., et al., *Chitosan Scaffolds Containing Hyaluronic Acid for Cartilage Tissue Engineering*. *Tissue Engineering: Part C*, 2010. **17**.
8. Menard, K.P., *Dynamic mechanical analysis: a practical introduction*2008: CRC Press.
9. Sobral, J.M., et al., *Three-dimensional plotted scaffolds with controlled pore size gradients: Effect of scaffold geometry on mechanical performance and cell seeding efficiency*. *Acta Biomaterialia*, 2011. **7**(3): p. 1009-1018.
10. Monteiro-Riviere, N.A., A.O. Inman, and L.W. Zhang, *Limitations and relative utility of screening assays to assess engineered nanoparticle toxicity in a human cell line*. *Toxicology and Applied Pharmacology*, 2009. **234**(2): p. 222-235.
11. Abe, K. and N. Matsuki, *Measurement of cellular 3-(4,5-dimethylthiazol-2-yl)-2,5-diphenyltetrazolium bromide (MTT) reduction activity and lactate dehydrogenase release using MTT*. *Neuroscience Research*, 2000. **38**(4): p. 325-329.
12. Ciapetti, G., et al., *In vitro evaluation of cell/biomaterial interaction by MTT assay*. *Biomaterials*, 1993. **14**(5): p. 359-364.
13. Hamid, R., et al., *Comparison of alamar blue and MTT assays for high through-put screening*. *Toxicology in Vitro*, 2004. **18**(5): p. 703-710.
14. Ulukaya, E., et al., *The MTT assay yields a relatively lower result of growth inhibition than the ATP assay depending on the chemotherapeutic drugs tested*. *Toxicology in Vitro*, 2008. **22**(1): p. 232-239.



***“Concentrate all your thought upon the work
at hand.
The sun’s rays do not burn until brought to a
focus”***

Alexander Graham Bell

CHAPTER III

NANOSTRUCTURED 3D CONSTRUCTS BASED ON CHITOSAN AND
CHONDROITIN SULPHATE MULTILAYERS FOR CARTILAGE TISSUE
ENGINEERING

Chapter III

Nanostructured 3D constructs based on chitosan and chondroitin sulphate multilayers for cartilage tissue engineering

Joana M. Silva, M.Sc.^{1,2}, Nicole Georgi M.Sc.³, Rui Costa, M.Sc.^{1,2}, Praveen Sher, Ph.D.^{1,2}, Rui L. Reis, Ph.D.^{1,2}, Clemens A. Van Blitterswijk, Ph.D.³, Marcel Karperien, Ph.D.³, and João F. Mano, Ph.D.^{1,2}.

¹ 3B's Research Group - Biomaterials, Biodegradables and Biomimetics, University of Minho, Headquarters of the European Institute of Excellence on Tissue Engineering and Regenerative Medicine, AvePark, 4806-909 Taipas, Guimarães, Portugal

² ICVS/3B's - PT Government Associate Laboratory, Braga/Guimarães, Portugal

³ Department of Tissue Regeneration, MIRA—Institute for Biomedical Technology and Technical Medicine, Twente University, Enschede,

ABSTRACT

Nanostructured 3D constructs combining layer-by-layer technology (LbL) and template leaching were processed and evaluated as possible support structures for articular cartilage. Chitosan (CHT) and chondroitin sulphate (CS) were used as polyelectrolytes and their ability to form multilayers was verified by Quartz crystal microbalance (QCM). The biological performance of 2D flat CHT/CS multilayers was first investigated, in which the viability, adhesion, morphology and proliferation of bovine chondrocytes (bch) were studied. The polymeric film was found to be non-cytotoxic and allowed the proliferation of bch. The technology was transposed to the 3D level by LbL coating followed by leaching of free-packet paraffin spheres. The obtained nanostructured 3D constructs has a high porosity and water uptake capability of about 300 %. Dynamical mechanical analysis (DMA) showed a clear viscoelastic nature of the scaffolds in which the storage modulus (E') is about one order of magnitude lower in the hydrated state when compared with the dry condition. Moreover enzymatic tests demonstrate that the structure could lose about 15 % of the initial weight after 15 days. To test the ability of these scaffolds as supports for cartilage TE, cellular tests were performed with the culture of bch and human mesenchymal stem cells (hMSCs) up to 21 days. SEM analysis, viability tests and DNA quantification showed that cells attached, proliferated and were metabolically active. Cartilaginous ECM formation was assessed and results showed that matrix production occurred indicating the maintenance of the chondrogenic phenotype and the chondrogenic differentiation of hMSCs.

Keywords: Layer-by-layer, chitosan, chondroitin sulphate, chondrocytes, human mesenchymal stem cells, cartilage tissue engineering.

III-1. INTRODUCTION

Articular cartilage is an avascular, alymphatic, aneural, anisotropic tissue with low mitotic and limited capacity to regenerate [1, 2]. It is known that due to articular cartilage properties, millions of people which suffer from traumatic injuries and degenerative diseases require treatments [3]. However, the current treatments present some limitations and fail to produce long-lasting repair, leading in some case to fibrocartilage formation instead of hyaline cartilage [4, 5].

Tissue Engineering (TE) has appeared as a new methodology which offers advantages when compared with current treatments [4, 6, 7]. Scaffolds play an important role in TE strategies because they provide the initial structure support, guiding the differentiation and development of the cartilaginous tissue [8-10]. Typically native tissues exhibit an hierarchical organization from the nano- to the macro-scale levels. The control from the nano-sizes of scaffold offers the possibility of develop structures with further capabilities, including the control of cell behaviour at the nano-level, the fabrication of hierarchical-organized devices, the inclusion of other functionalities, such as the possibility of incorporate bioactive molecules, or tune the mechanical and degradation behaviour of the scaffold. In this work we propose the use of bottom-up approaches to produce three-dimensional (3D) porous scaffolds with a nanostructured organization adequate to support cells development in context of articular cartilage. The layer-by-layer (LbL) methodology is a versatile technique that permits to fabricate layers nanostructured multilayered films using a variety of polyelectrolytes [11-13]. The principle of this technique is based on alternate deposition of polyelectrolytes that will self-organize on the material surface [11-14]. The main application of LbL is the build-up of polyelectrolytes multilayers (PEMs) onto flat surfaces [11-13]. Just a few works reported the use of LbL to fabricate scaffolds. Such technique may be used to coat free-packet leachable spherical templates [15] or to agglomerate beads [16], leading in both cases to porous structures.

A wide range of materials have been explored to cartilage tissue engineering approaches, among which polysaccharides based materials [7, 17]. Chitosan (CHT) is obtained by a partial deacetylation of chitin that has structural characteristics similar to glycosaminoglycan's (GAGs) [18]. Chondroitin sulphate (CS) is the major GAG component of native cartilage tissue and it is

responsible to generate electrostatic repulsion which provides much of the resistance to compression, and also cooperate in the shock absorbing capacity of aggrecans [14, 19].

The aim of this work is to prepare nanostructured 3D constructs, based on the LbL methodology, studying its effect on cartilage TE. For the proof of concept the build-up of CHT/CS PEMs onto flat surfaces were firstly characterized using quartz crystal microbalance (QCM) and its biological performance evaluated with a primary culture of bovine chondrocytes (bch), that are the cells present in the articular cartilage tissue. The biological performance of highly porous nanostructured 3D scaffolds was also evaluated using bch and cells with multilineage differentiation capacity, human mesenchymal stem cells (hMSCs). The maintenance of chondrogenic phenotype and the differentiation of hMSCs were also investigated.

III-2. MATERIALS AND METHODS

III-2.1. Materials

Chitosan (CHT) of medium molecular weight (M_w 190.000 - 310.000 Da, 75 – 85 % Degree of deacetylation, viscosity 200 - 800 cps) and chondroitin-4-sulphate (CS) (M_w 50.000 - 100.000 Da) were purchased from Sigma Aldrich. Before being used chitosan was purified by recrystallization. Paraffin wax spheres with 200 μ m were purchased from Jojoba Desert Whale (Tucson, USA) and then modified with polyethylene imine (PEI) (Sigma- Aldrich). Glass coverslips with 13 mm (L4097-3) were purchased from Agar Scientific. Lysozyme from chicken egg white (lyophilized powder \approx 10000 U/mg stored at 4°C) and hyaluronidase from bovine tests (Type VIII, 300 U/mg stored at -20°C) were purchased from Sigma- Aldrich.

III-2.2. Methods

III-2.2.1. Build-up Mechanism for film constructed

The build-up process of CHT/CS PEMs was followed *in situ* by quartz crystal microbalance (QCM-Dissipation, Q-Sense, Sweden), using gold coated sensor excited at a fundamental frequency of 5 MHz and at seventh overtone (35 MHz). The crystals were cleaned in an ultrasound bath at

30°C using successively acetone, ethanol and isopropanol. Adsorption took with a constant flow rate of 50 $\mu\text{L min}^{-1}$.

A 0.15 % (w/v) CHT solution was prepared in a 1 % acetic acid with 0.15 M NaCl. The pH of solution was adjusted at 5.5. CS at the same concentration was dissolved in 0.15 M NaCl and the pH of solution was also adjusted to 5.5. The CHT solution was injected standing for 10 min to allow the adsorption equilibrium at the crystal surface to be reached. Subsequently, the rinsing step was carried out by the injection of 0.15 M NaCl adjusted during 10 min. The same procedure was followed for the deposition of CS. The steps were repeated to the desire number of layers. The frequency and dissipation were monitored in real time. The thickness of the film was estimated using the Voigt model through the Q-Tools Software, from Q-Sense.

III-2.2.2. LbL assembly in 2D surfaces

The CHT/CS PEMs were constructed onto glass coverslips. The glass coverslips were placed in 70 % (v/v) ethanol during 2 hours and then immersed in 0.15 M sodium chloride (NaCl) for 10 min. After these two steps the glass coverslips were dried using nitrogen flow. The multilayered film build-up started by immersing first the substrate in CHT during 10 min followed by the immersion in 0.15 M NaCl solution during 5 min. Then the coverslips were dipped in CS solution for 10 min, followed by immersion in 0.15 M NaCl over 5 min. These four steps allowed the assembling of one double layer (dL). The process was repeated until 10 dL.

III-2.2.3. Scaffolds production by LbL

The PEMs was constructed onto free-packet paraffin spheres previously modified with PEI. Paraffin spheres modified with PEI were chosen as the porogen and 150 mg of them placed into a modified cylindrical container, with a porous base. CHT was used to make the initial coating. Drop wise addition of polyelectrolyte solutions and washing solutions over the top of assembly was done to form 10 dL of CS and CHT. The coated structure was placed in dichloromethane (DCM) to leach out the paraffin. After the leaching the samples were freeze dried.

III-2.2.4. Physicochemical characterization

III-2.2.4.1. Morphology

The morphology of the scaffolds after the leaching process and immersed in DCM was assessed by optical microscopy, using the Axioplan Imager Z1 microscope (*Zeiss*). Freeze-dried scaffolds were also observed by scanning electronic microscopy (SEM), using a Philips XL 30 ESEM-FEG operated at 15 kV accelerating voltage. Surface morphology of the glass coverslips was also performed using the same equipment at 7.5 kV accelerating voltage. All the samples were sputtered with a conductive gold layer, using a sputter coater (Cressington) for 40s at a current of 40 mA.

III-2.2.4.2. Fourier transform infrared (FTIR) spectroscopy

FTIR measurements were recorded using an IRPrestige-21 spectrophotometer, by averaging 34 individual scans over the range 4400 cm⁻¹ to 400 cm⁻¹. The samples were prepared in potassium bromide (KBr) discs.

III-2.2.4.3. Swelling test

The water uptake ability of the scaffolds with known weight was determined by soaking them in phosphate buffered saline solution (PBS, Gibco) at pH=7.4 up to 3 days at 37°C. The swollen scaffolds were removed at predetermined time points (t=15 min, 30 min, 1 h, 2 h, 3 h, 4 h, 5 h, 1 day, 2 days and 3 days). After removing the excess of water using a filter paper (Whatman Pergamyn Paper), the scaffolds were weighted with an analytical balance (Scaltec, Germany). The water uptake was calculated using Equation III-1, where W_w and W_d are the weights of swollen and dried scaffold, respectively.

$$\text{Water uptake\%} = \frac{W_w - W_d}{W_d} \times 100$$

Equation III-1: Determination of water uptake.

III-2.2.4.4. Enzymatic Degradation

The enzymatic degradation test is normally performed to evaluate the degradation profile of the scaffolds produced in simulated physiological environments. Scaffolds were placed at 37°C in PBS solution (pH=7.4) or at enzymatic solution containing 2 mg/ml of lysozyme and 0.33 mg/ml

of hyaluronidase (pH=7.4) [20]. PBS and enzymatic solution were changed every third day [20]. At predetermined time intervals $t=3, 7$ and 14 days the scaffolds were washed with distilled water to remove the salts. Then the scaffolds were immersed in ethanol 100 % and dried for 1 day at room temperature. The percentage of weight loss (WL) was calculated according to the Equation III-2, where W_i and W_f are the weights of dry scaffold and after incubation in PBS or enzymatic solution, respectively.

$$WL = \frac{W_i - W_f}{W_i} \times 100$$

Equation III-2: Determination of WL (%)

III-2.2.4.5. Mechanical Test

Compression tests were carried out by dynamic mechanical analysis (DMA), using a Triton 2000B equipment (Triton Technology, UK) to characterize the mechanical properties of cylindrical scaffolds in both the dry and wet states. The sizes of the samples were measured using a digital micrometer with precision of 0.001 mm. Prior to any measurements in the wet state the scaffolds were immersed in PBS until equilibrium was reached. The measurement was carried out at 37 °C under full immersion of the sample in liquid bath (PBS) placed in a Teflon® reservoir. Experiments were carried out in compression mode following cycles of increasing frequency ranging from 0.1 to 15 Hz, with constant strain amplitude of 30 μm . The frequency range chosen covers the characteristic timescales of the periodic loads felt by the scaffold *in vivo* (e.g. typical frequency of skeletal movement). The high frequency limit used in this study should provide information about the viscoelastic properties for the equivalent of short times (e.g. equivalent to a shock or sudden impact felt by the construct) [21].

III-2.3. Cellular assays

III-2.3.1. Bovine articular chondrocytes and human mesenchymal stem cells culture

Two different cell types were used in this study: the bovine chondrocytes (bch) and human mesenchymal stem cells (hMSCs). Bch cells were isolated by 0.2% collagenase overnight digestion from freshly collected cartilage of a calf knee. hMSCs were selected by adherence from the bone marrow of human donors undergoing total hip replacement. Ethical approval has been obtained

from the Almelo and Enschede hospital. The isolated bch were washed, centrifuged and re-suspended in chondrocytes proliferation medium containing dulbecco's modified eagle medium (DMEM, Invitrogen, USA), fetal bovine serum (FBS, 10 %, Sigma-Aldrich), non-essential aminoacids (0.1 mM, Sigma-Aldrich), penicillin/streptomycin (100 U/100 µg/mL, Invitrogen), proline (0.4 mM, Sigma-Aldrich) and Ascorbic acid 2-phosphate (ASAC, 0.2 mM, Invitrogen) in a humidified atmosphere with 5 % CO₂ and at 37°C. hMSCs were also washed, centrifuged and re-suspended in MSCs proliferation medium containing alpha modified eagle's medium (α-MEM, Invitrogen, USA), fetal bovine serum (FBS, 10 % Sigma-Aldrich), penicillin/streptomycin (100 U/100 µg/mL, Invitrogen), Glutamine (2 mM, Sigma-Aldrich), basic fibroblast growth factor (bFGF, 1 ng/mL, Sigma Aldrich) and ASAC (0.2 mM, Invitrogen) in a humidified atmosphere with 5 % CO₂ and at 37°C. bch and hMSCs were seeded in tissue culture flasks and the medium was change every third day until cells achieved 80 % of confluence. bch were used at passage 2 and hMSCs at passage 3. Prior to cell seeding scaffolds were sterilized with 70 % (v/v) ethanol overnight and then rinsed three times in PBS, whereas surfaces were treated with ultraviolet (UV) light for 10 min to avoid the damage of the coating. Scaffolds and flat surfaces were then immersed for 4 hours in the medium appropriate for each cell type. For the scaffolds the seeding was performed by applying the cell suspension, with a concentration of 0.5x10⁶ cells in 25 µL of medium (per scaffold). For surfaces the cell concentration was adjusted to 1.32x10⁴ cells in 25 µL of medium (per glass coverslips). After cell attachment for 2 hours (37°C in a 5 % CO₂), chondrocytes proliferation medium, MSCs proliferation medium or differentiation medium (DMEM, 2 mM glutamine (Gibco), 0.2 mM ASAC (Invitrogen), 100 µg/mL penicillin/Streptomycin (Invitrogen), 0.4 mM proline (Sigma-Aldrich), 100 µg/mL sodium pyruvate (Sigma-Aldrich) and 50 mg/mL insulin-Transferrin-selenite (ITS+premix, BD biosciences), 10 ng/mL TGFβ-3 (R&D systems) and 0.1 µM dexamethasone (Sigma-Aldrich)) was added.

III-2.3.2. Cell viability

The cell viability and morphology were assessed with live/dead assay, MTT assay and SEM analysis. The scaffolds were cut in half in order to perform live/dead and MTT at 1, 3, 14 and 21 days. Scaffolds were further observed by SEM. For the surfaces live dead assay was performed at 1, 3, 7, 14 and 21 days followed by SEM visualization. Medium was changed every third day to maintain an adequate supply of cell nutrients.

III-2.3.2.1. Live /dead assay

To perform this assay the proliferation medium was aspirated from the wells where scaffolds and surfaces were deposited. The scaffolds and surfaces were then incubated with ethidium homodimer-1 (4 μ M) and calcein-AM (2 μ M) in PBS for 30 min at 37°C in a 5 % CO₂ atmosphere incubator. After 30 min the samples were immediately examined in an inverted fluorescent microscope (Nikon Eclipse E600) using Fluorescein isothiocyanate (FITC) and Texas Red Filter, as well as the *NIS element-F.30* software. Calcein-AM is only capable of permeating into plasma membrane of living cells where it will be cleaved by esterases and produces green fluorescence. On the other side, ethidium homodimer-1 is only able to enter dead cells and bind to fragmented nucleic acid, emitting a red fluorescence. The live/dead assay pictures were analysed using *Image J*. to average the percentage of the surface area covered with cells.

III-2.3.2.2. MTT assay

The scaffolds were incubated in 900 μ L of proliferation medium and 100 μ L of MTT solution (5 mg/mL) per well for 2 h at 37°C in 5 % CO₂. The MTT assay measures the metabolic activity of viable cells once that dissolved MTT can be converted to an insoluble purple formazan by dehydrogenase enzymes that catalyse the cleavage of the tetrazolium ring in MTT. Images were captured using a stereomicroscope with colour camera (Nikon SMZ-10A) and the *Qcapture* software.

III-2.3.2.3. Scanning electron microscopy observation

The structures with cells were fixed in formalin 10 % and dehydrated using serial concentrations of ethanol [70 %, 80 %, 90 %, 96 % and 100 % (v/v), 30 min in each], before performing critical point drying (Balzers CPD 030). The surfaces of the materials were then coated with a conductive layer. The SEM observations were performed in a Philips XL 30 ESEM-FEG operated at 7.5-15 kV accelerating voltage.

III-2.3.3. DNA quantification

Scaffolds seeded with bch and hMSCS in differentiation medium at 1, 14 and 35 days were washed with PBS and frozen at - 80°C before proteinase K (Sigma Aldrich) digestion. Then the scaffolds were digested with 1 mg/mL of proteinase K in tris (hydroxymethyl) aminomethane

ethylenediaminetetraacetic (Tris\EDTA) buffer (pH 7.6) containing 18.5 µg/mL idoacetamide and 1 µg/mL pepstatin A (Sigma Aldrich) at 56°C for 20 hours. Quantification of total DNA in each sample was determined with CyQuant DNA kit according to manufacturer description (Molecular probes, Eugene, Orgeon, USA), using a spectrofluorometer (Victor3, Perkin-Elmer, USA) at an emission wavelength of 520 nm and an excitation wavelength of 480 nm.

III-2.3.4. Histology

Haematoxylin & eosin (H&E) and alcian blue stainings methods were used to analyse cell distribution and cartilage tissue formation, respectively. For histology analysis, scaffolds were fixed overnight in 10 % formalin, and then dehydrated using sequential ethanol series [70 %, 80 %, 90 %, 96 %, and 100 % (v/v), 30 min in each]. Once dehydrated, they were incubated in butanol overnight at 4°C and then in a solution of paraffin at 56°C for 12 hours. Sections with 4.5 µm of thickness were cut using a microtome (MicroM HM355S). After deparaffinization with xylene and rehydration using a graded ethanol series [from 100 % to 70 % (v/v)], the samples were stained using an automatic stainer (MicroM HMS740). For H&E staining samples were stained with haemotoxylin for 1 min and rinse up to 6 min before being stained with eosin for 30 s. For alcian blue staining the samples were placed in alcian blue solution (0.5%, pH=1) for 30 min and rinsed with tap water or distilled water for 4 min. In the last step nuclear fast red was added for 5 min before dehydration. Slides were assembled with resinous medium and mounted slides were examined under a light of Axioplan Imager Z1 microscope (Zeiss). Representative images were captured using a digital camera (AxioCAM MRCE) and treated using *Axiovision* software. Each assay was performed at 1, 14, 21 and 35 days of culture.

III-3. STATISTICAL ANALYSIS

The experiences developed were carried out in triplicate otherwise specified. The results were presented as mean ± standard deviation (SD). Statistical analysis was performed using one way ANOVA analysis followed by *Turkey test* (*Graph Pad Prism 5.0 for Windows*). Statistical significance was set to $p < 0.05$ (*) and $p < 0.01$ (**).

III-4. RESULTS AND DISCUSSION

III-4.1. Build-up Mechanism for film constructed

The build-up mechanism of the polymeric multilayered films made of CS and CHT was assessed *in situ* with QCM-D. This technique detects the adsorbed mass of polyelectrolytes and measures the viscoelastic properties of the surface [22, 23]. Figure III-1-A shows the build-up of 10 layers of CHT and CS in terms of variations on normalized frequency, $\Delta f/n$ (where n is the frequency overtone) and dissipation, ΔD_7 . As expected, the normalized frequency decreases with each CHT and CS solutions injection, reflecting the increase of mass over the gold sensor. The increase of ΔD_7 is due to the non-rigid adsorbed layer structure of the deposited film. During the washing step that follows the injection of each polyelectrolyte, the change of both $\Delta f_7/7$ and ΔD_7 were small relatively to the total frequency variation associated to the adsorption of the respective polymer. This indicates a strong association of the layers on the surface of the crystal.

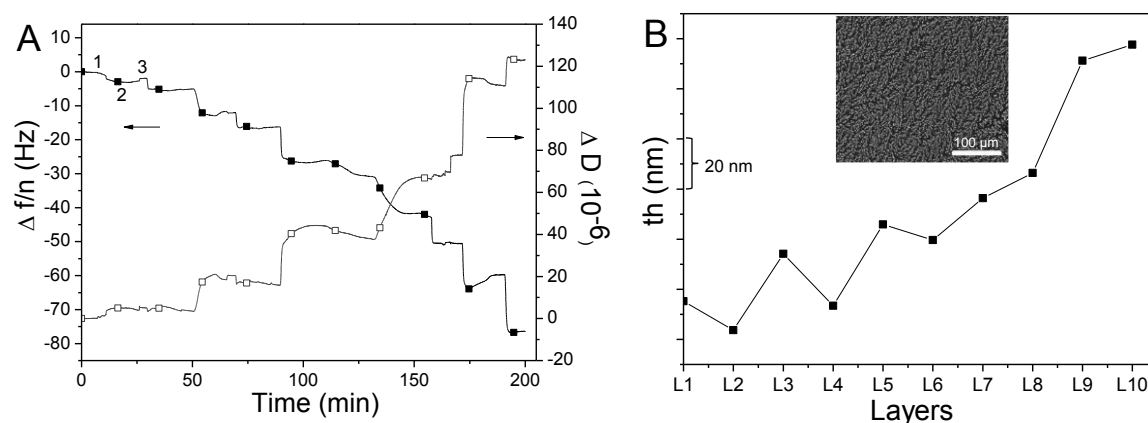


Figure III-1: Build-up monitoring of the CHT/CS polyelectrolyte multilayered using QCM for film constructed: A) Normalized frequency ($\Delta f_7/7$) and dissipation changes (ΔD_7) obtain at 35 MHz, 1) deposition of CHT, 2) washing step and 3) deposition of CS; B) Estimated thickness (th) evolution and SEM micrographs of the multilayer surface with 10 dL (inset image).

The combination of $\Delta f_7/7$ and ΔD_7 gives information about the adsorbed amount and the variations of the viscoelastic properties [22, 24, 25]. The thickness (th) of the film was estimated using the Voigt Model [26]. Figure III-1-B shows the th variation along the deposition of 10 layers [22, 25]. The results revealed a decrease of th from the first layer to the second one, which can be explained due to changes in water absorption [27]. The absorption of water occurs owing to the presence of some groups in the polysaccharides (hydroxyl, carboxyl and sulphate groups) that

interact favourably with water molecules [27]. When the second layer is adsorbed the presence of opposite charge leads to electrostatic interactions between them and the counterion-polymer. Consequently, water-polymer bonds are disrupted, resulting in an effective decrease of the hydrated film *th* [24, 27, 28]. The trend was observed during the first three pairs of layers. After the first three dL, this trend was no longer observed: there was an increase of *th* with the addition of CS. The SEM microphotography of the multilayered surface revealed a homogenous coating along the 2D flat surface - see inset image of Figure III-1B. Moreover, the texture of the surface presented a rough texture and some granularity, with characteristic sizes around 2 μm .

The results obtained through QCM measurements and SEM demonstrates that CS can be used successfully with CHT to conceive a homogeneous viscoelastic polymeric self-assembled coating using the LbL approach.

III-4.2. Multilayer surface

Using LbL methodology it is possible the production of surfaces with tuned properties [11-13]. In this work, multilayers of chitosan and chondroitin sulphate have been prepared in glass coverslips by using the LbL methodology, obtaining assemblies with 10 dL.

III-4.2.1. Cell behaviour in multilayers

In order to assess the cell viability in the surfaces, live/dead assay was performed – see Figure III-2 A, C, E, G and I. The results showed a large amount of living cells and low number of dead cells in any of the time points indicating that the film has no cytotoxic effects.

The cell adhesion/morphology was also studied using SEM - see micrographs in Figure III-2 B, D, F and H. The results revealed that the bch were attached to the surface in the earliest time points. Attachment, adhesion and spreading belong to the first phase of cell/material interaction and the quality of this stage influence the capacity of cells to proliferate and differentiate itself on contact with the implant[29, 30]. With increasing culture time, ECM production also increase and cells start to spread out along the surface, losing their round phenotype. After 7 days of culture a huge surface area was already covered and consequently a large amount of proliferation occurred. At 14 days a cellular confluence was achieved.

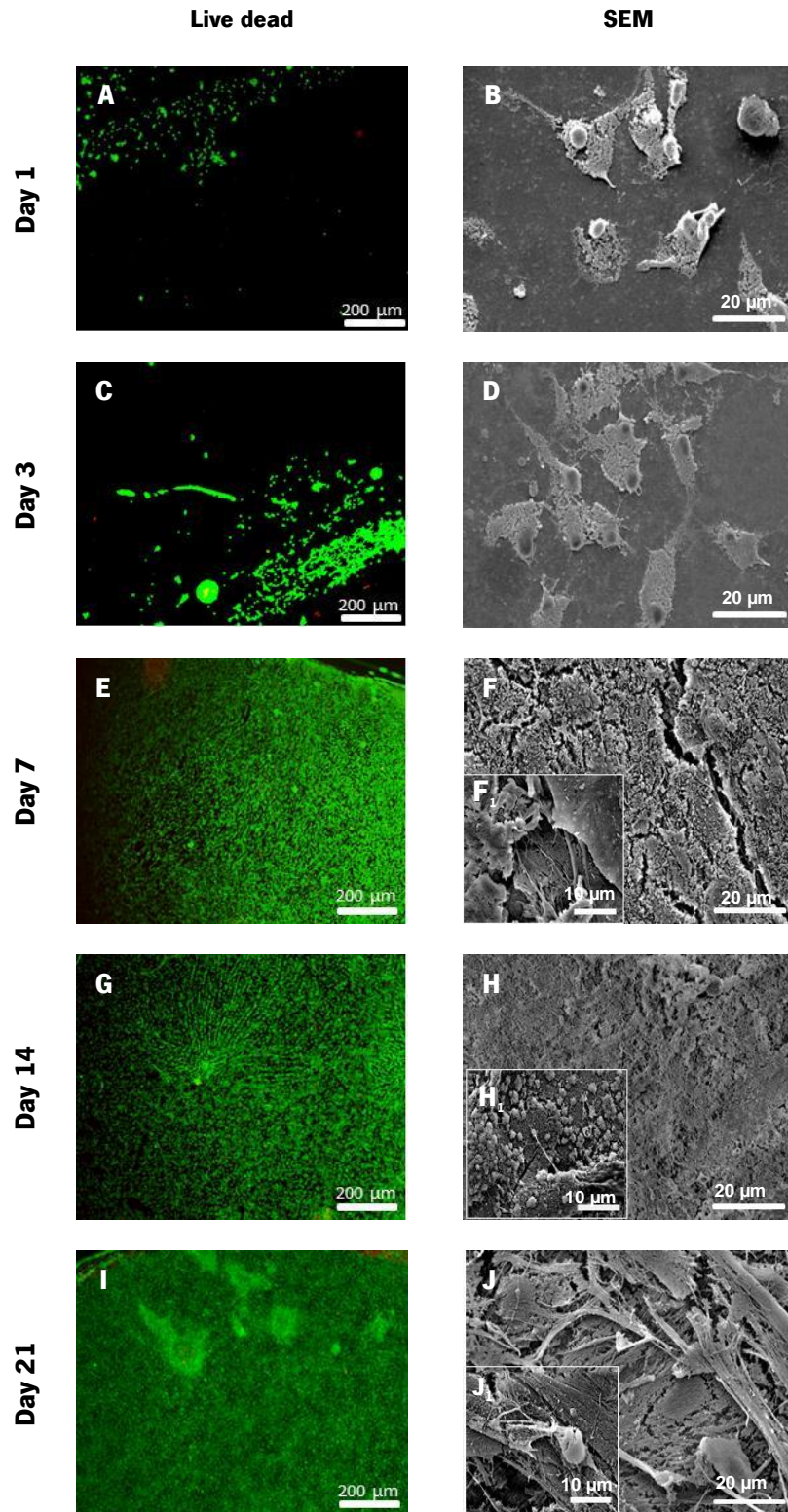


Figure III-2: Live/dead assay and SEM micrographs of bch seeded on glass coverslips coated with chitosan and chondroitin sulphate at day 1 (A, B), 3 (C, D), 7 (E, F), 14 (G, H) and 21 (I, J) of culture in proliferation medium.

The cell proliferation onto the CHT/CS multilayered film could be also observed in the live/dead assay images. The percentage of area coverage with the cells was measured using the calcein/ethidium positive staining and *Image J software* (Figure III-3). The results showed a high amount of living cells and low amount of dead cells.

Among day 1 and 3 no significant differences occurred which can be explained with the natural lag-phase of cells after seeding into a new environment. At 7 days of culture, a vast area ($\approx 60\%$) of surface was already covered and the cell number increase with the increase of culture time which is characteristic of the exponential growth phase of cells. Furthermore, between 14 days and 21 days no differences were achieved in cell proliferation, cells reached the confluence. The results showed no cytotoxic effects from the film and an increase in cell number. Consequently, CHT and CS were used as polyelectrolytes for the fabrication of the 3D nanostructure.

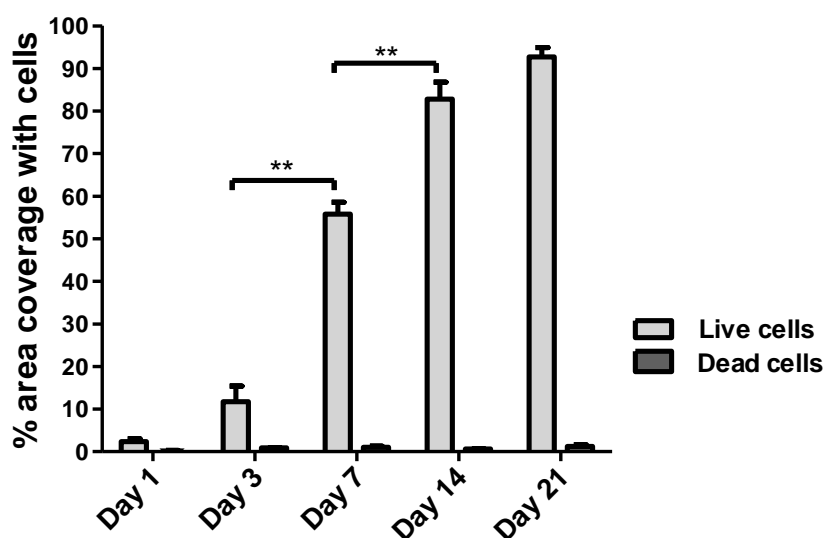


Figure III-3: Percentage of surface area coverage with cells at 1, 3, 7, 14 and 21 days of culture. Significant differences for $p < 0.01$ () were found.**

III-4.3. Nanostructured Scaffolds: Physicochemical characterization

III-4.3.1. Scaffold preparation and morphology

The use of bottom-up approaches to produce 3D porous structures is particularly relevant due to the hierarchical organization of the native tissues. It has been hypothesized that an interconnected 3D porous structure could be prepared combining LbL with leaching of free-packet paraffin spheres. A dropwise addition method of PEMS over the 3D template formed by free-packet paraffin spheres was applied. This technique allows the formation of a 3D lattice arrangement from a randomly placed paraffin spheres. After the coating the paraffin template was leached out and void spaces were created. Thus, the remaining material should be entirely composed by the CHT/CS multilayers - see Figure III-4-A.

The morphology of the obtained scaffolds after the leaching was seen by optical microscopy. The results clearly reveal a soap-bubble-like morphology with geometry and pore sizes consistent with the paraffin spheres used as the template – see Figure III-4B. The interconnectivity should be assured by the existence of physical contact points between the neighbouring paraffin beads that will result in a passage point between the two pores after the leaching process (see red arrow in Figure III-4A). Further structural information was obtained by SEM - see Figure III-4-C. SEM images of freeze-dried scaffolds revealed a noticeable hollow imprint of the porous spherical wax template morphology. This concept allows the production of highly porous structure with controlled pore size and interconnectivity. Consequently, this type of scaffolds should allow the diffusion of substances as well as the integration of cells, namely its infiltration, migration and distribution in the entire volume of the scaffold. The histological cross-sections of the freeze-dried scaffold stained by alcian blue (Figure III 4-D) and eosin (Figure III 4-E) showed a homogeneous distribution of the polysaccharides. Moreover the size of the pores is again consistent with the paraffin template used. Alcian blue stained chondroitin sulphate [31] and eosin chitosan due to the high ability of this polysaccharide to adsorb anionic dyes [32].

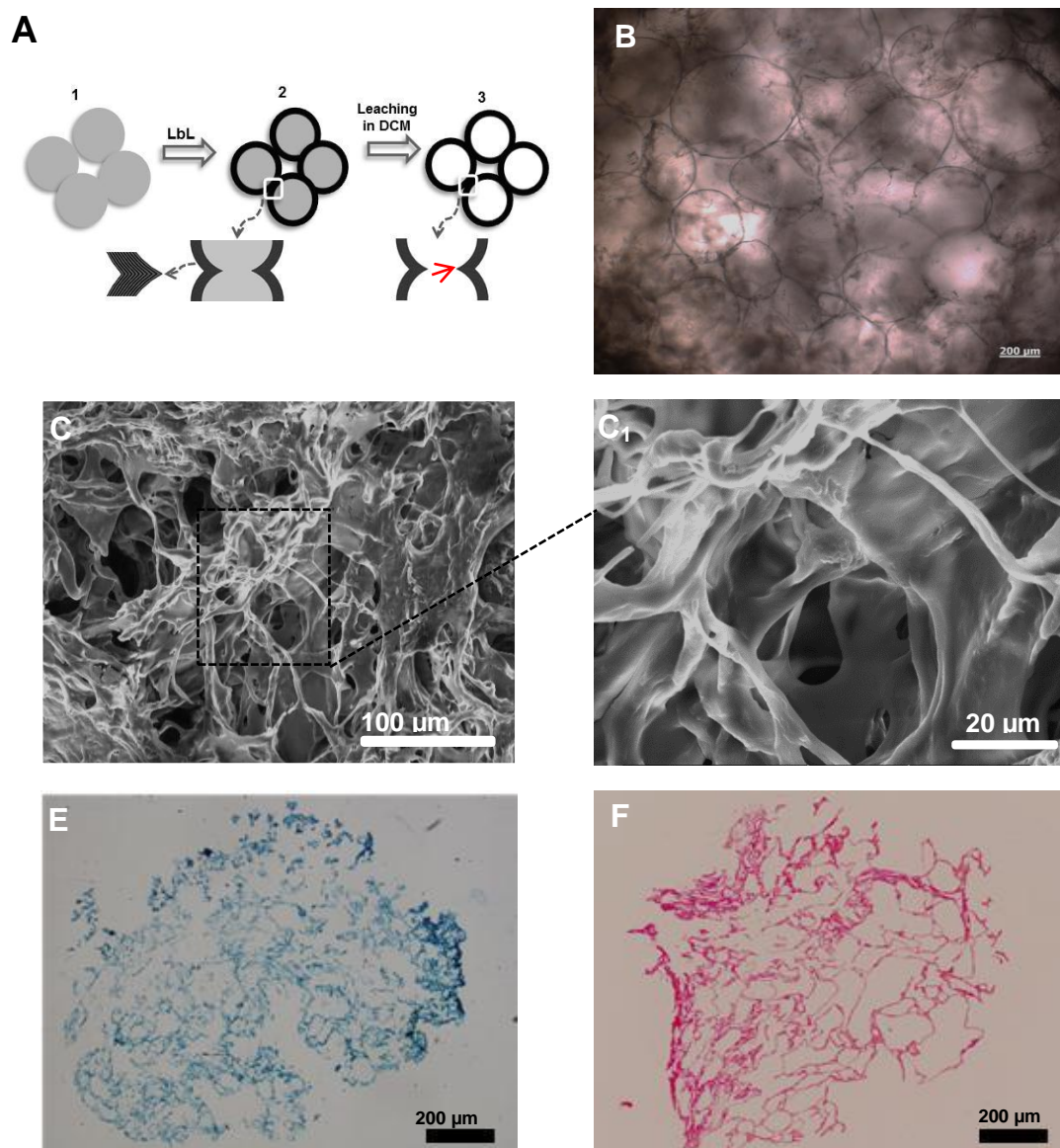


Figure III-4: Scaffold characterization: **A)** Production steps of scaffolds: LbL and leaching of free-packet paraffin spheres, **B)** Optical Microscopy image of the scaffolds after the leaching of the core material, **C)** SEM micrographs of cross-sections (two different magnifications) and Histological cross-sections of the scaffolds after staining with alcian blue **(E)** and eosin **(D)**.

III-4.3.2. Fourier transform infrared spectroscopy

FTIR measurements (Figure III-5A) were performed on the scaffold produced, as well as on both CHT and CS powders in order to identify the presence of both polysaccharides in the entire scaffold. The spectra of CHT and CS are very similar, as expected, reflecting the similarities in the chemical structure of both materials. As a result, they share some common peaks near around

3400 cm^{-1} corresponding to $-\text{OH}$ and N-H bond stretching vibrations, and the peaks around 2900 cm^{-1} corresponding to C-H stretching. Between 1020 cm^{-1} and 1080 cm^{-1} the peaks associated with the stretching of C-O bonds could be also observed. Moreover, the amide groups appeared at 1648 cm^{-1} [33, 34].

In the CHT spectrum the amine group bonds, characteristic of this polysaccharide, appeared at 1570 cm^{-1} [35] The representative peak of chondroitin sulphate was detected at 1250 cm^{-1} corresponding to the stretching in the S=O bond (SO_4^{2-}) [33, 34]. The spectrum of the scaffold shows globally the absorption peaks arising from both CHT and CS which is indicative of the presence of both raw materials in the final structure.

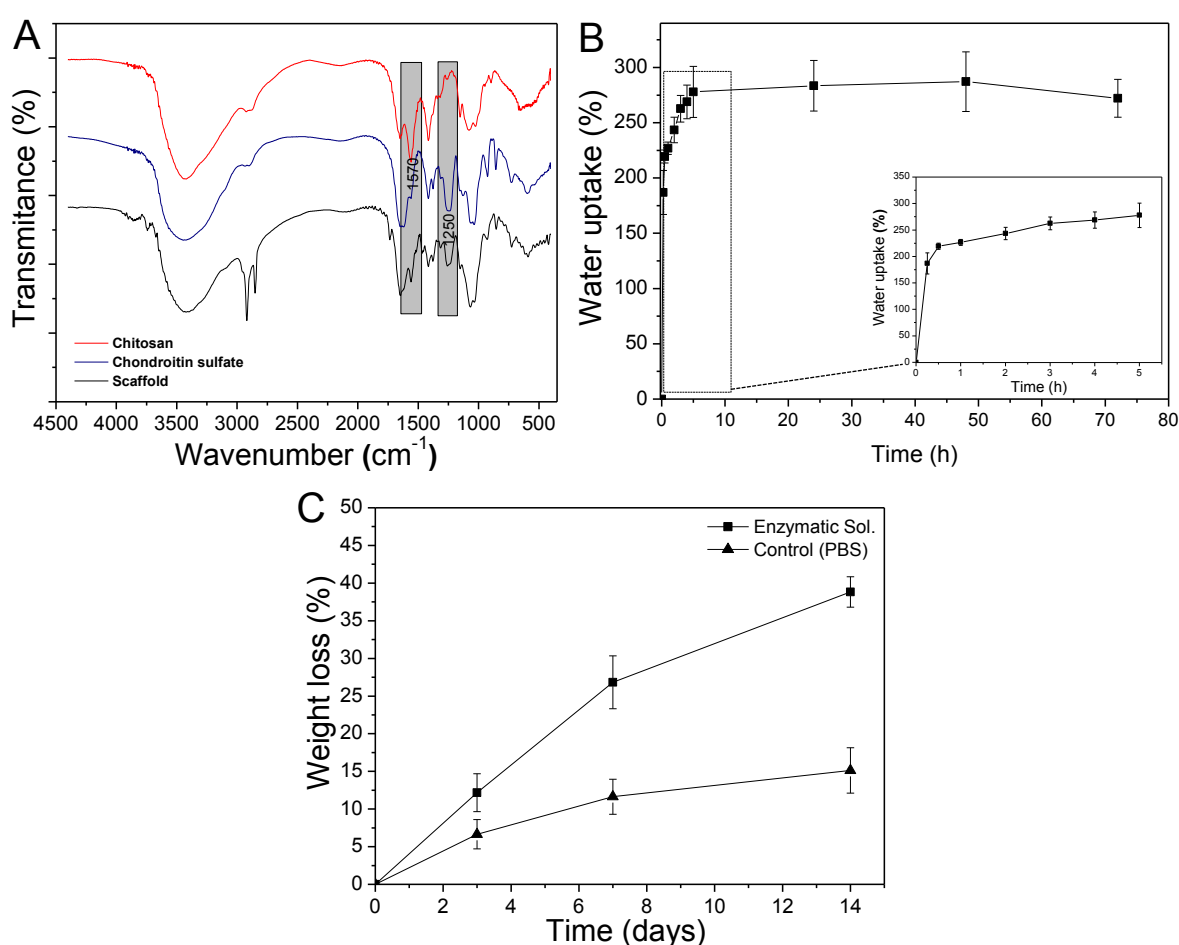


Figure III-5: Physicochemical characterization of scaffolds: A) FTIR measurements of CHT/CS scaffolds and pure polysaccharides (CHT and CS), B) Swelling test up to 3 days (The inset graphic expands the water uptake for the first 5 hours), C) Weight loss of the scaffolds in PBS (\blacktriangle) and in an enzymatic solution at 37°C (\blacksquare).

III-4.3.3. Swelling ability

Water uptake is particularly important for implantable materials because it allows the diffusion and exchange of nutrients and waste to the entire scaffold; moreover water uptake ability also influence the mechanical performance of the biomaterial [8]. The materials used in the scaffold have abundant number of hydrophilic groups, such as hydroxyl, amino, sulphate and carboxyl groups, which can promote the swollen state of the scaffold [36]. The swelling ability was evaluated by soaking scaffolds in PBS (pH=7.4) at 37°C for 3 days – see Figure III-5B. The results showed that the water uptake increase mainly in the first hour and then tends to remain stable, reaching the equilibrium after 5 h (water uptake=280 %). This results can be explained due to the existence of hydrophilic groups, mainly hydroxyl groups, but mostly to CS charge, as a result of the fully ionization of its diprotic anionic functional groups, carboxyl groups (–COOH) and sulphate groups (SO_4^{2-}) under neutral or low ionic strength media [37, 38]. The high density of charge increases the difference in osmotic pressure between the scaffold network and medium resulting in a swollen scaffold.

III-4.3.4. Enzymatic degradation

The biodegradability profile of scaffolds will dictate the changes of many properties of the structure that will occur upon the implantation. Enzymatic activity plays a fundamental role in the degradation of polysaccharides *in vivo* [39]. *In vitro* enzymatic degradation tests were performed with lysozyme and hyaluronidase solution and compared with weight loss in PBS (control). These two enzymes were chosen because they are present in the synovial fluid and they have as well the ability to cleave the polysaccharides used in this study [40, 41]. Lysozyme is able to degrade CHT and hyaluronidase has also the ability to degrade both CHT and CS [41-44]. The weight loss as a function of time is presented in Figure III-5C.

The results showed that the scaffolds are degradable in the presence of the selected enzymes, showing weight losses of ca. 40 % after 14 days. The degradation of scaffolds in the presence of enzymatic solution is facilitated by the high porosity and interconnectivity of the structures allowing the easy access of the enzyme to their substrate. Moreover, the high hydrophilicity of CS (revealed by the high water uptake) can increase the interaction of scaffolds with the enzymatic solution, promoting the weight loss. The scaffolds placed in PBS also suffer some weight loss ca. 15 % after 14

days. In this case the weight loss may be the result of some disaggregation of the multilayered structure, as the polyelectrolytes are self-assembled through electrostatic interactions. The ions present in PBS may interact to the structure and promote partial detachment between the macromolecules resulting in their release to the medium.

III-4.3.5. Mechanical Properties

The viscoelastic/mechanical properties of an implantable device are fundamental for its performance *in vivo* [21]. Dynamical mechanical analysis (DMA) is an adequate non-destructive tool to characterize the mechanical and viscoelastic properties of polymeric materials [45, 46]. Since articular cartilage often bears a dynamic compression force, DMA experiments performed in a hydrated environment and at 37°C allow the assessment of scaffolds in more realistic conditions [21]. The storage modulus (E') and loss factor ($\tan \delta$) as a function of frequency of the developed scaffolds, in the dry and wet state are presented in Figure III-6. The results for the hydrated scaffold showed a slightly increase in both E' and $\tan \delta$ with increasing frequency. In the dry state the values of E' are about one order of magnitude higher when compared with the wet state. Such result is consistent with the high water uptake ability of the scaffolds and the plasticization effect of water molecules in such kind of polysaccharides that increases their molecular mobility and decreases the stiffness of the material. A similar loss of the stiffness due to the effect of water was observed in CHT membranes [47]. In both cases no evident variation of E' along the frequency axis are seen, indicating that no relaxation phenomena takes place in the scaffolds within the time scale covered by the experiments. The $\tan \delta$ of the dry sample decreases slightly with an increasing of frequency. However an opposite trend was observed when the samples were immersed in PBS. $\tan \delta$ is higher in the wet samples, indicating that some dragging of entrapped water can participate in energy loss for the hydrated structure [48]. The DMA results demonstrated a viscoelastic behaviour of the scaffold which is particularly relevant for cartilage TE approaches owing to the viscoelastic nature of this tissue [49]. Moreover, the E' values obtained are similar to ones of the mandibular condylar cartilage which ranges from 0.1 MPa to almost 1.5 MPa in the range of 0.01 – 10 Hz [50].

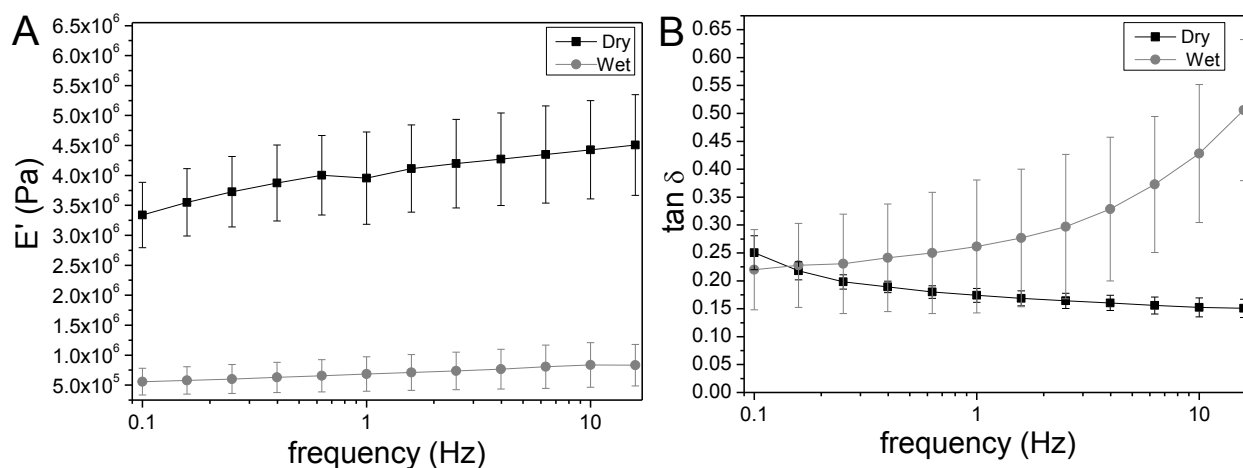


Figure III-6: Variations of (A) Storage modulus (E') and (b) loss factor ($\tan\delta$) of the CHT/CS scaffolds obtained by LbL methodology. Experiments are reported for dry samples (■) and hydrated samples in PBS at 37°C (●).

III-4.4. Cells behaviour in nanostructured scaffolds

III-4.4.1. Cell viability and adhesion\morphology

The cell viability tests with bch (Figure III-7 A, D, G and J) showed a large amount of live cells (green) and almost no dead cells (red), consistent with the results obtained in the flat surfaces indicate, these results indicate that the scaffolds have also no cytotoxic effects to bch cells. After 1 day it is possible to see that the cells tend to aggregate. Furthermore, the results obtained with MTT assay (Figure III-7 B, E, H and K) suggest an increase in cell number and metabolic due to the increase in dark purple staining over time. The results of live/dead assay for hMSCs (Figure III-8 A, D, G and J) also show low amount of dead cells, which indicate the absence of cytotoxic effects also for these types of cells. MTT results (Figure III-8 B, E, H and K) also shown metabolically active cells represented by the dark purple formazan precipitate, evidencing also an increase in the staining intensity with increasing time culture.

Cell adhesion and morphology was further studied by SEM – see Figure III-7 C, F, I and L. The results obtained for bch at day 1 showed that cells were attached to the surface, displaying a round shape. After 3 days of culture the adherent cells might start the deposition of their own ECM which leads to further and faster cell spreading in the following time points. It was also possible to verify that some cell agglomeration occurred after 3 days inside the scaffold. In the latest time point the cells are more adhered and an increase in ECM deposition occurred. The bch presented a round

shape in all time points which is an indication of phenotype retention and essential for matrix deposition [51]. The results for hMSCs (Figure III-8 C, F, I and L) revealed that the cells were attached to the surfaces and presented a more stretched morphology. After 1 day, cells started to adhere and an increase in ECM deposition occurred in the inner areas of the scaffolds (t=14 days).

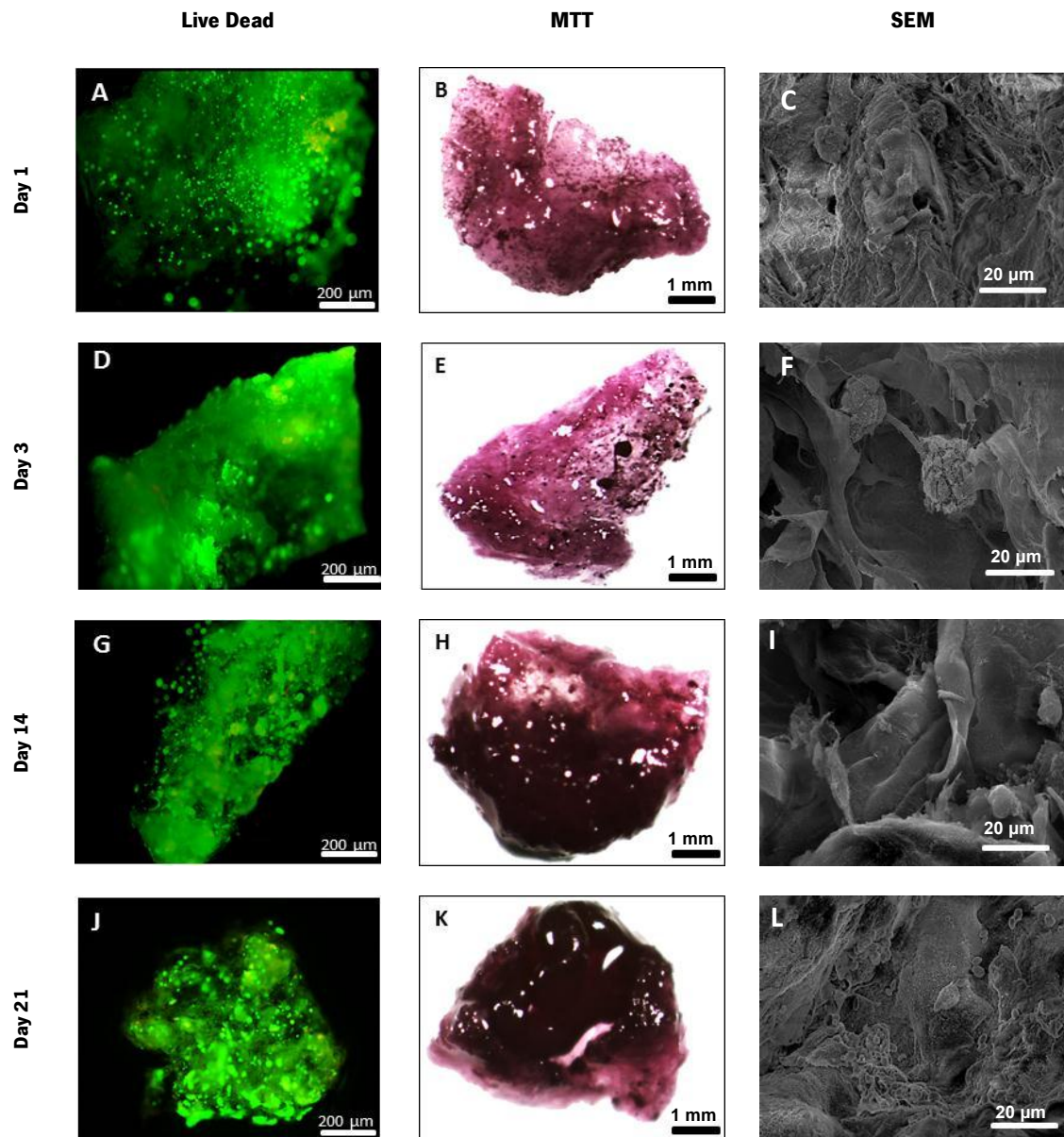


Figure III-7: Live/dead assay, MTT assay and cross-section SEM micrographs of Bch seeded on scaffold at day 1(A, B, C), 3(D, E, F), 14 (G, H, I) and 21(J, K, L) of culture in proliferation medium.

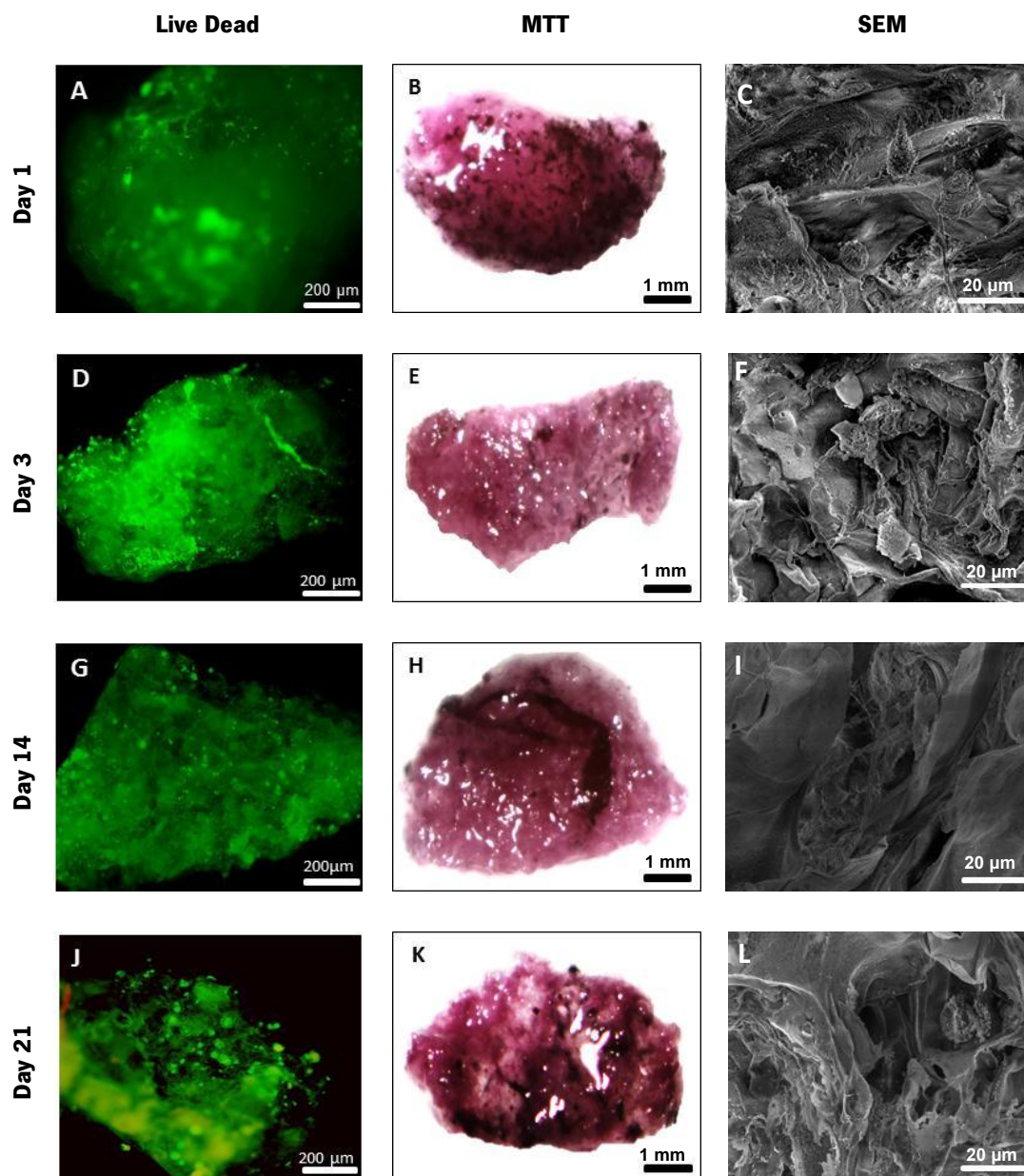


Figure III-8: Live/dead assay, MTT assay and cross-section SEM micrographs of HMSCs seeded on scaffold at day 1(A, B, C), 3(D, E, F), 14 (G, H, I) and 21(J, K, L) of culture in proliferation medium.

III-4.4.2. Cell proliferation

Cell proliferation in differentiation medium was evaluated using DNA assay (Figure III-9). The result obtained for the two types of cell showed that the number of both types of cells increased with increasing culture time. Between the first day of culture and after 35 days there were significant differences in the content of bch and hMSCs cells, indicating that the cells continue the

proliferation even after long time culture. Thus, it is possible that new cells might migrate and populate areas of the scaffold in outside the regions of initial cell seeding.

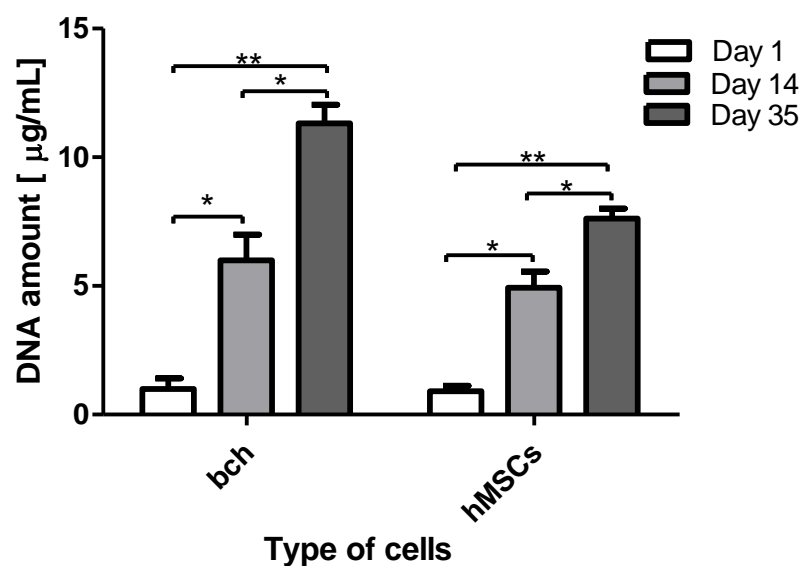


Figure III-9: DNA assay on the scaffolds seeded with bch and hMSCs in differentiation medium. Significant differences between each cell type at different time points were found for $p < 0.05$ (*) and $p < 0.01$ ().**

III-4.5. Histology

Cell distribution and matrix production in differentiation medium was evaluated using histology cross-sections stained with H&E and alcian blue (Figure III-10, Figure III-11).

The H&E staining of scaffold seeded with bch showed the round morphology of cells. Moreover, the abundance of cells per section is increased, which indicates again the occurrence of cell proliferation. At day 1, cells start to attach to the walls forming small aggregates. At day 14 the size of bch agglomerates increased. During the followed weeks, the cells presented a higher dispersion and distribution in the scaffolds. Sulphated GAGs, indicating new cartilage matrix formation, were stained by alcian blue. CS, which gives as well a positive staining for GAGs, can be distinguished from newly deposited matrix by comparing alcian blue staining at day 1 with later times. Secretion of GAGs by bch was seen at 14 days of culture. GAGs production increased during subsequent weeks. Lacunae formation was also seen in the matrix surrounding bch, namely at day 21 and 35. The maintenance of chondrogenic phenotype is indicated by the round shape of the cells by the matrix production.

The scaffolds seeded with hMSCs were also stained with H&E. At day 1 it is possible to see some agglomerate cells and after 2 weeks the size of this agglomerates increased. During the following times of *in vitro* culture the hMSCs were more spread out throughout the scaffold. The GAGs secretion was also assessed and at day 14 a small amount of secretion could be seen. The amount of secretion increased during the next weeks. The secretion of GAGs by hMSCs indicates the chondrogenic differentiation of these cells. The driving force for differentiation in this assay have been TGF- β , however CS might also has a positive influence on chondrogenic differentiation , as reported before [31].

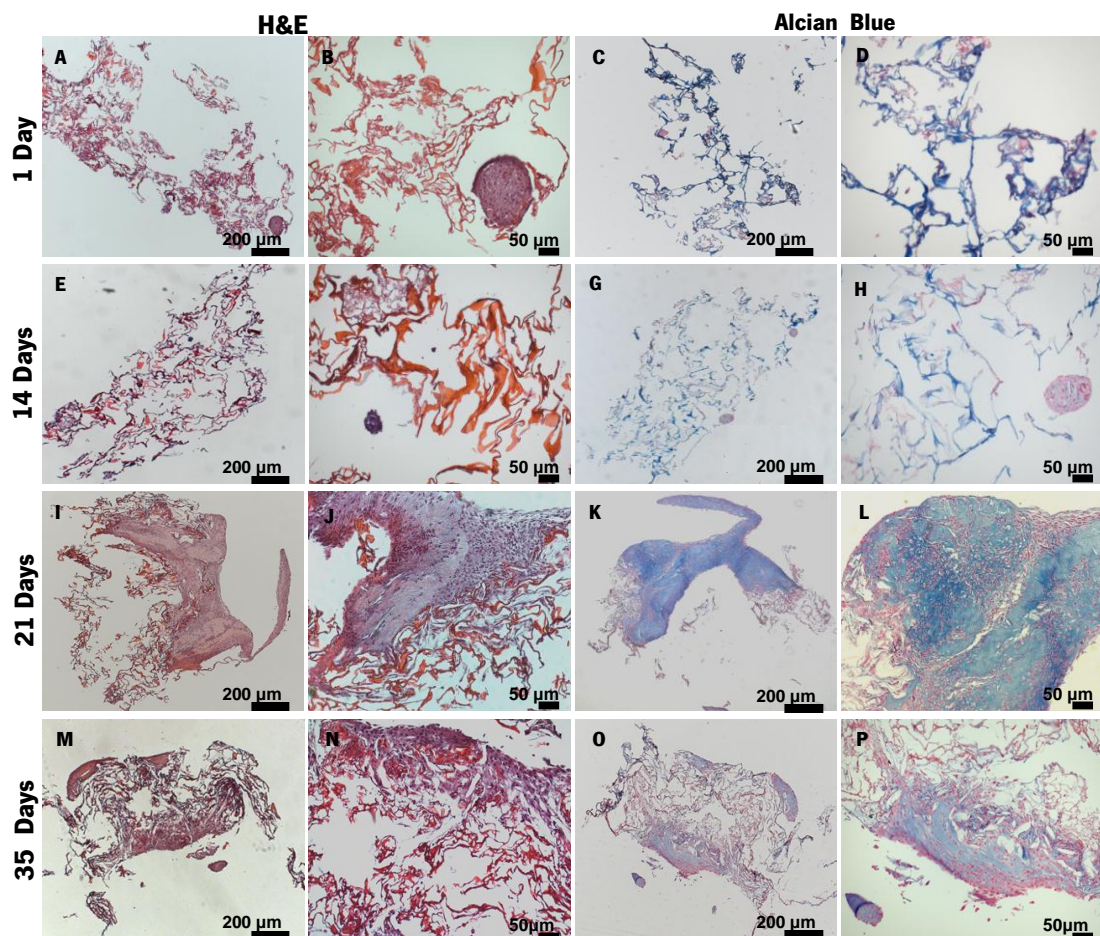


Figure III-10: Histological cross-sections of scaffolds seeded with hMSCs stained by H&E and Alcian blue at different days of culture in differentiation medium.

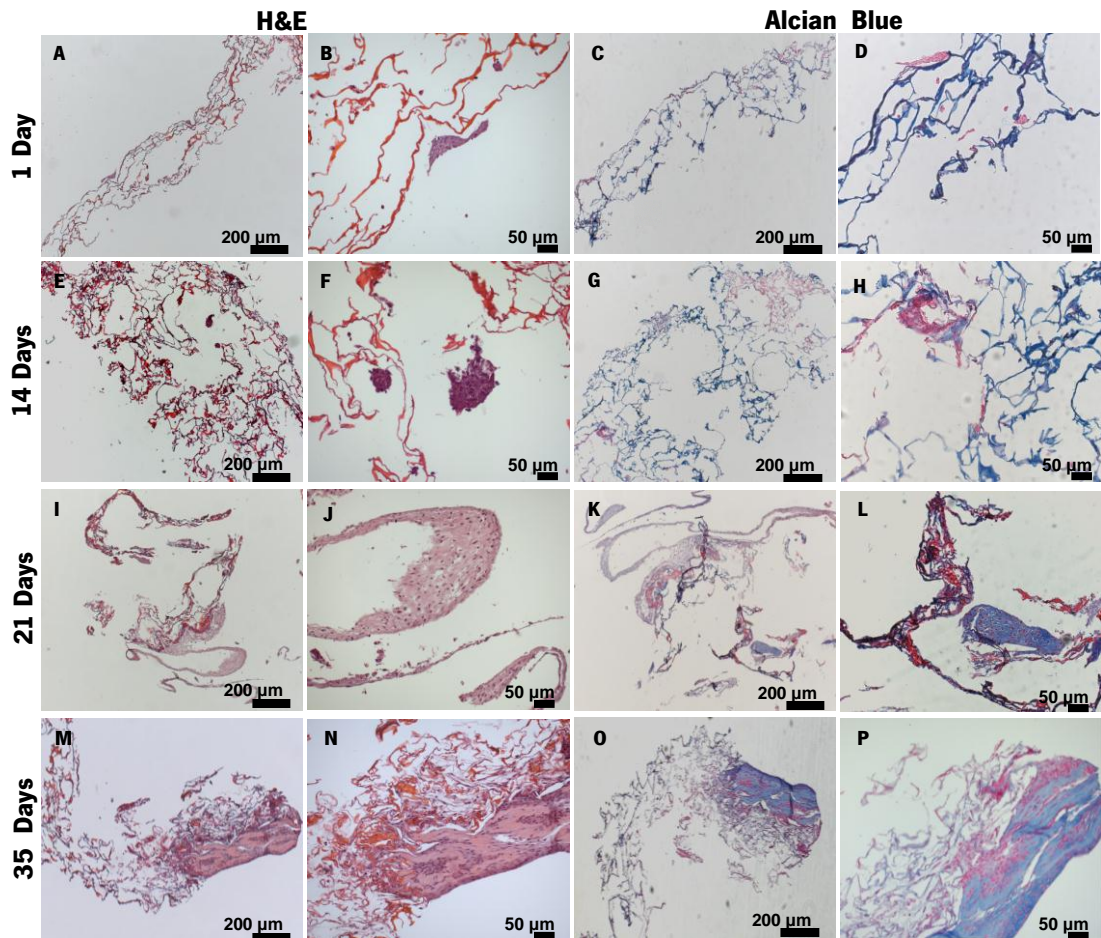


Figure III-11: Histological cross-sections of scaffolds seeded with hMSCs stained by H&E and Alcian blue at different days of culture in differentiation medium.

III-5. CONCLUSION

Flat CHT/CS PEMs prepared using LbL did not elicit any cytotoxic effects to bch cells. It was possible to use LbL combined with spherical template leaching to produce CHT/CS 3D structures with high porosity and interconnectivity, just composed by self-assembled multilayers of these polyelectrolytes. Both bch and hMSCs could adhere and proliferate in these scaffolds, demonstrating the potential of their use in cartilage TE. Production of cartilage matrix production was observed upon culture in chondrogenic differentiation medium indicating that chondrogenic phenotype was maintained and hMSCs differentiation. Our results suggest that the nanostructured scaffolds of chitosan and chondroitin sulphate could have potential use in TE approaches for cartilage.

III-6. REFERENCES

1. LeBaron, R.G. and K.A. Athanasiou, *Ex vivo synthesis of articular cartilage*. Biomaterials, 2000. **21**(24): p. 2575-2587.
2. Fan, H., Y. Hu, and C.e.a. Zhang, *Cartilage regeneration using mesenchymal stem cells and a PLGA-gelatin/chondroitin/hyaluronate hybrid scaffold*. Biomaterials, 2006. **27**: p. 4573-4580.
3. Heng, B., T. Cao, and E. Lee, *Directing stem cell differentiation into the chondrogenic lineage in vitro*. Stem cells, 2004. **22**: p. 1152-1167.
4. Temenoff, J.S. and A.G. Mikos, *Review: tissue engineering for regeneration of articular cartilage*. Biomaterials, 2000. **21**(5): p. 431-440.
5. Mano, J.F. and R.I. Reis, *Osteochondral defects: present situation and tissue engineering approaches*. Journal of Tissue Engineering and Regenerative Medicine, 2007. **4**: p. 263-273.
6. Buckwalter, J. and H. Mankin, *Articular repair and transplantation*. Arthritis Rheum 1998. **20**: p. 1331-1342.
7. Chung, C. and J.A. Burdick, *Engineering cartilage tissue*. Advanced Drug Delivery Reviews, 2008. **60**(2): p. 243-262.
8. Puppi, D., et al., *Polymeric materials for bone and cartilage repair*. Progress in Polymer Science, 2010. **35**(4): p. 403-440.
9. Lee, S. and H. Shin, *Matrices and scaffolds for delivery of bioactive molecules in bone and cartilage tissue engineering*. Advanced Drug Delivery Reviews, 2007. **59**: p. 3393-33959.
10. Chen, F.H., K.T. Rousche, and R.S. Tuan, *Technology Insight: adult stem cells in cartilage regeneration and tissue engineering*. Nat Clin Pract Rheum, 2006. **2**(7): p. 373-382.
11. Boudou, T., et al., *Multiple Functionalities of Polyelectrolyte Multilayer Films: New Biomedical Applications*. Advanced Materials, 2010. **22**(4): p. 441-467.
12. Detzel, C.J., A.L. Larkin, and P. Rajagopalan, *Polyelectrolyte Multilayers in Tissue Engineering*. Tissue Engineering part B., 2011. **17**: p. 1-13.
13. Tang, Z., et al., *Biomedical Applications of Layer-by-Layer Assembly: From Biomimetics to Tissue Engineering*. Advanced Materials, 2006. **18**: p. 3203-3224.
14. Almodóvar, J., et al., *Layer-by-Layer Assembly of Polysaccharide-Based Polyelectrolyte Multilayers: A Spectroscopic Study of Hydrophilicity, Composition, and Ion Pairing*. Biomacromolecules, 2011. **12**(7): p. 2755-2765.
15. Sher, P., C.A. Custódio, and J.F. Mano, *Layer-By-Layer Technique for Producing Porous Nanostructured 3D Constructs Using Moldable Freeform Assembly of Spherical Templates*. Small, 2010: p. n/a-n/a.
16. Miranda, E.S., T.H.S. Silva, and J.F. Mano, *Nanostructured Natural-Based Polyelectrolyte Multilayers to Agglomerate Chitosan Particles into Scaffolds for Tissue Engineering*. Tissue Engineering part A., 2011: p. 2663-2674.
17. Vinatier, C., et al., *Cartilage engineering: a crucial combination of cells, biomaterials and biofactors*. Trends in biotechnology, 2009. **27**(5): p. 307-314.
18. Francis Suh, J.K. and H.W.T. Matthew, *Application of chitosan-based polysaccharide biomaterials in cartilage tissue engineering: a review*. Biomaterials, 2000. **21**(24): p. 2589-2598.
19. Malafaya, P.B., G.A. Silva, and R.L. Reis, *Natural-origin polymers as carriers and scaffolds for biomolecules and cell delivery in tissue engineering applications*. Advanced Drug Delivery Reviews, 2007. **59**(4-5): p. 207-233.
20. Correia, C., et al., *Chitosan Scaffolds Containing Hyaluronic Acid for Cartilage Tissue Engineering*. Tissue Engineering: Part C, 2010. **17**.
21. Sobral, J.M., et al., *Three-dimensional plotted scaffolds with controlled pore size gradients: Effect of scaffold geometry on mechanical performance and cell seeding efficiency*. Acta Biomaterialia, 2011. **7**(3): p. 1009-1018.
22. Costa, R.R., et al., *Stimuli-Responsive Thin Coatings Using Elastin-Like Polymers for Biomedical Applications*. Advanced Functional Materials, 2009. **19**(20): p. 3210-3218.
23. Costa, R.R., et al., *Layer-by-Layer Assembly of Chitosan and Recombinant Biopolymers into Biomimetic Coatings with Multiple Stimuli-Responsive Properties*. Small, 2011. **7**(18): p. 2640-2649.

24. Martins, G., J.F. Mano, and N. Alves, *Nanostructured self-assembled films containing chitosan fabricated at neutral pH*. Carbohydrate Polymers, 2010. **80**: p. 570-573.
25. Alves, N.M., C. Picart, and J.F. Mano, *Self Assembling and Crosslinking of Polyelectrolyte Multilayer Films of Chitosan and Alginate Studied by QCM and IR Spectroscopy*. Macromolecular Bioscience, 2009. **9**(8): p. 776-785.
26. Voinova, M.V., et al., *Viscoelastic acoustic response of layered polymer films at fluid-solid interfaces: continuum mechanics approach*. Physica Scripta, 1999. **59**: p. 391-396.
27. Crouzier, T., T. Boudou, and C. Picart, *Polysaccharide-based polyelectrolyte multilayer*. Current Opinion in Colloid&Interface Sciene, 2010. **15**: p. 417-426.
28. Kohler, K., et al., *Thermal behavior of polyelectrolyte multilayer microcapsules 1. the effect of odd and even layer number*. Journal physics chemical, 2005. **109**: p. 18250-18259.
29. Anselme, K., *Osteoblast adhesion on biomaterials*. Biomaterials, 2000. **21**: p. 667-681.
30. Kirkpatrick, C. and A. Dekker, *Quantitative evaluation of cell interaction with biomaterials in vitro*. Adanced Biomaterials, 1992. **10**: p. 31-42.
31. Chen, W.-C., et al., *Compare the effects of chondrogenesis by culture of human mesenchymal stem cells with various type of the chondroitin sulfate C*. Journal of bioscience and bioengineering, 2011. **111**(2): p. 226-231.
32. Chatterjee, S., et al., *Adsorption of a model anionic dye, eosin Y, from aqueous solution by chitosan hydrobeads*. Journal of Colloid and Interface Science, 2005. **288**(1): p. 30-35.
33. Servaty, R., et al., *Hydration of polymeric components of cartilage — an infrared spectroscopic study on hyaluronic acid and chondroitin sulfate*. International Journal of Biological Macromolecules, 2001. **28**: p. 121–127.
34. Sui, W., et al., *Preparation and properties of chitosan and chondroitin sulfate complex microcapsules*. Colloids and Surfaces B: Biointerfaces, 2008. **65**: p. 69-73.
35. Neves, S.C., et al., *Chitosan/Poly([ε- caprolactone) blend scaffolds for cartilage repair*. Biomaterials, 2010. **In Press, Corrected Proof**.
36. Varghese, J.M., et al., *Thermoresponsive hydrogels based on poly(N-isopropylacrylamide)/chondroitin sulfate*. Sensors and Actuators B: Chemical, 2008. **135**(1): p. 336-341.
37. Fajardo, A.R., et al., *Time- and pH-dependent self-rearrangement of a swollen polymer network based on polyelectrolytes complexes of chitosan/chondroitin sulfate*. Carbohydrate Polymers, 2010. **80**(3): p. 934-943.
38. Piai, J.F., A.F. Rubira, and E.C. Muniz, *Self-assembly of a swollen chitosan/chondroitin sulfate hydrogel by outward diffusion of the chondroitin sulfate chains*. Acta Biomaterialia, 2009. **5**(7): p. 2601-2609.
39. Hutmacher, D.B., *Scaffolds in tissue engineering bone and cartilage*. Biomaterials, 2000. **21**: p. 2529-2543.
40. Fraser, J., T. Laurent, and U. Laurent, *Hyaluronan: its nature, distribution, functions and turnover*. Journal of Internal Medicine, 1997. **242**: p. 27-33.
41. Martins, A.M., et al., *Natural origin scaffolds with in situ pore forming capability for bone tissue engineering applications*. Acta Biomaterialia, 2008. **4**(6): p. 1637-1645.
42. Menzel, E. and C. Farr, *Hyaluronidase and its substrates hyaluronan: biochemistry, biological activities and therapeutic uses*. Cancer Letters, 1998. **131**: p. 3-11.
43. Mao, J., et al., *The properties of chitosan-gelatin membranes and scaffolds modified with hyaluronic acid by different methods*. Biomaterials, 2003. **24**: p. 1621-1629.
44. Jin, R., et al., *Synthesis and characterization of hyaluronic acid-poly(ethylene glycol) hydrogels via Michael addition: An injectable biomaterial for cartilage repair*. Acta Biomaterialia, 2010. **6**(6): p. 1968-1977.
45. Yan, L.-P., et al., *Macro/microporous silk fibroin scaffolds with potential for articular cartilage and meniscus tissue engineering applications*. Acta Biomaterialia, (0).
46. Yan, L.-P., et al., *Genipin-cross-linked collagen/chitosan biomimetic scaffolds for articular cartilage tissue engineering applications*. Journal of Biomedical Materials Research Part A, 2010. **95A**(2): p. 465-475.
47. Mano, J.F., *Viscoelastic Properties of Chitosan with Different Hydration Degrees as Studied by Dynamic Mechanical Analysis*. Macromolecular Bioscience, 2008. **8**(1): p. 69-76.
48. Ghosh, S., et al., *Dynamic mechanical behavior of starch-based scaffolds in dry and physiologically simulated conditions: Effect of porosity and pore size*. Acta Biomaterialia, 2008. **4**(4): p. 950-959.

49. Moutos, F.T., L.E. Freed, and F. Guilak, *A biomimetic three-dimensional woven composite scaffold for functional tissue engineering of cartilage*. *Nat Mater*, 2007. **6**(2): p. 162-167.
50. Franke, O., et al., *Dynamic nanoindentation of articular porcine cartilage*. *Materials Science and Engineering: C*, 2011. **31**(4): p. 789-795.
51. Von der Mark, K., et al., *Relationship between cell shape and type of collagen synthesized as chondrocytes lose their cartilage phenotype in culture*. *Nature*, 1977. **267**: p. 531-532.

***“One never notices what has been done;
one can only see what remains to be done”***

Marie Curie

CHAPTER IV

GENERAL CONCLUSION AND FUTURE PERSPECTIVES

Chapter IV

General Conclusion and Future Perspectives

The objective of this dissertation was the development and characterization of 2D and 3D structures based on LbL methodology. Porous 3D structures can be useful for cartilage TE approaches. To accomplish this aim, two polyelectrolytes were selected: CHT and chondroitin CS. Herein a summary of major achievements will be given.

IV-1. GENERAL CONCLUSIONS

A novel type of nanostructured scaffolds based on CHT and CS was obtained, combining LbL and leaching of spherical templates. The potential of these structures for cartilage TE was evaluated.

For the proof of concept, biological assays were first performed in multilayer surfaces with bovine chondrocytes (bch) and no cytotoxic effects of the film were found. Thus, PEMs was transposed to 3D level and originated a structure with a soap-bubble-like morphology, as proven by optical microscopy after the leaching of the all core material. Moreover, the scaffolds present a high porosity and interconnectivity, owing to the leaching of all the paraffin and physical contact points between the original paraffin beads. After the freeze drying, SEM images revealed a noticeable hollow imprint of the porous spherical wax templates geometry. The histological cross-sections of the freeze dried scaffolds showed a pore size consistent with the paraffin template and a homogeneous distribution of the both polysaccharides, as proven with FTIR.

Swelling test and enzymatic degradation demonstrated a structure with ability to diffuse substances and gradual degradation. Mechanical tests performed with DMA revealed the viscoelastic properties of the scaffolds which corroborate the results obtained at QCM (an increase of dissipation (ΔD) in each polyelectrolyte injection).

The applicability of the nanostructured scaffold for cartilage TE approaches was evaluated in cellular assays with bch and human mesenchymal stem cells (hMSCs). The cells were viable, metabolically active and proliferate during 35 days of *in vitro* studies, as live dead/MTT assay, SEM

analysis and DNA quantification showed. Histological cross-sections revealed the maintenance of chondrocyte phenotype and chondrogenic differentiation of hMSCs. The physicochemical and biological advantages presented in this study will make it probably possible to apply the current scaffolds to cartilaginous lesions.

IV-2. FUTURE PERSPECTIVES

A number of valuable results were obtained in this research project which will hopefully be of utility in future investigations. The usefulness of nanostructured 3D constructs based on CHT and CS multilayers for cartilage TE approaches are the most significant contributions of this thesis. The next steps may include the following studies:

1. The production of structures with gradients of porosity, using different size of paraffin wax spheres;
2. Increase the mechanical properties of the constructs using for that a high number of layers, crosslinking or fillers;
3. Evaluate the behaviour of cells with different number of layers;
4. Assess gene expression with polymeric chain reaction (PCR);
5. Study the effect of chondroitin sulphate in chondrogenic differentiation.